THE EFFECT OF HERBICIDES, PESTICIDES, AND FERTILIZERS ON THE OPTICAL PROPERTIES OF WATER

Marvin R. Querry
Principal Investigator

Richard C. Waring
Senior Investigator

Department of Physics
University of Missouri-Kansas City

MISSOURI WATER RESOURCES RESEARCH CENTER
University of Missouri-Columbia

Project Number: A-030-MO
Agreement Number: 14-31-0001-3025
Dates: 1 September 1969 - 15 August 1971

COMPLETION REPORT

13 August 1971

The work upon which this publication is based was supported in part by funds provided by the United States Department of the Interior, Office of Water Resources Research, as authorized under the Water Resources Act of 1964.

FOREWORD

The research results outlined in this report represent the accomplishments of a two year research program sponsored by the Missouri Water Resources Research Center (OWRR) as Project A-030-Mo. Based on the results of the research program, we estimate that reflectance techniques will ultimately have definite and very interesting applications in measuring water quality from remote platforms and by measuring reflectance in the laboratory for samples collected in the field (Section VIII). We are grateful for the opportunity to serve the Missouri Water Resources Research Center and the Office of Water Resources Research of the Department of Interior. We invite your comments and discussion of the results from the research program.

10 August 1971

Marvin R. Querry

ABSTRACT

THE EFFECTS OF HERBICIDES, PESTICIDES, AND FERTILIZERS ON THE OPTICAL PROPERTIES OF WATER

M. R. Querry and R. C. Waring
Department of Physics
University of Missouri-Kansas City

A reflectometer accessory for a spectrophotometer was designed and constructed in our laboratory. Using distilled water as the reflectance standard, the reflectometer was used to measure relative specular reflectance of 0.5M aqueous solutions of K_2SO_4 and $NH_4H_2PO_4$ in the 2-12μm wavelength region and for 1M $(NH_2)_2CO$ in the 2-20μm wavelength region for infrared radiant flux incident at about 70° and linearly polarized perpendicular to the plane of incidence. Absolute reflectances of the solutions were computed for 70° angle of incidence by using the relative reflectance measurements, one of the Fresnel equations, and the optical constants of water. The optical constants of the aqueous solutions were then computed by applying a Kramers-Kronig phase-shift dispersion analysis to the absolute reflectance spectra. The report provides a description of the instrumentation and the experimental procedures for making the measurements.

The relative reflectances, absolute reflectances, and optical constants are presented in graphical form in the text and are tabulated in Appendix I. Spectral signatures characteristic of the solutes are discussed in the text.

In addition, further investigations of the optical constants of distilled water were made in that they are related to the investigations of aqueous solutions. The work on distilled water was accomplished in cooperation with Dr. Dudley Williams at Kansas State University. A reprint describing the work is presented in Appendix I.

LIST OF FIGURES

Figure

TABLE OF CONTENTS

"THE EFFECTS OF HERBICIDES, PESTICIDES, AND FERTILIZERS ON THE OPTICAL PROPERTIES OF WATER"

M. R. Querry and R. C. Waring
Department of Physics
University of Missouri-Kansas City

I. INTRODUCTION

The research program associated with project A-030-Mo had four objectives:

(1) to measure the effects of a pesticide, a herbicide, and a fertilizer on the infrared reflectance and transmittance of water.

(2) To compute the optical constants, i.e. the index of refraction and the extinction coefficient, from reflectance and transmittance data.

(3) To compute the absorption and reflectance of radiant energy for water solutions of pesticides, herbicides, and fertilizers relative to that of pure water, and to relate the results of these computations to possible changes in the thermodynamic equilibrium of rivers and lakes.

(4) To study the interaction of solutes with the water substance.

In accordance with the objectives as stated above and as they were altered by mutual consent of the Principal Investigator and the Director of the Missouri Water Resources Research Center, we did not investigate aqueous solutions of pesticides and herbicides but rather measured the relative infrared reflectance of three different aqueous solutions of chemical fertilizers. The three aqueous solutions investigated had solute content of 0.5M K_2SO_4, 0.5M $NH_4H_2PO_4$, and 1M $(NH_2)_2CO$. The reflectance was measured respectively in the 2-12μm and 2-20μm wavelength regions of the infrared for the 0.5M and 1M solutions. Optical constants were then computed by applying a Kramers-Kronig phase-shift dispersion analysis to the absolute reflectance spectra.

The purpose of this report is to present, in some detail, the results derived from the two year research program. In Section II we present an analysis of a transmission polarizer because results of the analysis are applied in Section III to the experimental procedure for making relative reflectance measurements. The relative reflectances of the aqueous solutions are presented in graphical form and the effects of the solutes on the relative reflectance spectra are discussed in Section IV. Methods for computing absolute reflectances from relative reflectances are outlined in Section V. In Section VI the Kramers-Kronig analysis for computing the optical constants is outlined as it was applied

to the oblique angle of incidence reflectance data. The optical constants of the aqueous solutions are presented in graphical form in Section VII. Conclusions related to the application of results from the research program are presented in Section VIII. The report ends with a list of publications and presentations derived from the project[1-4] and references important to the research program. The relative reflectances and optical constants are tabulated in the final pages of the report.

II. TRANSMISSION POLARIZERS

The reflectometer unit constructed in our laboratory has two transmission polarizers for the 2-20μm infrared wavelength region. Each polarizer consists of six silver chloride plates oriented at the Brewster angle. Querry[5] in 1968 was the first to measure leakage and insertion loss for such a polarizer as applied to investigations of the infrared reflectance of distilled water. His analyses are produced here to provide background information that is important to the experimental procedure presented in Section III.

A transmission polarizer, consisting of a stack of transparent plates oriented at the Brewster angle, is placed in a completely unpolarized, collimated, beam of radiant flux, of radiant intensity I_o, which propagates along the Z-axis of a Cartesian Coordinate system. Before passing through the polarizer the radiant intensity

$$I_o = I_x + I_y \quad , \tag{2-1}$$

where I_x, I_y are the radiant intensities derived from a superposition of the respective x-, y- components of the electric field vectors of the many electromagnetic plane waves that make up the unpolarized beam of radiant flux. Let the polarizer be characterized by a transmission coefficient τ and a leakage coefficient ℓ. The coefficients

τ, ℓ can be computed by using the Fresnel equations. Orienting the polarizer to transmit the x-component and to not transmit the y-component; after passing through the polarizer the radiant intensity I will be

$$I = \tau I_x + \ell I_y . \qquad (2\text{-}2)$$

If the transmitted beam of radiant flux is then monitored with a spectrophotometer system, the recorder reading X could be computed by using the equation

$$X = m\,(\tau k_x I_x + \ell\, k_y\, I_y), \qquad (2\text{-}3)$$

where k_x, k_y are characteristic constants of the monochromator that account for all the reflection and transmission losses due to mirrors, prisms, or window materials and m is a proportionality constant characteristic of the detector-amplifier-recorder system of the spectrophotometer.

Similarly, when the polarizer is rotated 90° to transmit the I_y component and not transmit the I_x component, the recorder reading Y is given by

$$Y = m(\ell k_x I_x + \tau k_y I_y) . \qquad (2\text{-}4)$$

When two similar polarizers are crossed in such a manner that one is to transmit the I_x component and the other the I_y

component, the recorder reading N will be

$$N = m\tau\ell(k_x I_x + k_y I_y) \quad . \tag{2-5}$$

And when there is no polarizer in the beam the recorder reading will be

$$U = m(k_x I_x + k_y I_y) \quad . \tag{2-6}$$

Equations (2-5) and (2-6) may be combined to yield

$$N = \tau\ell U \quad . \tag{2-7}$$

Equations (2-3) - (2-7) are solved for the coefficients τ, ℓ as follows: Add equation (2-3) to equation (2-4) to get

$$X + Y = U(\tau + \ell) \quad . \tag{2-8}$$

Substituting for ℓ from equation (2-7) in equation (2-8) gives

$$U\tau^2 - (X + Y)\tau + N = 0 \quad . \tag{2-9}$$

Equation (2-9) is a quadratic in τ having the solution

$$\tau = \frac{X + Y + \sqrt{(X + Y)^2 - 4UN}}{2U} \quad , \tag{2-10}$$

where the plus sign was chosen because τ is nearly unity. Equation (2-10) gives τ in terms of measurable quantities. The value of ℓ is found by using equation (2-7) with τ as computed from equation (2-10). Figure 1 shows graphs of the parameters τ and ℓ for a four plate, silver chloride, polarizer as determined by Querry in 1968. There was no need to complete this type analysis for our two six plate polarizers, because for two six plate polarizers in series, i.e. a twelve plate polarizer, the parameters would be τ^3 and ℓ^3 where τ and ℓ are the parameters shown in Figure 1 for the four plate polarizer. Reading from the graph in Figure 1 at wavelength 5μm we have $\tau = 0.894$ and $\ell = 0.075$, or $(\ell/\tau)^3 = 0.0006$. Thus about 0.06 per cent of the beam transmitted by the twelve plate polarizer is due to leakage.

III. EXPERIMENTAL TECHNIQUES

The new reflectometer for measuring specular reflectance is an improved design of the reflectometer that Querry et al.[6] used in 1968 to measure the specular reflectance of distilled water. The new system was designed for the 0.2-30μm wavelength region, but for the investigation reported here, we operated the system only in the 2-20μm wavelength region. A diagram of the reflectometer spectrophotometer system is shown in Figure 2. When operating the system in the infrared spectral region, a glower G emits radiant flux which is chopped at C and is then collected and collimated by a Cassegrain unit consisting of spherical mirrors M_1 and M_2. A partially collimated pencil of radiant flux of about 18 mrad divergence passes horizontally to mirror M_3, and then enters a Cassegrain condenser unit consisting of spherical mirrors M_5 and M_6. From the condenser unit a convergent cone of radiant flux, with apex angle of about 75 mrad at the entrance slit of the monochromator, passes through a transmission polarizer consisting of 12 silver chloride plates positioned at the Brewster's angle relative to the system's optical axis. The 12 plate polarizer passes less than .1 per cent of the undesired polarization component. A thermopile detector having a CsI window provides a measure of the spectral energy. Interference filters at the monochromator's exit slit prevent overlapping diffraction orders and scattered radiant flux from reaching

the detector. The monochromator, chopper, detector assembly, amplifier, recorder, and scan control are a Perkin-Elmer E System. A photograph of the reflectometer is shown in Figure 3.

The reflectometer was designed and constructed in such a manner that measurements can be made of absolute specular reflectance or of the specular reflectance relative to a calibrated reflectance standard. To measure absolute reflectance we must move mirrors B, C to positions B', C'; as shown in Figure 4; so that the only change is in the optical path length. A He-Ne laser beam provided a reference for carefully repositioning the two mirrors. This technique consistently introduced an additional random error of ± 2-3 per cent in the absolute reflectance measurements. To measure relative specular reflectance, we substitute the reflectance standard for the sample and then carefully move the standard reflector to the sample's original position by adjusting a small laboratory jack while viewing the edge of the reflectance surface through the telescope of a cathetometer. A series of relative reflectance measurements typically have a standard deviation of less than 1.0 per cent. Since the optical constants of distilled water are now known with reasonable certainty[5-10] in the 2-20μm wavelength region of the infrared, we chose distilled water as the reflectance standard and measured the relative reflectance of the aqueous solutions.

The technique for measuring the relative specular reflectance of an aqueous solution for polarized radiant flux was as follows: An aqueous solution was placed at the sample position in the reflectometer. The transmission polarizer was oriented to transmit the H (horizontal polarization) component of radiant intensity I_h and to not transmit the V (vertical polarization) component of radiant intensity I_v. The recorder reading h_s from the spectrophotometer was

$$h_s = m(\tau R_{\perp s} k_h I_h + \ell R_{\parallel s} k_v I_v) \ , \qquad (3\text{-}1)$$

where $R_\perp$, $R_\parallel$ are respectively the reflectances for radiant flux linearly polarized with the electric field vector perpendicular and parallel to the plane of incidence and the other quantities were defined in Section II. Now, it was shown in Section II that (ℓ/τ) is about 0.0006 for two, six plate polarizers in series. For a grating monochromator $1/3 \lesssim (k_h/k_v) \lesssim 3$, and for water or weak water solutions $(R_s/R_s) \gtrsim 2$ at about 70° angle of incidence which was the angle of incidence for our investigations. The last term in equation (3-1) was relatively small ($\sim 10^{-3}$); therefore

$$h_s = maR_{\perp s} k_h I_h \ . \qquad (3\text{-}2)$$

Similarly for distilled water placed at the sample position in the reflectometer the recorder reading h_w was given by

$$h_w = maR_{\perp w}k_h I_h \quad , \tag{3-3}$$

where R_w was the reflectance of the distilled water for horizontally polarized radiant flux. The relative reflectance R_h, the ratio of equation (3-2) to (3-3), was

$$R_h = (h_s/h_w) = (R_{\perp s}/R_{\perp w}). \tag{3-4}$$

We measured h_s and h_w in order to obtain R_h, which is the reflectance of the aqueous solution relative to distilled water for horizontally polarized radiant flux. Measurements of h_s and h_w were alternately repeated until three independent values of R_h were determined in accordance with equation (3-4). The standard deviation of the three values of R_h was then determined by using the theory of errors for a small number of observations.

The monochromator was operated with spectral slit widths as shown in the table at the end of the report. A cathetometer, having a protractor ocular as the eye piece for the telescope, was used to measure the angle of incidence Θ to about $\pm$ 4 mrad for the central ray of the slightly divergent pencil of radiant flux.

IV. EXPERIMENTAL RESULTS

The experimental techni ues for measuring the relative specular reflectance of aqueous solutions by using distilled water as the reflectance standard were outlined in Section III. We used those techniques to measure the relative, infrared reflectance of aqueous solutions of K_2SO_4, $NH_4H_2PO_4$, and $(NH_2)_2CO$ in the 2-12μm wavelength region. The data from our relative reflectance measurements are shown graphically in Figures 5-7. All reflectance measurements were made for infrared radiant flux incident at an angle of about 70° as measured relative to the vertical and for polarization perpendicular (horizontal) to the plane of incidence.

The measured average, relative, infrared reflectances are shown in Figures 5-7 for aqueous solutions of $(NH_4)H_2PO_4$, and K_2SO_4 at 0.5 molar concentration and for $(NH_2)_2CO$ at 1.0 molar concentration.

The strong infrared reflectance band of SO_4^{-2} in the 8-10μm wavelength region produces a strong spectral signature in the relative reflectance spectrum which is characteristic of the ionic sulfate solute. The strong spectral signatures are quite evident in relative reflectance spectra shown in Figure 5. The strong spectral signature extends beyond the 10μm and is possibly caused by a band due to $(HSO_4)^{-1}$ or other molecular compounds that are

formed in the solution. The phosphate ion PO_4^{-3} has a medium strength reflectance band in the in the 8-10μm wavelength region, as shown in Figure 6, which also produces a medium strength spectral signature characteristic of the phosphate. The medium strength spectral signature is extended to wavelengths greater than 10μm, as seen in Figure 6, possibly due to spectral signatures of $(HPO_4)^{-2}$ and $(H_2PO_4)^{-1}$ or other molecular compounds that are formed in the solution. The $(NH_4)^{-1}$ ion has only weak bands which we did not observe. We also noticed the distinctness of the spectral signatures due to the sulfate and phosphate.

The measured, average, relative reflectance spectrum of the 1M $(NH_2)_2CO$ aqueous solution is shown in Figure 7 through the 2-20μm wavelength region. We noted in the relative reflectance spectrum some vibration bands of the solute. There are: two bands at about 2.8μm due to NH_2 vibrations, a vibration band at 4.8μm possibly due to CO_2, vibration bands due to NH_2 and NH_2-CO in the 6-7μm region, a vibration band in the 8.4-9.2μm region due to NH_2-CO, a broad band due to CO in the 7.7-11.3μm region, and a possible band of unknown origin in the 17-19μm wavelength region. The correlation of the vibration bands with the solutes was based on information available in reference number 17. The band assignments are tentative and therefore subject to additional investigation.

V. ABSOLUTE REFLECTANCE

The absolute reflectances of the aqueous solutions were computed from the measured values for the relative reflectance, the Fresnel reflectance equations,[11] and the optical constants of distilled water.[7] The average, absolute reflectances of the aqueous solutions are shown graphically in Figures 5-7. The procedure for computing the absolute reflectance is as follows. We measure $\overline{R}_h$ the average, relative reflectance for aqueous solutions with horizontally polarized infrared radiant flux incident at an oblique angle Θ as measured from a normal to the surface of the solution. In the form of an equation we write the average, relative reflectance $\overline{R}_h$ as

$$\overline{R}_h = R_{\perp s}/R_{\perp w} \quad , \tag{5-1}$$

where $R_{\perp s}$ and $R_{\perp w}$ are respectively the absolute reflectance for horizontally polarized radiant flux reflected at the same angle Θ from the surface of the aqueous solution and from the distilled water. The absolute reflectance for the aqueous solution is therefore

$$R_{\perp s} = \overline{R}_h \, R_{\perp w} \quad . \tag{5-2}$$

The Fresnel equation describing the absolute specular reflectance for radiant flux polarized (horizontally) perpendicular to the plane of incidence as applied to distilled water gives

$$R_{\perp w} = \frac{(Q_w - \cos\Theta)^2 + P_w^2}{(Q_w + \cos\Theta)^2 + P_w^2} \quad , \tag{5-3}$$

where Θ is the angle of incidence, Q_w and P_w are given by

$$Q_w = \sqrt{\frac{(n^2-k^2-\sin^2\Theta) + \sqrt{(n^2-k^2-\sin^2\Theta)^2+4n^2k^2}}{2}} \tag{5-4}$$

and

$$P_w = nk/Q_w \quad , \tag{5-5}$$

where n and k are the optical constants of the distilled water and are respectively the index of refraction and the extinction coefficient. These equations were programmed on an IBM 360/50 computer and the absolute reflectances of the aqueous solutions were computed according to equation (5-2) and were then plotted as shown in Figures 5-7.

VI. KRAMERS-KRONIG RELATIONS*

In this section we present an outline of the Kramers-Kronig analysis which was developed for computing the optical constants of aqueous solutions from the absolute reflectance spectrum. The Kramers-Kronig analysis has been used by many different investigators[12-15] to compute the optical constants of different materials from the characteristic, normal incidence, absolute reflectance spectra of the materials. We have developed what we believe to be the first application of a Kramers-Kronig analysis for computing the optical constants of a material from the absolute reflectance spectrum measured at oblique angles of incidence.

To develop the Kramer-Kronig analysis for absolute reflectance data measured at normal incidence, one must consider the normal incidence complex reflectivity P,

$$P = re^{i\phi} = \frac{n-ik-1}{n-ik+1} \quad , \qquad (6\text{-}1)$$

where $r = \sqrt{R_o}$, the square root of the reflectance R_o as measured at normal incidence; ϕ is the phase change of the incident wave due to reflection from the surface of the sample; k is the extinction coefficient of the sample; and $i = \sqrt{-1}$. Solving equation (6-1) for n and k gives

---

*A computer code for the Kramers-Kronig analysis outlined here was developed at the University of Missouri-Kansas City by M. R. Querry with joint support from contract 14-08-0001-12636 with the U.S. Geological Survey and grant A-030-Mo with the Missouri Water Resources Research Center.

$$n = \frac{1-r^2}{1+r^2-2r\cos\phi} \quad , \quad \text{and} \tag{6-2}$$

$$k = \frac{-2r\sin\phi}{1+r^2-2r\cos\phi} \tag{6-3}$$

Taking the natural logarithm of the first two terms in equation (6-1) and multiplying both sides of the equation by $1/(w-w_o)$, where w is the frequency of the electromagnetic radiant flux, and then applying complex integration techniques,[16] it can be shown that

$$\phi(\lambda o) = \text{Prin.} \left[-\frac{2\lambda o}{\pi} \int_0^\infty \frac{\ell n(r)}{\lambda^2-\lambda_o^2} d\lambda \right] \quad , \tag{6-5}$$

where Prin. denotes the Cauchy principal value of the integral. The integral in equation (6-5) is to be evaluated over the entire reflectance spectrum. The integral can be evaluated numerically on a high speed digital computer. In our development of the Kramers-Kronig codes for the computer, we used the optical constants of distilled water[2] to generate the normal incidence reflectance spectrum of distilled water in the wavelength region 2-30μm. In the wavelength region 0-2μm we assumed the reflectance was constant and equal to the reflectance at 2μm. In the wavelength region 20-∞μm we assumed the reflectance at 30μm.

We then evaluated the integral in equation (6-5) and determined ϕ . From the values of ϕ we determined n and k from equations (6-2) and (6-3). The program returned the optical constants used to generate the reflectance spectrum except in the long wavelength regions where the assumption of constant reflectance in the wavelength region 30-$\infty\mu$m begins to seriously influence the validity of the computations.

Next we developed the code for applying the Kramers-Kronig analysis at oblique angles of incidence. The complex reflectivity at oblique angles of incidence for radiant flux polarized perpendicular to the plane of incidence is

$$P_{\perp} = r_{\perp} e^{i\phi_{\perp}} = \frac{Q - iP - \cos\Theta}{Q - iP + \cos\Theta} \quad , \tag{6-6}$$

where the subscript $\perp$ denotes the polarization, Θ is the angle of incidence, $\phi_{\perp}$ is the phase change of the electromagnetic wave due to reflection, $r_{\perp}$ is the square root of the reflectance, and Q and P are as defined by equations (5-4) and (5-5). The index of refraction n and the extinction coefficient k are given in terms of Q, P, and Θ by the equations[4]

$$n = \sqrt{\frac{(Q^2 - P^2 + \sin^2\Theta) + \sqrt{(Q^2 - P^2 + \sin^2\Theta)^2 + 4Q^2P^2}}{2}} \tag{6-7}$$

and

$$k = QP/n \quad . \tag{6-8}$$

The Kramers-Kronig method is now similar to that at normal incidence. Solving equation (6-6) for Q and P gives

$$Q = \frac{(1-r_\perp^2)\cos\Theta}{1+r_\perp^2-2r_\perp\cos\phi} \quad \text{and} \tag{6-9}$$

$$P = \frac{-2r_\perp \sin\phi\cos\Theta}{1+r_\perp^2-2r_\perp\cos\phi} \quad . \tag{6-10}$$

the phase change is given by

$$\phi_h(\lambda o) = \text{Prin.}\left[-\frac{2\lambda o}{\pi}\int_0^\infty \frac{\ell n(r_\perp)}{\lambda^2-\lambda_o^2}d\lambda\right] \quad . \tag{6-11}$$

We used the optical constants of distilled water to generate the oblique angle of incidence reflectance spectrum of distilled water for perpendicular polarization in the wavelength region 2-30μm. In the wavelength regions 0-2μm and 30-∞μm we assumed the reflectance was constant and respectively equal to the values at 2μm and 30μm and thus programmed a high speed digital computer to evaluate the integral of equation (6-11). We computed ϕ from (6-11), then computed

P and Q from equations (6-9) and (6-10), and then computed n and k from equations (6-7) and (6-8). Again the program returned the optical properties used to generate the reflectance spectrum except in the long wavelength part of the 2-30μm region. We have modified the computer code recently to correct the invalid assumption of constant reflectance at wavelength less than 2μm and greater than 30μm. The optical constants presented in Section VII, however, were computed with the unmodified computer code.

VII. OPTICAL CONSTANTS

The optical constants of a substance are the index of refraction and the extinction coefficient, i.e. the real and imaginary parts of the complex refractive index. The optical constants of the aqueous solutions of $NH_4H_2PO_4$, K_2SO_4, and $(NH_2)_2CO$ were computed according to the Kramers-Kronig analysis outlined in Section VI. The results of the computations are shown graphically in Figures 8-11. The spectral signatures due to the sulfates are more evident in the graphs of the extinction coefficient than in the graphs of the index of refraction.

A knowledge of the optical constants of a substance enables one to compute reflectances and emittances of the substance for any desired geometrical configuration. Therefore, an application of results from project A-30-Mo would be, to use the optical constants of the solutions as the basis for a feasibility study to determine if sulfates, phosphates, or urea can be detected remotely by reflectance techniques.

VIII. CONCLUSIONS

The application of spectral reflectance to qualitatively and quantitatively measure water quality must ultimately use the spectral signatures of the solutes as the basis for the analysis. The discovery of strong spectral signatures for sulfate, phosphate, and urea in the relative reflectance spectra, as shown in Figures 5-7, form the basis for immediate laboratory analysis of samples collected in the field and then sent to the laboratory.

Water quality measurements from remote platforms must also use the spectral signatures of the solutes as the basis for the analysis. The 8-14μm wavelength region, the position of the sulfate, phosphate, and some urea spectral signatures, is in the thermal region where the performance of remote reflectance measurements that use natural infrared radiant flux would be difficult. There are several ways to overcome the difficulties. One method would be to use a wavelength tunable infrared laser[18] system as the source of radiant energy, and then measure the spectral intensity of the reflected laser beam thus obtaining the spectral signature of the solute. Based on our reflectance measurements of the concentrated solutions of sulfate, phosphate and urea, we estimate the maximum theoretical sensitivity of reflectance techniques would be detection of solutes at concentrations of one solute molecule per 10^8 water molecules. To obtain this estimate of maximum

theoretical sensitivity, we considered the laser system infrared source,[18] an integrating data acquisition system, such as those in multispectral scanner systems, and correlation techniques for analysis of the reflectance data. In actual practice the sensitivity may be to detect say only one solute molecule in 10^6 water molecules rather than the theoretical estimate. The values of the optical constants, that were computed from our reflectance data, would be the basis for calculations during a feasibility study and the design of actual remote sensing experiment.

We are grateful for the opportunity to serve the Missouri Water Resources Research Center. We invite your comments and discussion of the results from the research program.

REFERENCES

1. "Optical Properties of Water in the Infrared," A. N. Rusk, D. Williams, M. R. Querry, Bull. Am. Phys. Soc. 16, 501 (1971).

2. "Infrared Reflectance of Aqueous Solutions of Sulfates and a Phosphate," M. R. Querry, W. E. Holland, R. C. Waring, Bull. Am. Phys. Soc. 16, 502 (1971).

3. "The Reflectance of Aqueous Solutions," M. R. Querry, R. C. Waring, W. E. Holland, and G. R. Mansell, Proceedings 7th International Symposium on Remote Sensing of Environment, University of Michigan (Ann Arbor, May 1971).

4. "Optical Constants of Water in the Infrared," A. N. Rusk, D. Williams, and M. R. Querry, J. Opt. Soc. Am. 61, 895 (1971).

5. "The Infrared Reflectance of Liquid Water," M. R. Querry, Ph.D. Dissertation, Kansas State University (1968).

6. "Refractive Index of Water in the Infrared," M. R. Querry, B. Curnutte, and D. Williams, J. Opt. Soc. Am. 59, 1299 (1969).

7. "Optical Constants of Water in the Infrared," A. Rusk, D. Williams, and M. R. Querry, J. Opt. Soc. Am. 61, 895 (1971).

8. "Determination Des Constantes Optiques De L'eau Liquide," L. Pontier and C. Dechambenoy, Ann. Geophys. 22, 633 (1966).

9. "Mesure Du Pouvior Réflecteur Monochromatique De L'eau sous Incidence Normale Entre 1 et 38 μ, L. Pontier and C. Dechambenoy, Ann. Geophys. 21, 462 (1965).

10. "Dispersion and Absorption of Liquid Water in the Infrared and Radio Regions of the Spectrum," V. M. Zolatarev, B. A. Mikhailov, L. I. Aperovich, and S. I, Popov, Opt. Spektrosk. 27, 790 (1969). [Opt. Spectrosc. 27, 430 (1969)].

11. Electromagnetic Theory, J. A. Stratton. McGraw-Hill, New York (1941), pp. 505-506.

12. "Optical Properties of Lithium Fluoride in the Infrared," M. Gottlieb, J. Opt. Soc. Am. 50, 343 (1960).

13. "Optical Constants of Germanium in the Region 1 to 10 eν," H. R. Phillip and E. A. Taft, Phys. Rev. 113, 1002 (1959).

14. "Improved Infrared Optical Index Values for M_gO," J. Opt. Soc. Am. 60, 53 (1970).

15. "Optical Properties of Molybdenum and Ruthenium," K. A. Kress and G. J. Lapeyre, J. Opt. Soc. Am. 60, 1681 (1970).

16. Optical Physics, S. G. Lipson and H. Lipson, Cambridge U.P., London (1969), pp. 431-434.

17. Handbook of Chemistry and Physics, 48th Ed., R. C. Weast ed., The Chemical Rubber Co., Cleveland, Ohio (1967), pp. F159-F177.

FIGURE CAPTIONS

Figure 1.--The coefficients as measured for a transmission polarizer composed of four silver chloride plates for the wavelength region 2-25μm. ℓb is the polarizer leakage and τ is the fraction of the desired polarization component transmitted by the polarizer.

Figure 2.--Reflectometer Spectrophotometer System. The components are a glower G, Chopper C, Cassegrain Collimator unit M_1 and M_2, plane mirrors M_3 and M_4, sample S, Cassegrain condenser unit M_5 and M_6, polarizer P, and Perkin-Elmer E-system spectrophotometer. The angle of incidence is shown as Θ.

Figure 3.--The Reflectometer. The components are a source assembly A which consists of an infrared glower and a chopper, a collimating Cassegrain unit B which collects and collimates radiant energy from the glower, polarizers C, and a helium-neon laser D which is used to align the optical system. Other components are as shown in Figure 2. The reflectometer as shown in this photograph is set up to measure the intensity of the radiant energy incident on the sample.

Figure 4.--The geometry of our reflectometer system. A, B, C, D, and E are plane mirrors for directing a nearly collimated beam of radiant flux to the sample through the polarizer, and then to a Cassegrain unit which focuses the beam on to the entrance slit of a monochromator.

Figure 5.--The measured relative reflectance and the computed absolute reflectance in the 2-12μm wavelength region for a 0.5 molar aqueous solution of K_2SO_4. The relative reflectance was measured for horizontally polarized radiant flux incident at 70.03° ± 0.23°. Distilled water was the standard mirror. The uncertainty in the measurements was about one per cent. The strong spectral signature of the SO_4^{-2} ion is most easily seen in the relative reflectance spectrum.

Figure 6.--The measured relative reflectance and the computed absolute reflectance in the 2-12μm wavelength region for a 0.5 molar aqueous solution of $NH_4H_2PO_4$. The relative reflectance was measured for horizontally polarized radiant flux incident at 70.03° ± 0.23°. Distilled water was the standard mirror. The uncertainty in the measurements was about one per cent. The strong spectral signature of the phosphate is most easily seen in the relative reflectance spectrum.

Figure 7.--The measured relative reflectance and the computed absolute reflectance in the 2-20μm wavelength region for 1.0 molar aqueous solution of $(NH_2)_2CO$. The relative reflectance was measured for horizontally polarized radiant flux incident at 70.03° ± 0.23°. Distilled water was the standard mirror. The uncertainty in the measurements was about one per cent. The strong spectral signature of the solute is most easily seen in the relative reflectance spectrum.

Figure 8.--The optical constants in the 2.5-12μm wavelength region for a 0.5 molar aqueous solution of K_2SO_4 as computed from a Kramers-Kronig analysis of the absolute reflectance spectrum for the oblique angle of incidence 70.03° ± 0.23°. The Kramers-Kronig analysis was applied by using assumptions that limit the accuracy of its application (see text), and the optical constants should therefore be considered tentative values that are subject to further investigation.

Figure 9.--The optical constants in the wavelength region 2.5-12μm for a 0.5 molar aqueous solution of $NH_4H_2PO_4$ as computed from a Kramers-Kronig analysis of the absolute reflectance spectrum for the oblique angle of incidence 70.03° ± 0.23°. The Kramers-Kronig analysis was applied by using assumptions that limit the accuracy of its application (see text), and the optical constants should therefore be considered tentative values that are subject to further investigation.

Figure 10.--The optical constants of a 1 molar aqueous solution of $(NH_2)_2CO$ as computed from a Kramers-Kronig analysis of the absolute reflectance spectrum for the oblique angle of incidence 70.03° ± 0.23°. The Kramers-Kronig analysis was applied by using assumptions that limit the accuracy of its application (see text), and the optical constants should therefore be considered tentative values that are subject to further investigation.

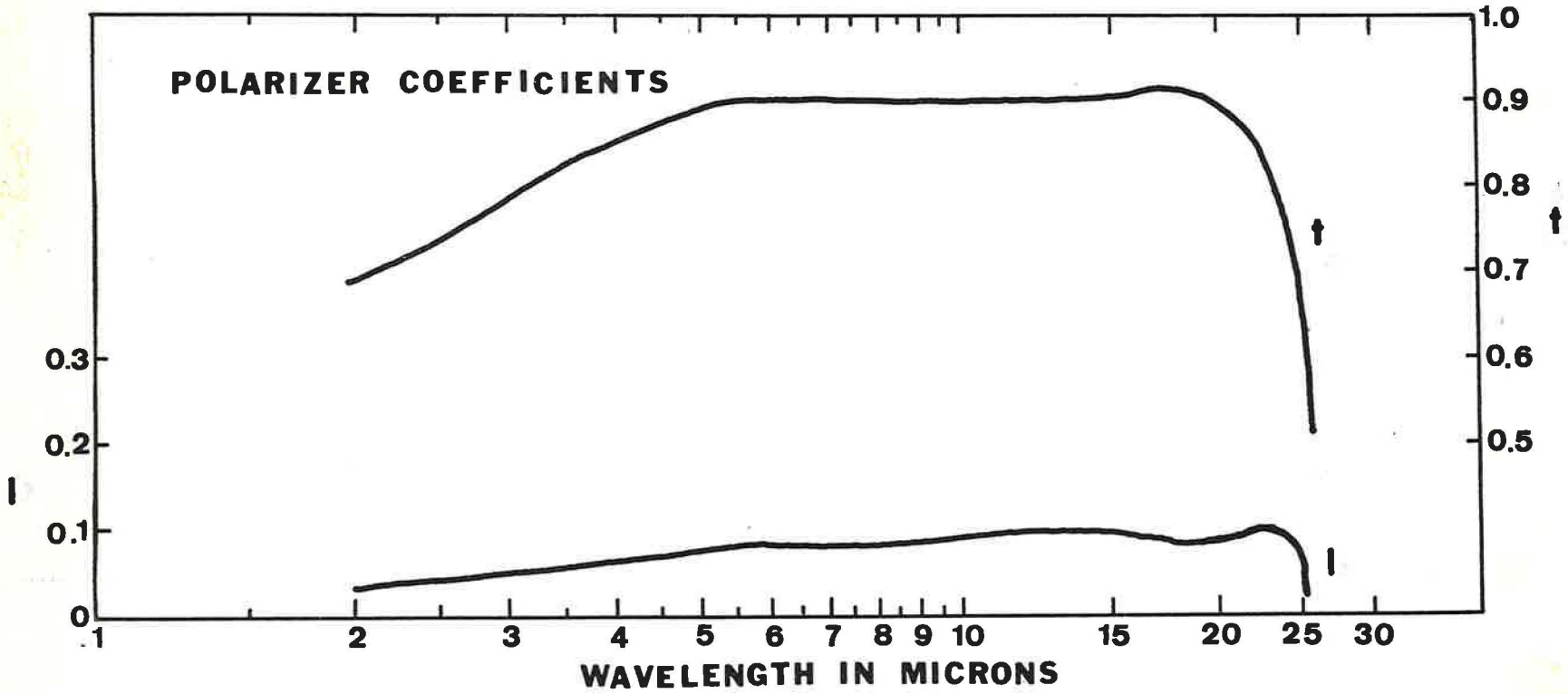
POLARIZER COEFFICIENTS
1.0
0.9
0.8
0.7
0.6
0.5
t
0.3
0.2
0.1
0
I
.1
2
3
4
5
6
7
8
9
10
15
20
25
30
WAVELENGTH IN MICRONS

Figure 1

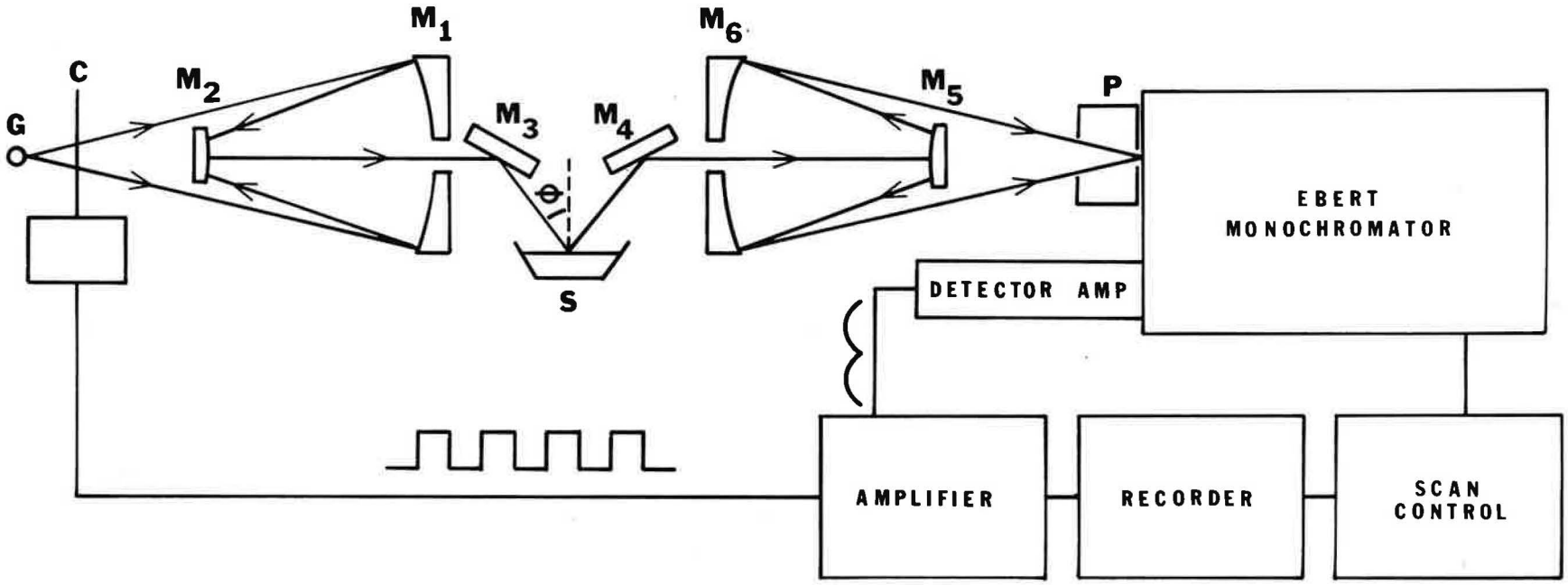
G
C
M1
M2
M3
M4
M5
M6
P
S
EBERT
MONOCHROMATOR
DETECTOR AMP
AMPLIFIER
RECORDER
SCAN
CONTROL

Figure 2

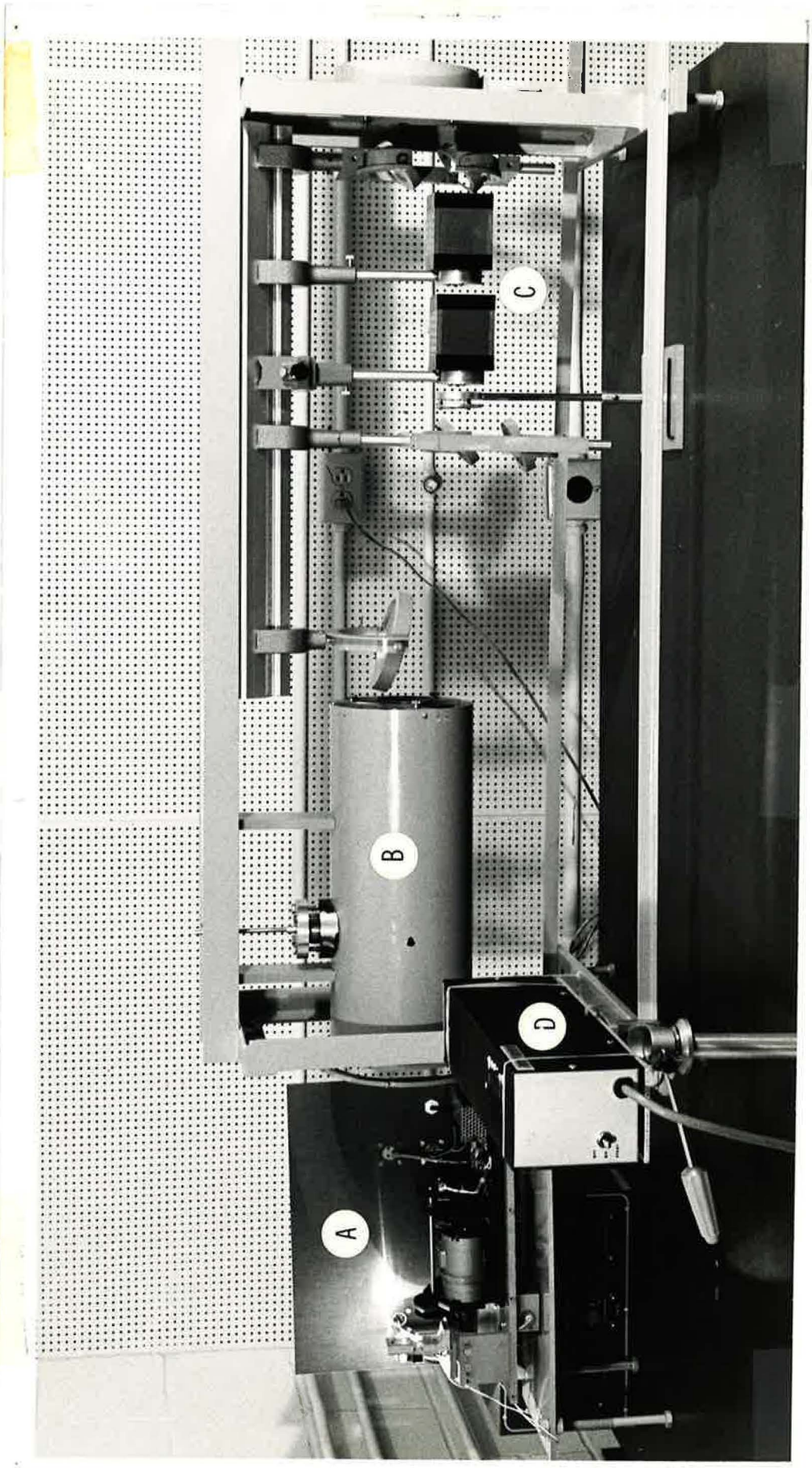

Figure 3

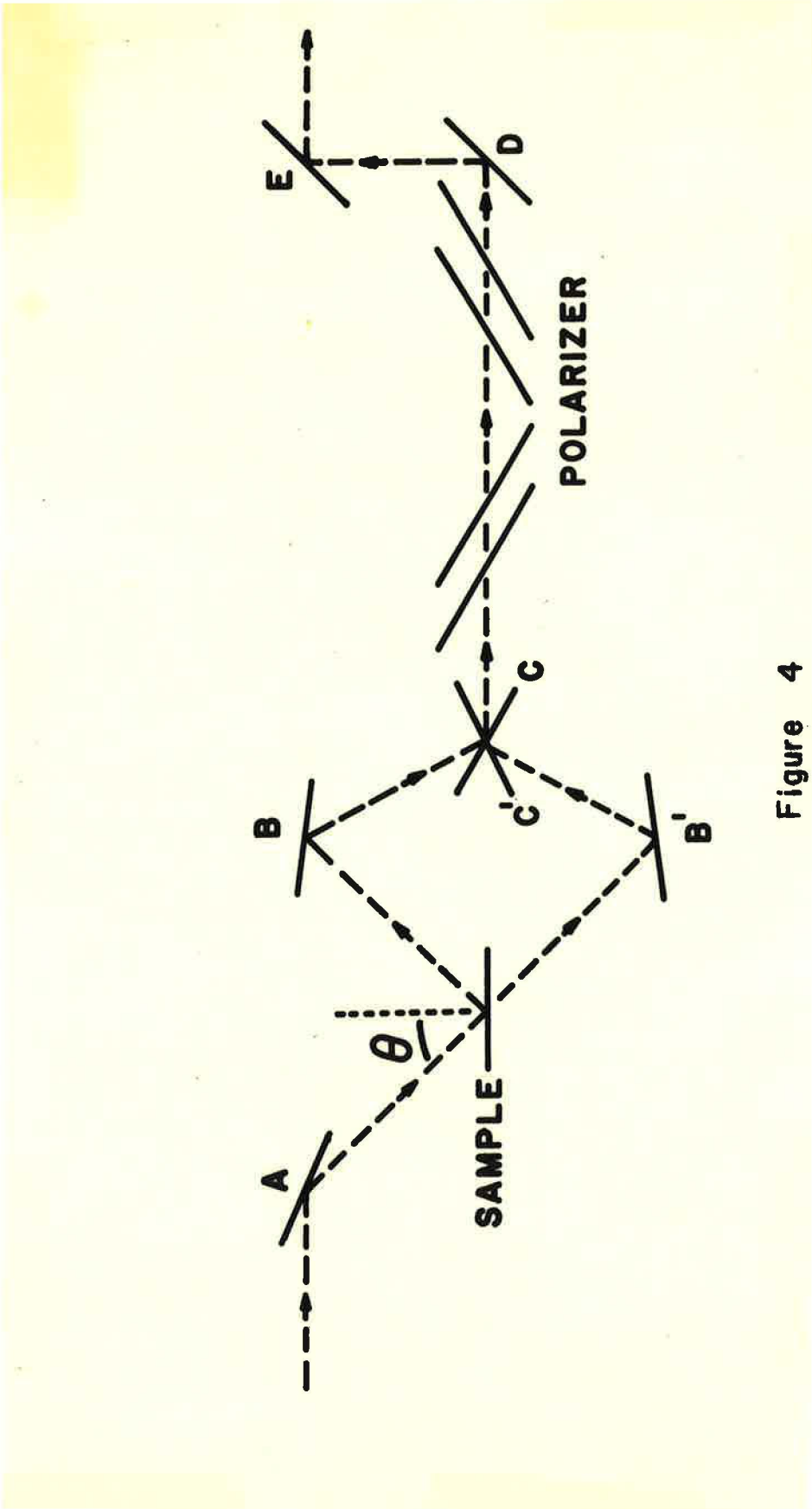

Figure 4

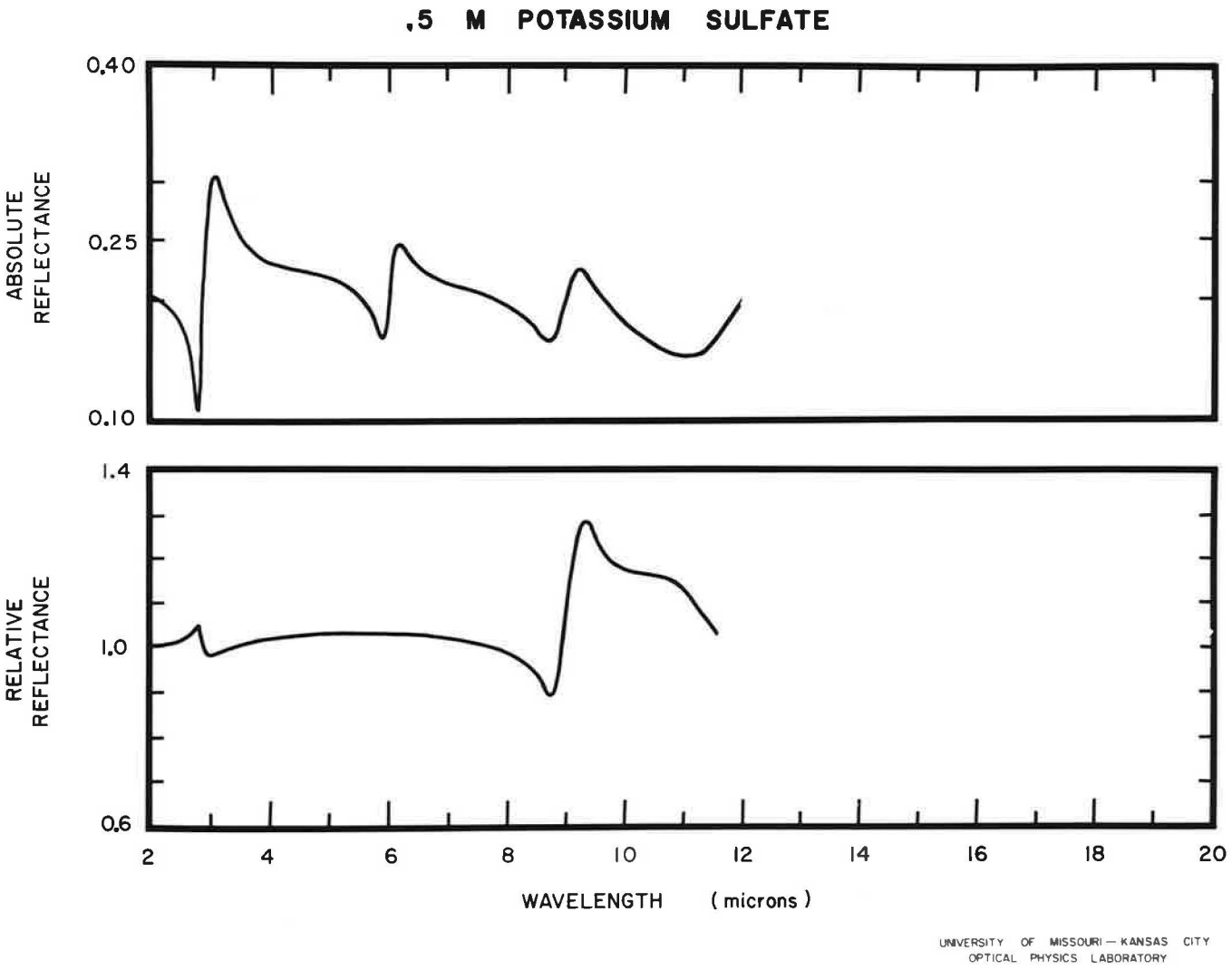
.5 M POTASSIUM SULFATE
ABSOLUTE REFLECTANCE
0.40
0.25
0.10
RELATIVE REFLECTANCE
1.4
1.0
0.6
2
4
6
8
10
12
14
16
18
20
WAVELENGTH (microns)
UNIVERSITY OF MISSOURI — KANSAS CITY
OPTICAL PHYSICS LABORATORY

Figure 5

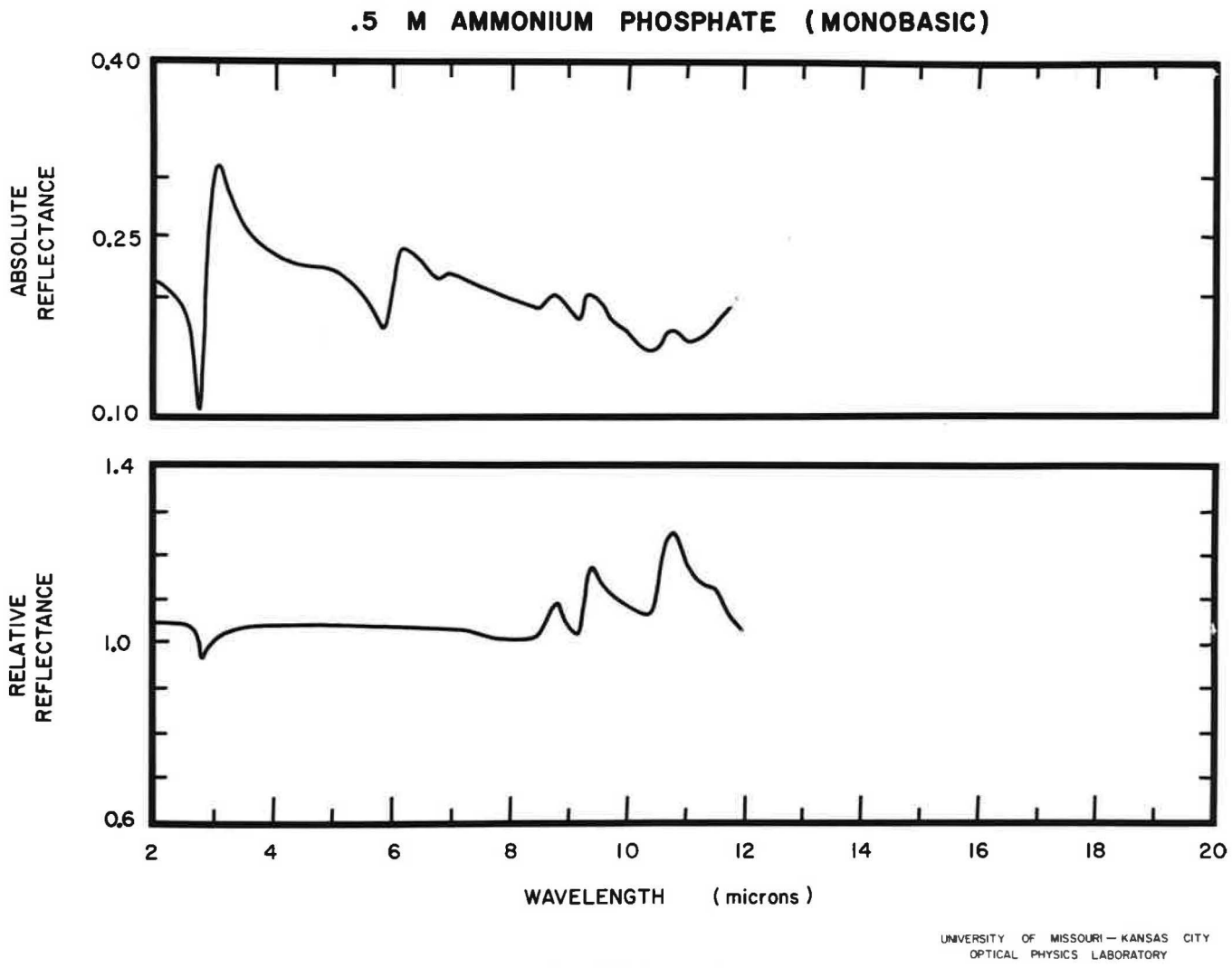
.5 M AMMONIUM PHOSPHATE (MONOBASIC)
ABSOLUTE REFLECTANCE
0.40
0.25
0.10
RELATIVE REFLECTANCE
1.4
1.0
0.6
2
4
6
8
10
12
14
16
18
20
WAVELENGTH (microns)
UNIVERSITY OF MISSOURI — KANSAS CITY
OPTICAL PHYSICS LABORATORY

Figure 6

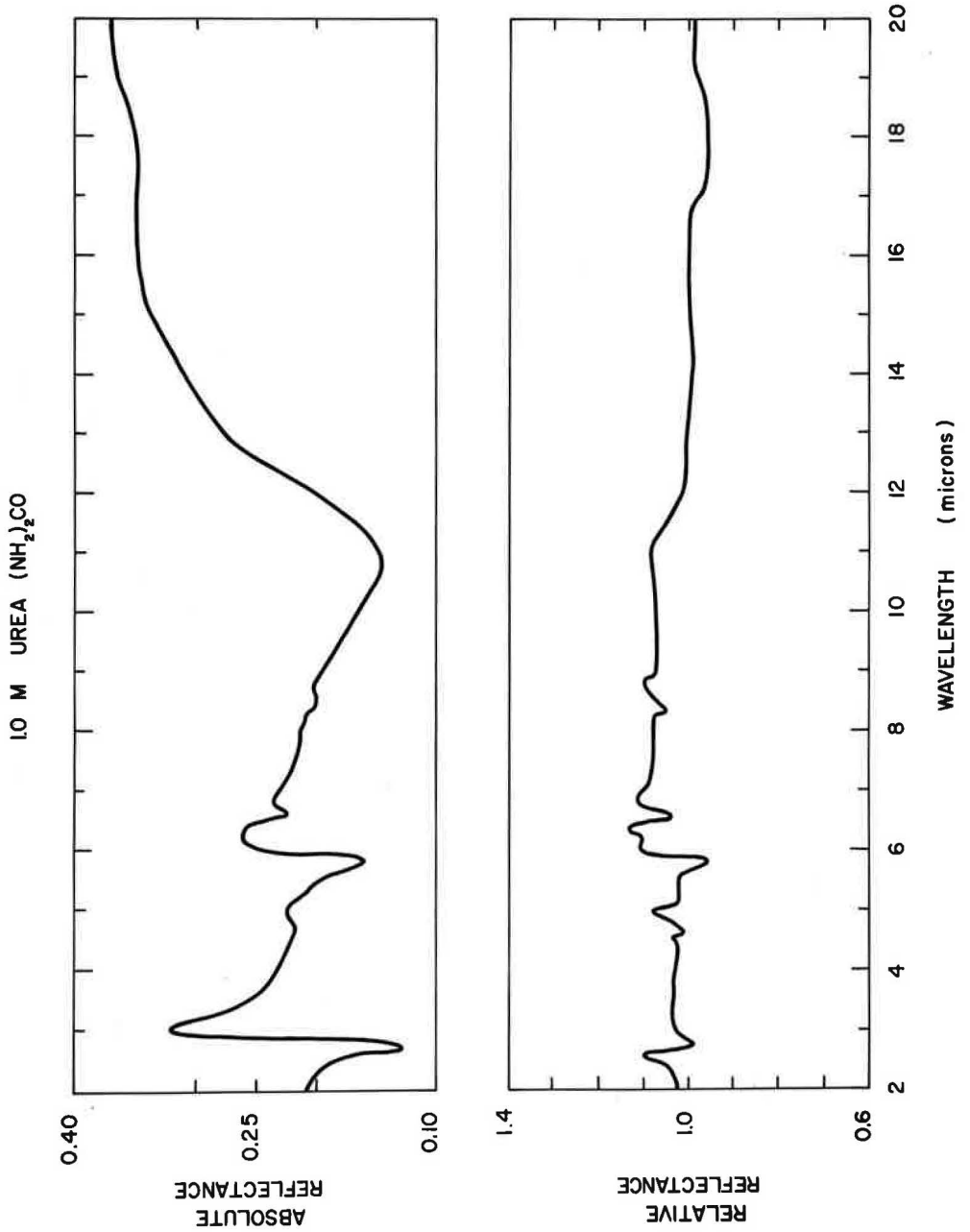
1.0 M UREA $(NH_2)_2CO$
ABSOLUTE REFLECTANCE
0.40
0.25
0.10
RELATIVE REFLECTANCE
1.4
1.0
0.6
2
4
6
8
10
12
14
16
18
20
WAVELENGTH (microns)

Figure 7

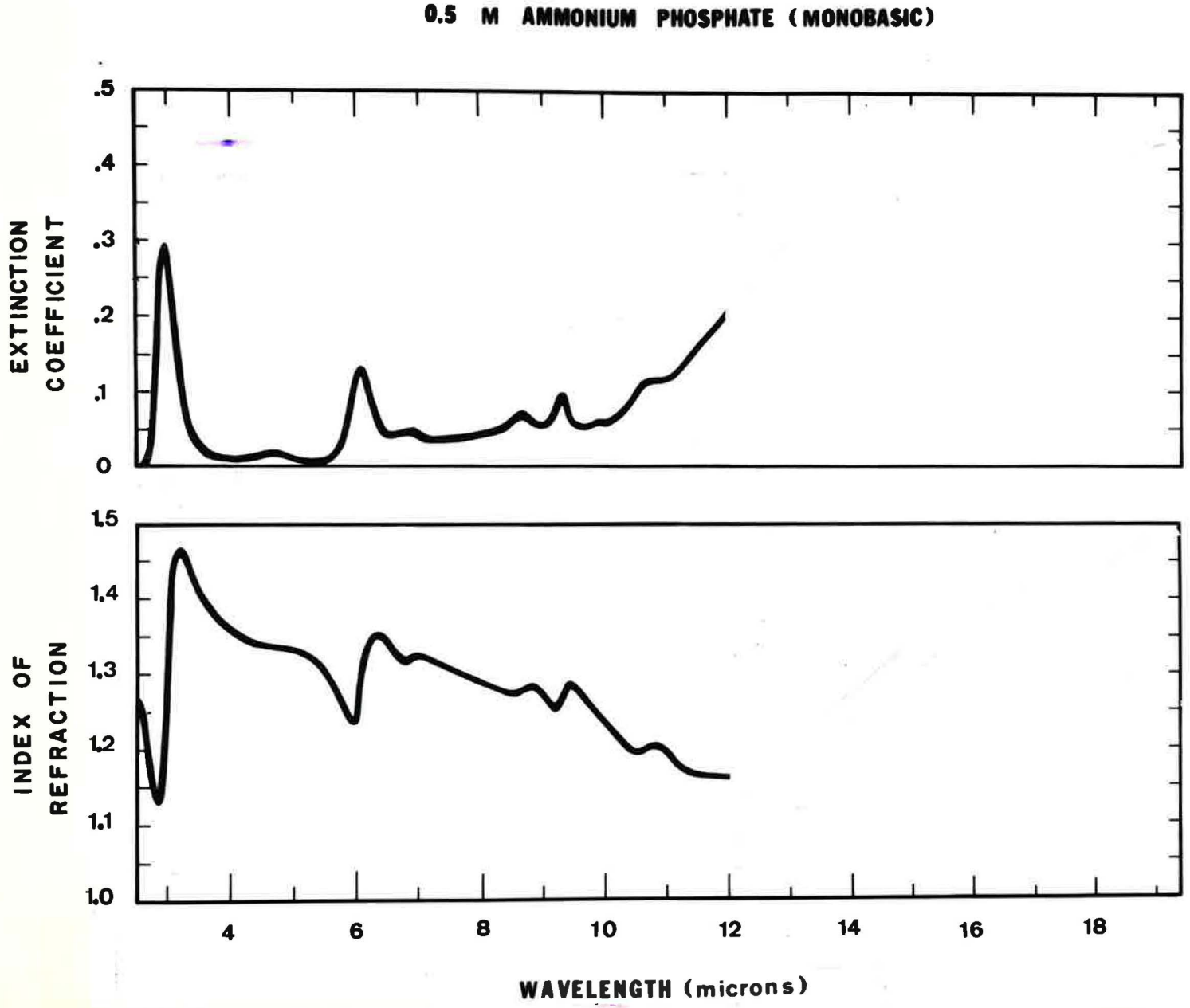
0.5 M AMMONIUM PHOSPHATE (MONOBASIC)
EXTINCTION COEFFICIENT
.5
.4
.3
.2
.1
0
INDEX OF REFRACTION
1.5
1.4
1.3
1.2
1.1
1.0
4
6
8
10
12
14
16
18
WAVELENGTH (microns)

Figure 8

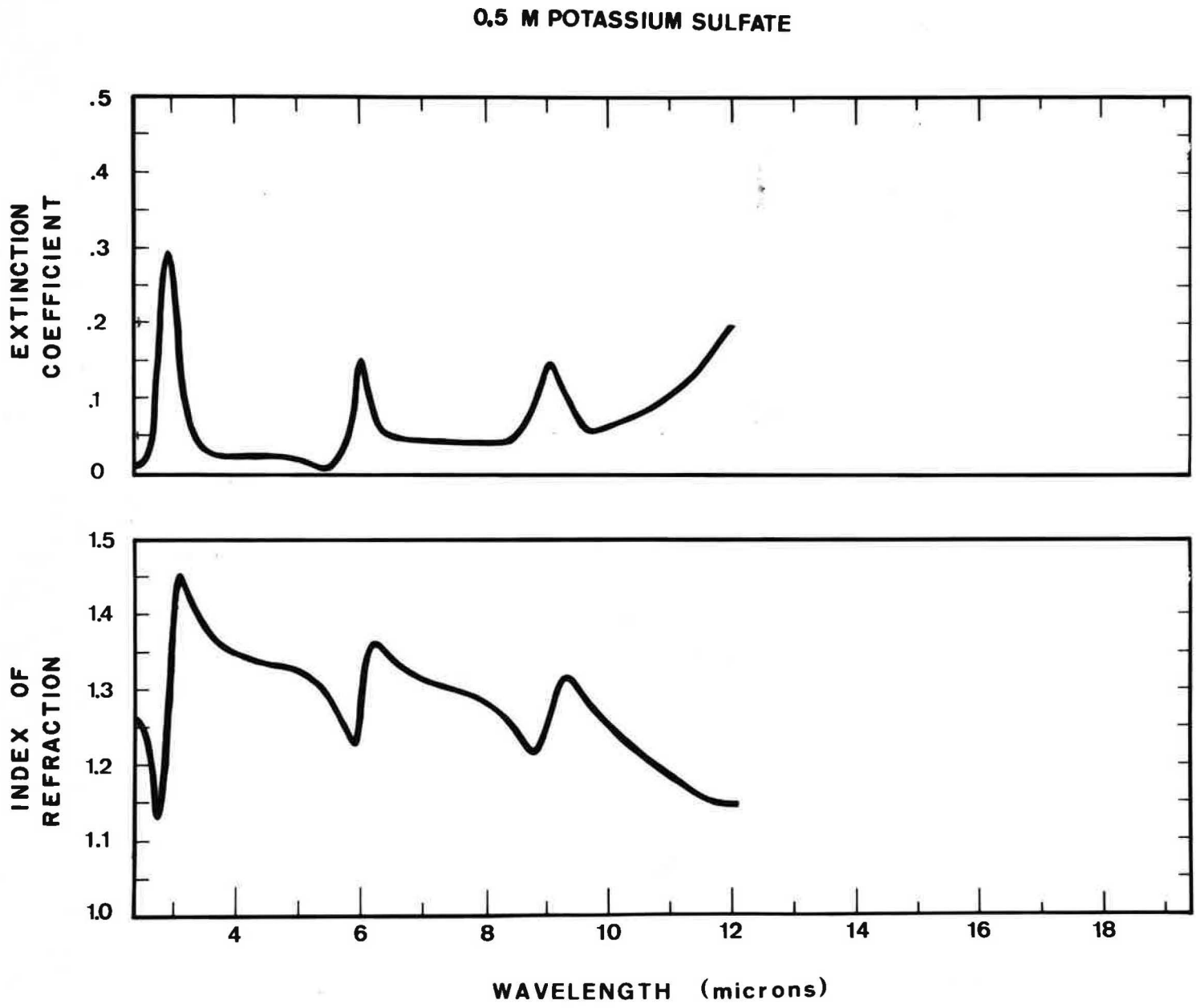
0.5 M POTASSIUM SULFATE
EXTINCTION COEFFICIENT
.5
.4
.3
.2
.1
0
INDEX OF REFRACTION
1.5
1.4
1.3
1.2
1.1
1.0
4
6
8
10
12
14
16
18
WAVELENGTH (microns)

Figure 9

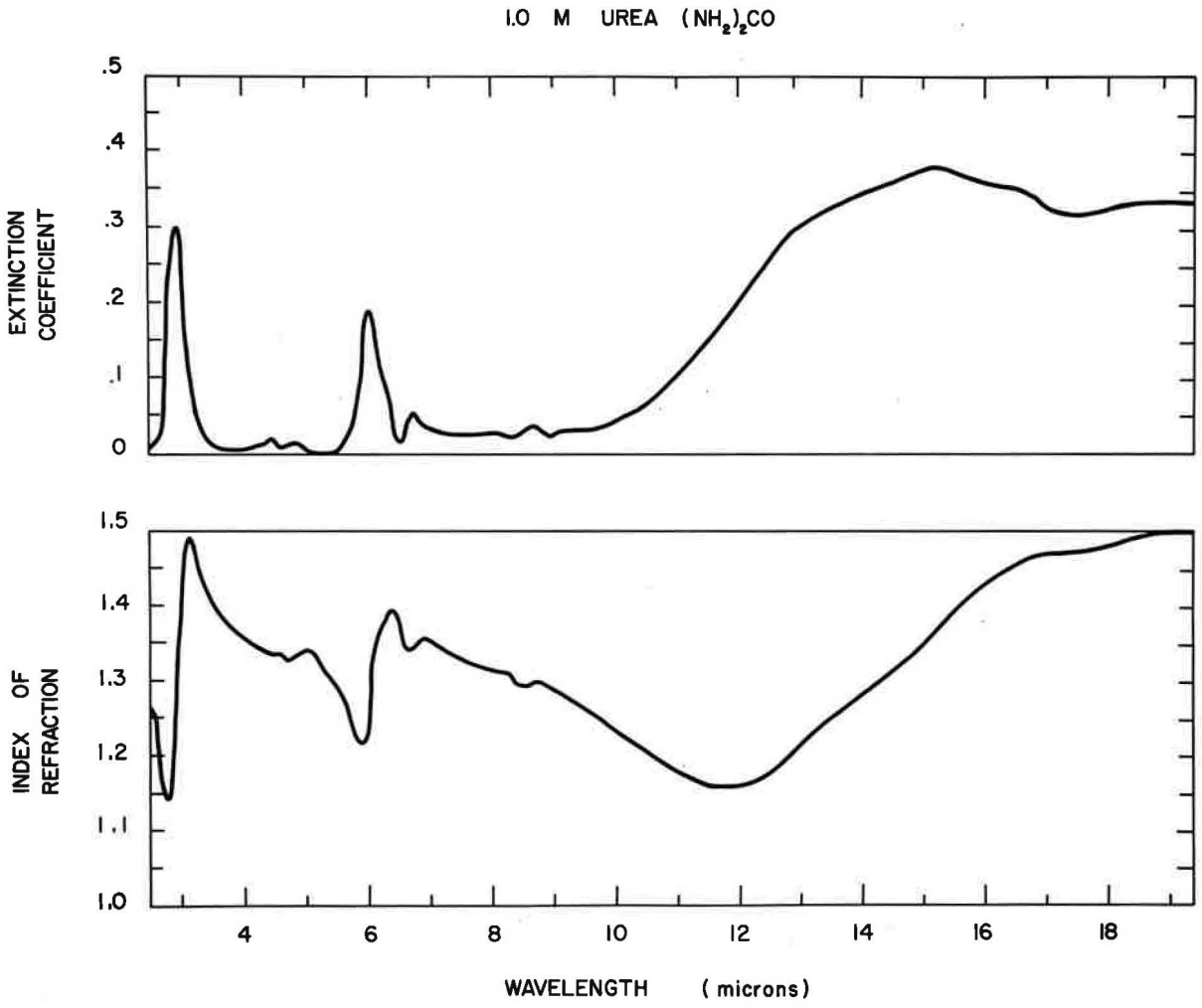
1.0 M UREA $(NH_2)_2CO$
EXTINCTION COEFFICIENT
.5
.4
.3
.2
.1
0
INDEX OF REFRACTION
1.5
1.4
1.3
1.2
1.1
1.0
4
6
8
10
12
14
16
18
WAVELENGTH (microns)

Figure 10[6]

Table 1.--Spectral Slit Width of Monochromator During Measurements of Relative Reflectance. λ and ν Respectively are the Wavelength and Wavenumber. $\Delta\lambda$ and $\Delta\nu$ respectively are the Spectral Slit Width in Units of nm and cm^{-1}

$\lambda(\mu m)$	$\Delta\lambda$(nm)	$\nu(cm^{-1})$	$\Delta\nu(cm^{-1})$
2.5	10.6	4000	17.0
3.5	23.5	2857	19.2
4.5	54.0	2222	26.7
5.5	52.0	1818	17.2
7.5	46.0	1333	8.2
8.5	42.0	1176	5.8
9.5	38.0	1052	4.2
10.5	135.0	952	12.2
12.5	133.	800	8.5
15.0	126.	667	5.6
17.5	119.	571	3.9
20.0	110.	500	2.8

APPENDIX I

The following pages are a preprint of a paper that is to appear in the Proceedings of the Seventh International Symposium on the Remote Sensing of Environment, which was held at the University of Michigan, Ann Arbor, 17-21 May 1971, and a reprint of a paper entit ed "Optical Constants of Water in the Infrared" which was published in The Journal of the Optical Society of America.

Reprinted from JOURNAL OF THE OPTICAL SOCIETY OF AMERICA, Vol. 61, No. 7, 895–903, July 1971
Printed in U. S. A.

Optical Constants of Water in the Infrared*

ALVIN N. RUSK AND DUDLEY WILLIAMS
Kansas State University, Manhattan, Kansas 66502

AND

MARVIN R. QUERRY
University of Missouri, Kansas City, Missouri 64110

(Received 2 January 1971)

The infrared reflectance of water in the region 5000–300 cm^{-1} has been measured at near-normal incidence and at an incidence angle of 53°. On the basis of the measured values of spectral reflectance and the existing data on spectral transmittance, we have obtained values for the real and imaginary parts of the refractive index of water. The resulting values, which are presented in both graphical and tabular form, are compared with recent determinations by other investigators.

INDEX HEADINGS: Refractive index; Water; Infrared; Reflectance.

On the basis of a critical survey of the existing literature, Irvine and Pollack[1] pointed out the lack of reliable values for the real n_r and imaginary n_i parts of the refractive index of water in the infrared. A knowledge of these quantities is of great importance to an understanding of the earth's heat balance and to the effective application of Mie theory to calculations of the transmission of infrared radiant flux through fog and cloud layers in the earth's atmosphere.

In principle, the value of n_i can be determined from the relation $n_i=k\lambda/4\pi$, where k is the Lambert absorption coefficient for radiation of wavelength λ and is based on laboratory measurements of spectral transmittance $T=(1-\rho)\exp(-kx)$, where x is the thickness of the water layer and ρ is the fraction of the incident radiant flux that is reflected at the cell windows. In practice, the necessity of providing extremely thin but accurately measured absorbing layers makes the determination of n_i very difficult at the centers of strong absorption bands. Determination of n_i from transmission studies in much of the infrared is further complicated by the lack of transparent, insoluble cell windows of high optical quality.

However, in spectral regions where n_i is known from transmission measurements, the corresponding values of n_r can be determined from n_i and from measured values of spectral reflectance. At the time of the Irvine–Pollack survey,[1] no detailed experimental studies of reflectance had been reported for nearly two decades. Since that time several pertinent investigations have been made.

Pontier and Dechambenoy[2] have published a table of optical constants based on transmission measurements in the spectral range 10 000–250 cm^{-1} and measurements of the reflectance of polarized radiant flux at incidence angles of 50° and 60° in the spectral range 10 000–360 cm^{-1}. Querry, Curnutte, and Williams[3] have measured the spectral reflectance of polarized radiant flux for incidence angles of 70° and 75° in the spectral range 5000–400 cm^{-1}; these authors used their reflectance measurements to determine both n_r and n_i in spectral regions of strong absorption and their own reflectance measurements, along with the Irvine–Pollack[1] values of n_i, to obtain n_r in other spectral ranges.

Still more recently, Zolatarev *et al.*[4] have used a variety of techniques to obtain values of n_i and n_r at selected points in the spectral range between the visible and radiofrequency regions. Their experimental work included transmission measurements in the 5000–250-cm^{-1} region, attenuated total reflection measurements in the 5000–1000-cm^{-1} region, and reflection measurements at an incidence angle of 12° between 5000 and 200 cm^{-1}. They used their own results, along with those of several other investigators, to compute values of n_i and n_r by means of Kramers–Kronig methods; although their calculations involve a hypothetical ultraviolet band centered at 100 000 cm^{-1}, they assert that the choice of parameters for this "model band" does not influence the calculated values of n_r in the infrared.

Although there is now fair agreement of the optical constants n_i and n_r reported by different investigators, certain discrepancies still remain. The present work was undertaken with the purpose of resolving some of the remaining disagreements and of obtaining more detailed information in the 5000–300-cm^{-1} region. Our major purpose was to obtain reliable experimental data that would permit calculations of n_r and n_i by methods not involving the use of band models of any kind.

EXPERIMENTAL MEASUREMENTS

The reflectometers employed in the present study are shown schematically in Figs. 1 and 2. Radiant flux from Globar A is directed by mirrors B and C to the water sample or to a reference-mirror surface at D; the reflected flux is directed by mirrors E and F to the spectrometer entrance slit at G. In the reflectometer used for near-normal incidence, which is shown in Fig. 1, converging mirror C was masked in such a way that the maximum incidence angle in the cone of radiant flux reaching D was 7° and the angle of incidence for the central ray was approximately 4°; for this arrangement the Cauchy relation giving reflectance in terms of n_r and n_i can be used with confidence. In

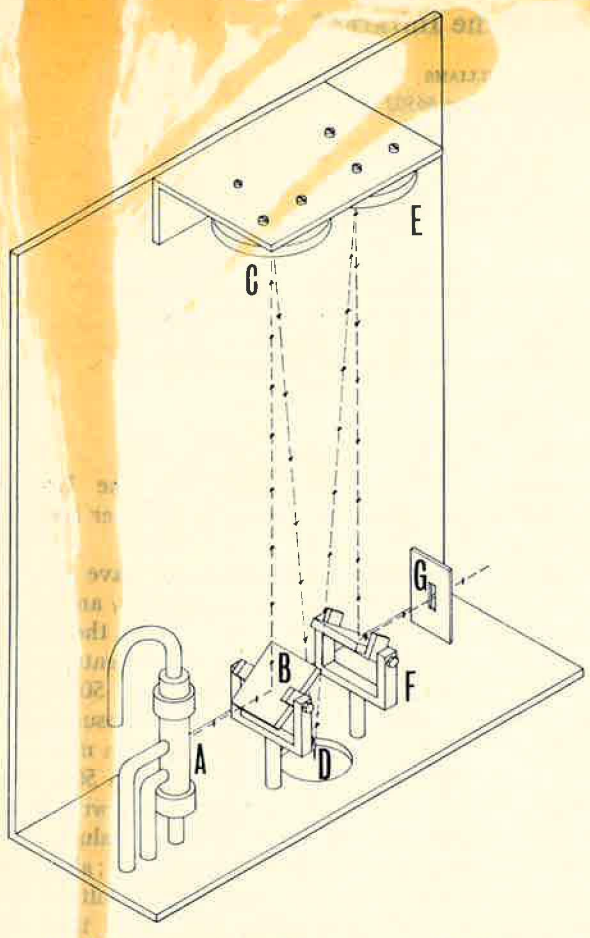

FIG. 1. Reflectometer used for near-normal incidence.

the reflectometer used for oblique incidence, which is shown in Fig. 2, converging mirror C was equipped with a slotted mask. For the slotted mask used in most of the work, all radiant flux reaching D had incidence angles in the range $53.0°\pm0.8°$; however, for the lowest-frequency region covered, we sometimes widened the slot in order to increase the radiant flux reaching the spectrometer; and with this arrangement, the incidence angles were in the range $53.0\pm1.5°$. The geometry of the oblique-incidence reflectometer permitted the insertion of a polarizer in the beam between F and G; the polarizer consisted of six AgCl plates oriented at Brewster's angle with respect to the beam direction.

In earlier studies, Pontier and Dechambenoy[2] determined water reflectance by comparing the radiant flux reflected by water with the flux reflected by a high-quality front-surface mirror, which was assumed to be a perfect reflector. Querry *et al.*[3] made absolute measurements of water reflectance by repositioning two plane mirrors in their reflectometer; although direct measurement of absolute reflectance is desirable, the difficulties of achieving exact repositioning of mirrors introduced more scatter in the resulting data than in those of Pontier and Dechambenoy. In the present study, we first obtained values of nominal reflectance R_N by comparing the reflectance of water with that of an aluminized reference mirror. Then, by means of an auxiliary reflectometer, we made absolute measurements of the mirror reflectance μ; from these two measurements, we obtained the water reflectance R from the product μR_N. For normal incidence, values of μ_0 for the reference mirror ranged from 0.950 at 5000 cm^{-1} to 0.975 in the low-frequency region; for an incidence angle of 53°, values of μ_θ were somewhat higher. For both incidence angles, the probable error in μ was approximately 1%; checks of μ were made from time to time in the course of the investigation. We used a cathetometer to match the vertical positions of water and mirror surfaces at D in Figs. 1 and 2 and employed an auxiliary laser beam to ensure that the surface of the reference mirror was horizontal.

We used a Perkin–Elmer model 112 single-beam spectrometer employing a Reeder thermocouple with a CsBr window as a detector; we used LiF, CaF_2, NaCl, and CsBr prisms in various spectral regions. The spectrometer was used in its double-pass mode with an internal radiation chopper. Because water reflectance for most of the infrared is small compared with that of the reference mirror, the voltages produced at the thermocouple by radiant flux from the water sample are much smaller than the voltages obtained with the reference mirror. In their measurements, Pontier and Dechambenoy[2] relied on amplifier linearity and made use of amplifier-gain steps in comparing amplified signals. In the present work, we used the scheme employed by Querry *et al.*[3] and Zolatarev *et al.*[4] and placed a rapidly rotating calibrated sector wheel in front of the spectrometer entrance slit when the

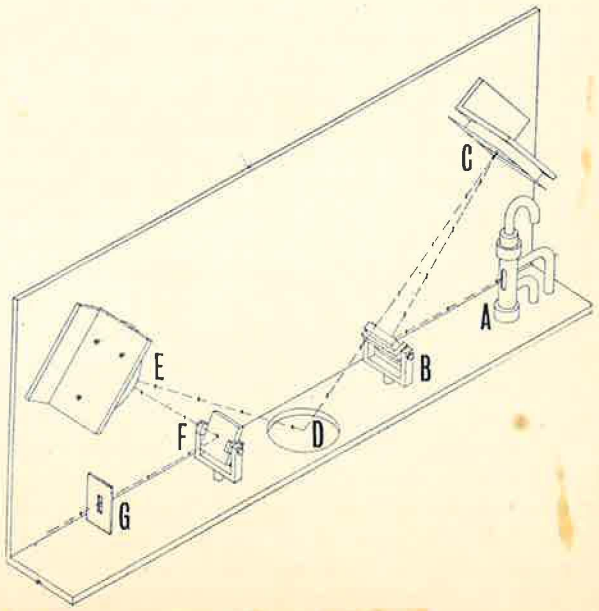

FIG. 2. Reflectometer used for an incidence angle of 53°.

reference mirror was in position, so that the flux reaching the detector from the reference mirror was not greatly different from that reaching the detector from the water surface when the sector wheel had been removed. Without change of amplifier gain controls, the two output signals were compared by noting recorder-chart deflections from a zero position recorded when a shutter interrupted the beam leaving the source. Because the rotating sector wheel was somewhat warmer than its surroundings, the shutter-zero trace with the wheel running was displaced from its normal chart position; therefore it was necessary to run one shutter-zero trace for the reference-mirror measurements and a second shutter-zero trace for water measurements. An opaque metal shutter was used in the 5000–800-cm^{-1} region and, in order to minimize the effects of possible stray radiation, a glass shutter was employed at lower frequencies.

Because Brewster's angle for water is near 53°, the radiant flux reflected by the water surface at this angle is nearly completely polarized; its electric vector $\mathbf{E}_H$ is parallel to the horizontal water surface and is also horizontal in the path through the spectrometer. Because the beam reflected by the metallic surface of the reference mirror is largely unpolarized, it might be thought that the reflectance R_H for horizontal polarization could be determined directly from the recorder tracings for water and reference-mirror reflections. However, initially unpolarized flux entering the spectrometer is partially polarized by the time it reaches the detector, chiefly as a result of preferential reflection of vertically polarized radiant flux by the prism surfaces. Therefore, it was necessary to determine the discrimination factor of the spectrometer. We did this in an auxiliary arrangement by placing a 12-plate AgCl polarizer in front of the entrance slit and comparing chart deflections obtained with V-polarized flux with those obtained with an equal flux having H polarization. Assuming negligible leakage of undesired flux through the 12-plate polarizer, we obtained the spectrometer discrimination factor α from the relation $D_V=\alpha D_H$, where D_V and D_H are chart deflections when equal quantities of V-polarized and H-polarized flux pass through the entrance slit. The measured values of α are a function of frequency and depend upon the prism used in the spectrometer; the largest values of α were obtained with the LiF prism and the lowest with the CsBr prism, as would be expected if preferential reflection at the prism faces is the dominant effect involved.

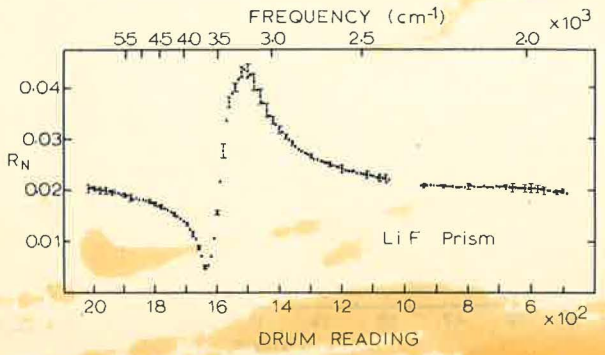

FIG. 3. Nominal spectral reflectance at near-normal incidence as determined with an LiF prism.

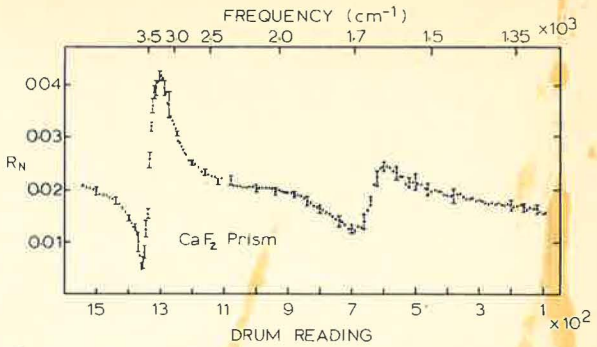

FIG. 4. Nominal spectral reflectance at near-normal incidence as determined with a CaF_2 prism.

In spectral regions for which $n_r \gg n_i$ the radiant flux reflected by water at an incidence angle of 53° has nearly complete H polarization. This condition is realized throughout most of the near infrared except in the vicinity of strong absorption bands. We made measurements of reflectance without the use of polarizers throughout the entire spectral range covered in the investigation and, in regions of large n_i, also made measurements with the 6-plate AgCl polarizer in the beam. When a polarizer is employed, the effects of leakage of undesired flux must be considered. Although Pontier and Dechambenoy[2] assumed zero leakage for their 6-plate polarizer, Querry[3] showed that leakage λ through such a polarizer can be as great as 0.1. With the 6-plate polarizer used in the present study, λ was considerably less than 0.1 for frequencies greater than 400 cm^{-1}. The discrimination characteristics of our spectrometer serve to reduce still further the effects of V-polarized flux.

The distilled deionized water samples employed were at a temperature of 25°C. Care was taken to avoid contamination of the free surfaces during the course of the reflection measurements.

REFLECTANCE MEASUREMENTS

The results of our measurements of nominal reflectance at near-normal incidence are shown in Figs. 3–6 for each prism used in the study. Each point shown in these plots represents the mean of at least four sets of independent measurements; the probable errors are given by the error bars at various points in the plots. The uncertainty is somewhat larger in spectral regions where spectral reflectance is changing rapidly and we attribute the increased uncertainty in R_N to slight failures to reproduce prism settings on successive runs.

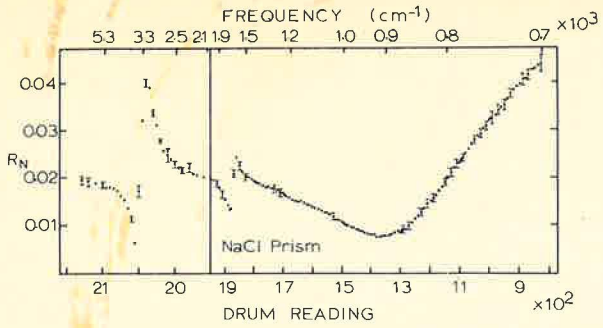

FIG. 5. Nominal spectral reflectance at near-normal incidence as determined with an NaCl prism.

The probable errors are quite small in most spectral regions but become larger in the low-frequency region in which we used the CsBr prism; these increased uncertainties are due in part to the low emissive power of the source and in part to the reduction of flux produced by the pure rotational lines of water vapor in the atmospheric path through the reflectometer and spectrometer. It was impossible to obtain reliable data in the vicinity of the strong ν_3 band of atmospheric carbon dioxide; however, inspection of Fig. 3 indicates that reliable values of R_N can be obtained in this region by interpolation.

Nominal-reflectance measurements of water for an incidence angle $\theta=53°$ are summarized in the plots of Figs. 7–10; the general features of these curves are similar to those noted in Figs. 3–6. We maintained the same schedule of slit widths for corresponding nominal reflectance spectra shown in these two sets of figures. Because of the slotted mask on mirror C, the radiant flux in the oblique-incidence measurements was smaller than that available for the normal-incidence measurements, and it was necessary to use higher amplifier-gain settings in obtaining the results shown in Figs. 7–10. However, the scatter of the data points shown in the two sets of figures is approximately the same; this result is attributable, at least in part, to the increased water reflectance for oblique incidence.

The data shown in Figs. 3–10 were obtained without the use of a polarizer in the reflectometer. Because the assumption that the reflection of V-polarized flux is negligible is of doubtful validity in spectral regions where n_r is significantly different from 1.3 and where n_i is larger, we also measured the nominal reflectance R_N' for H-polarized flux in the vicinity of absorption bands. The results were essentially similar to those shown in Figs. 7–10; however, the nominal reflectance R_N' was, of course, numerically different from the values of R_N in Figs. 7–10. Because the use of AgCl polarizing plates involves a significant loss of radiant flux, the scatter of points in plots of R_N' is somewhat greater than the corresponding scatter in Figs. 7–10.

The measured values of fractional spectral reflectance R_0 are summarized in the lower curve in Fig. 11 and represent the product of mirror reflectance μ_0 and R_N as given in Figs. 3–6. There are slight differences between the values of R_0 as determined by the CaF_2 and NaCl prisms in the vicinity of 1600 cm^{-1} and by the NaCl and CsBr prisms in the vicinity of 900 cm^{-1}. The uncertainty of spectral reflectance at normal incidence is given by the expression $\delta R_0=[(R_N\delta\mu_0)^2+(\mu_0\delta R_N)^2]^{\frac{1}{2}}$, where $\delta\mu_0$ and δR_N are the probable errors of μ_0 and R_N, respectively. Except at low frequencies, the uncertainties δR_0 were too small to plot in Fig. 11 but were tabulated for use in subsequent computations of n_r and n_i.

Our later computations involved expressions for these optical constants in terms of R_0 and $R_{\theta H}$, where $R_{\theta H}$ is the spectral reflectance for H-polarized flux at incidence angle $\theta=53°$. On the assumption that at this angle the water reflectance for V-polarized flux is negligible and that the reflectance μ_θ of the metallic reference mirror is the same for H- and V-polarized flux, we obtain

$$R_{\theta H}=\mu_\theta(1+\alpha)R_N, \tag{1}$$

where R_N is the measured nominal reflectance plotted in Figs. 7–10 and α is the discrimination factor of the spectrometer. Because μ_θ, α, and R_N were measured independently, the uncertainty $\delta R_{\theta H}$ is given by the expression

$$\delta R_{\theta H}=\{[R_N(1+\alpha)\delta\mu_\theta]^2+[\mu_\theta(1+\alpha)\delta R_N]^2+(\mu_\theta R_N\delta\alpha)^2\}^{\frac{1}{2}}, \tag{2}$$

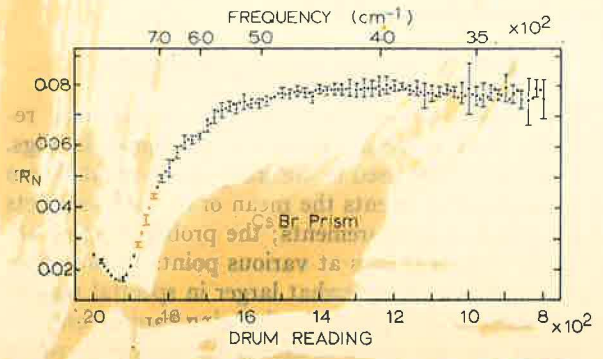

FIG. 6. Nominal spectral reflectance at near-normal incidence as determined with a CsBr prism.

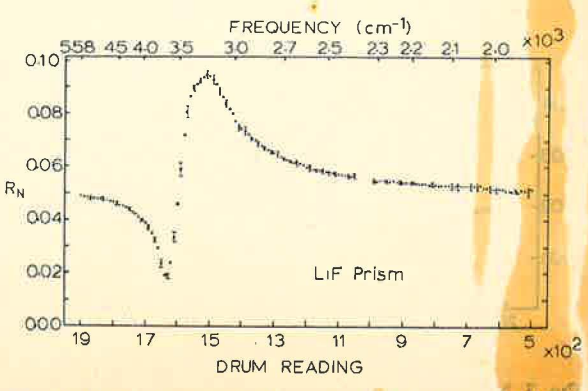

FIG. 7. Nominal spectral reflectance at an incidence angle of 53° as determined with an LiF prism.

where δR_N, $\delta\mu_\theta$, and $\delta\alpha$ are the probable errors. The results obtained for $R_{\theta H}$ are given by points in the upper curve of Fig. 11.

Also shown in Fig. 11 are points based on measurements in which the polarizer was employed. With the polarizer set to transmit H-polarized flux, we obtain

$$R_{\theta H}=\mu_\theta(1+\lambda\alpha)R_N'-R_{\theta V}\lambda\alpha, \quad (3)$$

where R_N' is the nominal water reflectance as determined with the polarizer in the beam, λ is the leakage factor of the polarizer, and $R_{\theta V}$ is the water reflectance for V-polarized flux. On the assumption that $\lambda<0.1$, the last term in Eq. (3) can be safely neglected because $\alpha<0.5$ for all prisms and independent tests with the polarizer set to pass V-polarized flux showed that $R_{\theta V}$ was too small for measurement. In computing the values of $R_{\theta H}$ plotted in Fig. 11, we also assumed that the product $\lambda\alpha$ was small compared with unity and used the expression $R_{\theta H}=\mu_\theta R_N'$.

The proper computation of the uncertainty $\delta R_{\theta H}$ should include consideration of the uncertainties of all quantities in Eq. (3). However, since the uncertainty $\delta\lambda$ is difficult to establish, because the measured uncertainty $\delta\alpha$ involves the assumption that $\lambda=0$ for a 12-plate polarizer, and since $R_{\theta V}$ is itself too small for accurate measurement, we used the expression

$$\delta R_{\theta H}=[(R_N'\delta\mu_\theta)^2+(\mu_\theta\delta R_N')^2]^{\frac{1}{2}}. \quad (4)$$

Although this expression probably underestimates $\delta R_{\theta H}$, the computed values of this quantity are in general larger than those given by Eq. (2) and become very large at low frequencies.

As indicated in Fig. 11 the values of $R_{\theta H}$ determined from R_N and R_N' agree to within $\pm 5\%$ of their mean values in all spectral regions except for frequencies below 700 cm^{-1}. Because the spectral transmittance of AgCl decreases for the lowest frequencies studied, the uncertainties of the plotted $R_{\theta H}$ values in this region are large. Since the refractive index of AgCl decreases rapidly with decreasing frequency in this spectral region and the AgCl plates are no longer oriented at Brewster's angle, our neglect of the term $\lambda\alpha$ in Eq. (3) is open to question in the low-frequency region.

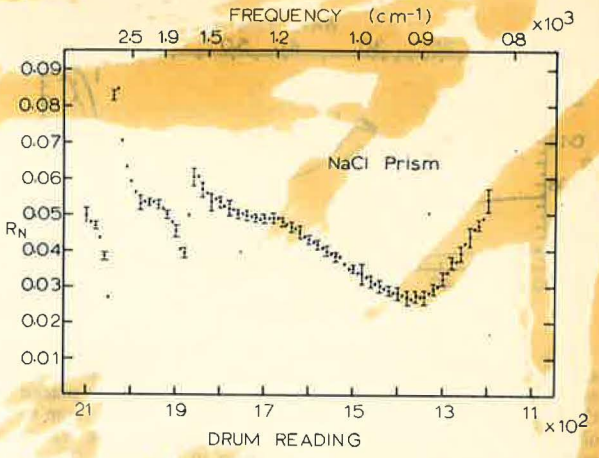

FIG. 9. Nominal spectral reflectance at an incidence angle of 53° as determined with an NaCl prism.

COMPUTATION OF OPTICAL CONSTANTS

Because reflection measurements can, in general, provide accurate values of n_r but can give reliable values of n_i only for large values of this quantity[5]: (a) We first used our measured values of R_0 together with values of n_i based on transmission studies to obtain one set of n_r values. (b) Then we used a computer program to obtain both n_r and n_i from our measured values of R_0 and $R_{\theta H}$. (c) We next obtained a set of weighted-mean values of n_r, based on plots of this quantity as given by the earlier steps; these best values of n_r are our final tabulated values. (d) Using the final values of n_r, and our measured values of R_0, we obtained a set of n_i values. (e) Our final tabulated values of n_i are based on our computed values in regions of strong absorption and on transmittance studies in regions of weak absorption. As a consistency check of

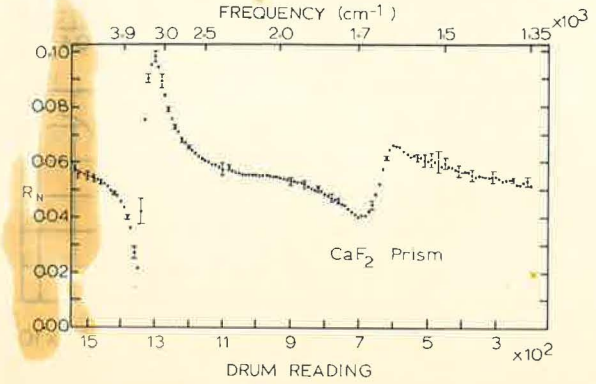

FIG. 8. Nominal spectral reflectance at an incidence angle of 53° as determined with a CaF_2 prism.

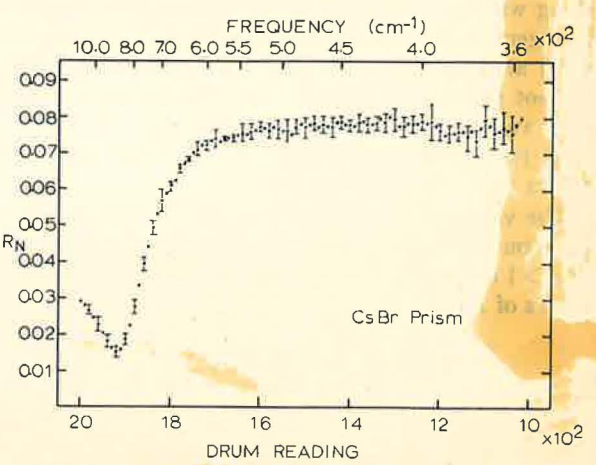

FIG. 10. Nominal spectral reflectance at an incidence angle of 53° as determined with a CsBr prism.

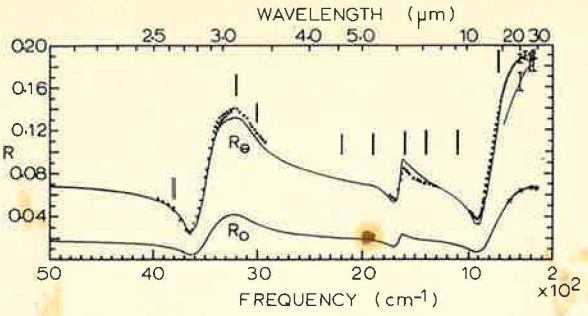

FIG. 11. The reflection spectrum of water in the infrared for R_0 and R_θ. Spectral slit widths, indicated by the vertical bars, are noted for various spectral regions. Uncertainty bars are placed on the solid curves in regions where they are sufficiently large to be observable on the plots. The points shown near the R_θ curve represent data obtained with a polarizer in the beam. The light curve for R_θ in the 300–600-cm^{-1} region represents data taken with an inefficient polarizer.

the tabulated values of n_r and n_i, we used them to compute values of R_0 and $R_{\theta H}$ for comparison with our measured values of these quantities.

In step (a) we obtained n_r from the expression

$$n_r=\frac{(1+R_0)}{(1-R_0)}+\left[\frac{4R_0}{(1-R_0)^2}-n_i^2\right]^{\frac{1}{2}} \tag{5}$$

obtained from the Cauchy relation. The values of n_i are based on the transmittance measurements of Plyler and Griff[6] in the 4000–1400-cm^{-1} range, on those of Plyler and Acquista[7] in the 1400–1000-cm^{-1} range, and on those of Draegert *et al.*[8] in the 1200–300-cm^{-1} range; at frequencies higher than 4000 cm^{-1} n_i is negligible, compared with the other quantities in Eq. (5). Plyler and his associates used CaF_2 absorption cells in the 4000–1000-cm^{-1} region and KRS-5 cells in the 1000–250-cm^{-1} region; probably as a result of the use of nonuniform layers, their results for frequencies less than 1000 cm^{-1} gave complex values of n_r when substituted along with our values of R_0 in Eq. (5). The results of Draegert *et al.* were obtained with water samples in AgCl and polyethylene cells, which like KRS-5 cells, are not entirely satisfactory for the purpose; although their values for n_i had uncertainties as large as 25%, their results were compatible with R_0 and gave real values of n_r when used in Eq. (5).

The values of n_r obtained in step (b) were based on a computer program leading to a consistent set of values of $n_r>1$ and $n_i\geq 0$ that were compatible with measured values of R_0 and $R_{\theta H}$

$$R_0=\frac{(n_r-1)^2+n_i^2}{(n_r+1)^2+n_i^2}$$

$$R_{\theta H}=\frac{(Q-\cos\theta)^2+P^2}{(Q+\cos\theta)^2+P^2}, \tag{6}$$

where $P=n_rn_i/Q$, and

$$Q=\left[\frac{n_r^2-n_i^2-\sin^2\theta+\left[(n_r^2-n_i^2-\sin^2\theta)^2+4n_r^2n_i^2\right]^{\frac{1}{2}}}{2}\right]^{\frac{1}{2}}. \tag{7}$$

In step (c) we plotted the values of n_{ra} and n_{rb} obtained in steps (a) and (b) as functions of frequency and drew a smooth curve through the plotted series. The agreement between the curves for n_{ra} and n_{rb} was nearly perfect in the 5000–3000-cm^{-1} range; in the 3300–2800-cm^{-1} region, the curves were within ±2% of their unweighted mean; agreement between the two curves was excellent in the 2800–850-cm^{-1} range. Between 850 and 650 cm^{-1}, the agreement was poorest; in this region n_{ra} and n_{rb} differed from their unweighted mean by as much as 8%, with $n_{rb}>n_{ra}$. Between 650 and 450 cm^{-1}, there was fair agreement between the n_{ra} and n_{rb} curves, but between 450 and 330 cm^{-1} the curves again diverged, so that they were separated from their unweighted mean by as much as 3%, with $n_{ra}>n_{rb}$.

Inspection of the plots of n_{ra} and n_{rb} as functions of frequency indicated that the scatter of individual n_{rb} values from the smooth curve was approximately twice as great as the corresponding scatter for n_{ra} points. Therefore, in completing step (c), we arbitrarily selected the weighted mean $(2n_{ra}+n_{rb})/3$ as the best value of n_r, where n_{ra} and n_{rb} are the values of these quantities read from the smooth curves. These best values of n_r are plotted in the lower panel of Fig. 12 and are listed in Table I.

In step (d), we substituted our best values of n_r along with the measured values of R_0 in the Cauchy equation to obtain

$$n_i=\{[(n_r+1)^2R_0-(n_r-1)^2]/(1-R_0)\}^{\frac{1}{2}}. \tag{8}$$

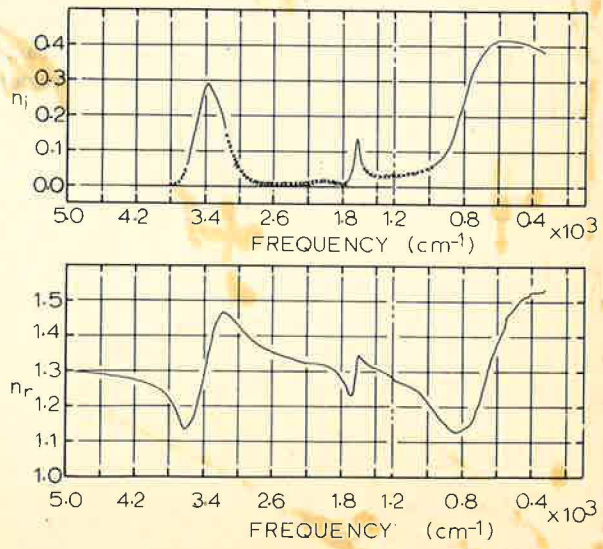

FIG. 12. The optical constants of water obtained in the present study. The crosses on the curve for n_i are based on transmission measurements. Estimates of uncertainties are given in the text.

TABLE I. Optical constants of water.

ν in cm^{-1}	n_r	n_i	λ in μm	ν in cm^{-1}	n_r	n_i	λ in μm
5000	1.300	···	2.00	2440	1.343	0.006	4.10
4920	1.299	···	2.03	2400	1.339	0.006	4.17
4840	1.297	···	2.07	2360	1.336	0.006	4.24
4760	1.296	···	2.10	2320	1.334	0.007	4.31
4680	1.294	···	2.14	2280	1.330	0.008	4.39
4600	1.292	···	2.17	2240	1.329	0.009	4.46
4520	1.290	···	2.21	2200	1.327	0.011	4.54
4440	1.286	···	2.25	2180	1.326	0.012	4.59
4360	1.283	···	2.29	2160	1.324	0.014	4.63
4280	1.280	···	2.34	2140	1.324	0.015	4.67
4200	1.275	···	2.38	2120	1.324	0.015	4.72
4160	1.273	···	2.40	2100	1.323	0.015	4.76
4120	1.271	···	2.43	2080	1.323	0.015	4.80
4080	1.267	···	2.45	2060	1.322	0.015	4.85
4040	1.264	···	2.47	2040	1.321	0.015	4.90
4000	1.260	0.003	2.50	2020	1.320	0.015	4.95
3960	1.255	0.003	2.52	2000	1.319	0.015	5.00
3920	1.249	0.003	2.55	1980	1.318	0.015	5.05
3880	1.241	0.003	2.58	1960	1.316	0.014	5.10
3840	1.232	0.004	2.60	1940	1.314	0.013	5.15
3800	1.220	0.004	2.63	1920	1.312	0.012	5.21
3780	1.215	0.004	2.65	1900	1.308	0.010	5.26
3760	1.206	0.005	2.66	1880	1.305	0.009	5.32
3740	1.200	0.005	2.67	1860	1.302	0.008	5.38
3720	1.186	0.009	2.69	1840	1.294	0.008	5.43
3700	1.174	0.015	2.70	1820	1.288	0.008	5.50
3680	1.160	0.021	2.72	1800	1.280	0.008	5.56
3660	1.146	0.032	2.73	1780	1.270	0.009	5.62
3640	1.135	0.045	2.75	1760	1.262	0.009	5.68
3620	1.136	0.067	2.76	1740	1.253	0.023	5.75
3600	1.140	0.083	2.78	1720	1.240	0.026	5.81
3580	1.145	0.104	2.79	1700	1.234	0.047	5.88
3560	1.150	0.126	2.81	1680	1.235	0.072	5.95
3540	1.159	0.148	2.82	1660	1.257	0.114	6.02
3520	1.175	0.173	2.84	1640	1.302	0.139	6.10
3500	1.190	0.199	2.86	1620	1.338	0.120	6.17
3480	1.207	0.225	2.87	1600	1.350	0.077	6.25
3460	1.227	0.247	2.89	1580	1.345	0.064	6.33
3441	1.245	0.270	2.91	1560	1.338	0.054	6.41
3420	1.274	0.281	2.92	1540	1.333	0.046	6.49
3400	1.297	0.290	2.94	1520	1.325	0.042	6.58
3380	1.320	0.291	2.96	1500	1.323	0.038	6.67
3360	1.345	0.284	2.97	1480	1.320	0.033	6.76
3340	1.367	0.278	2.99	1460	1.316	0.033	6.85
3320	1.385	0.269	3.01	1440	1.314	0.032	6.94
3300	1.405	0.258	3.03	1420	1.312	0.030	7.04
3280	1.420	0.248	3.05	1400	1.310	0.029	7.14
3260	1.436	0.234	3.07	1380	1.308	0.029	7.25
3240	1.447	0.222	3.09	1360	1.306	0.029	7.35
3220	1.457	0.209	3.11	1340	1.303	0.029	7.46
3200	1.465	0.194	3.12	1320	1.301	0.029	7.57
3180	1.468	0.162	3.14	1300	1.298	0.029	7.69
3160	1.465	0.143	3.16	1280	1.296	0.030	7.81
3140	1.464	0.124	3.18	1260	1.293	0.030	7.94
3120	1.460	0.112	3.20	1240	1.290	0.031	8.06
3100	1.455	0.098	3.23	1220	1.286	0.031	8.20
3080	1.450	0.086	3.25	1200	1.282	0.032	8.33
3060	1.445	0.075	3.27	1180	1.275	0.032	8.47
3040	1.440	0.065	3.29	1160	1.272	0.034	8.62
3020	1.432	0.054	3.31	1140	1.269	0.036	8.77
3000	1.426	0.048	3.33	1120	1.264	0.037	8.93
2960	1.415	0.035	3.38	1100	1.258	0.038	9.09
2920	1.407	0.025	3.42	1080	1.254	0.042	9.26
2880	1.397	0.017	3.47	1060	1.246	0.045	9.43
2840	1.389	0.013	3.52	1040	1.238	0.047	9.61
2800	1.383	0.009	3.57	1020	1.222	0.058	9.80
2760	1.376	0.007	3.62	1000	1.216	0.054	10.0
2720	1.370	0.006	3.67	980	1.200	0.067	10.2
2680	1.366	0.006	3.73	960	1.187	0.075	10.4
2640	1.361	0.005	3.79	940	1.175	0.079	10.6
2600	1.356	0.005	3.85	920	1.164	0.091	10.9
2560	1.353	0.005	3.91	900	1.150	0.110	11.1
2520	1.349	0.005	3.97	880	1.142	0.132	11.4
2480	1.345	0.005	4.03	860	1.134	0.160	11.6

TABLE I (*continued*)

ν in cm^{-1}	n_r	n_i	λ in μm	ν in cm^{-1}	n_r	n_i	λ in μm
840	1.130	0.193	11.9	560	1.435	0.416	17.9
820	1.132	0.228	12.2	540	1.459	0.415	18.5
800	1.137	0.261	12.5	520	1.469	0.415	19.2
780	1.142	0.295	12.8	500	1.476	0.413	20.0
760	1.150	0.324	13.2	480	1.494	0.411	20.8
740	1.168	0.343	13.5	460	1.509	0.408	21.7
720	1.190	0.364	13.9	440	1.518	0.405	22.7
700	1.225	0.378	14.3	420	1.523	0.402	23.8
680	1.260	0.392	14.7	400	1.527	0.397	25.0
660	1.300	0.398	15.1	380	1.527	0.392	26.3
640	1.330	0.407	15.6	360	1.528	0.387	27.8
620	1.348	0.402	16.1	340	1.531	0.383	29.4
600	1.353	0.415	16.7	330	1.535	0.380	30.3
580	1.393	0.416	17.2				

Computation of the uncertainty of n_i associated with uncertainties of R_0 and n_r shows that the uncertainty of n_i is inversely proportional to n_i and thus δn_i becomes unacceptably large for small values of n_i. Therefore, in our final tabulation of n_i, we used values of this quantity based on transmittance measurements in all cases for which $n_i<0.05$. We also adopted n_i values based on transmittance in the region 3200–3000 cm^{-1}, where the values of n_i given by Eq. (8) are in the range 0.05–0.15 but have uncertainties greater than the uncertainties of the values of n_i based on transmittance measurements. Our best values of n_i are plotted in the upper panel of Fig. 12 and are listed in Table I.

The determinations of n_i by reflection methods complement determinations based on transmittance studies, from which it is difficult to determine large values of n_i at the centers of strong absorption bands. However, we note that our values of n_i are in excellent agreement with those obtained by Plyler and Griff[6] in their careful studies of the 1640- and 3400-cm^{-1} absorption bands.

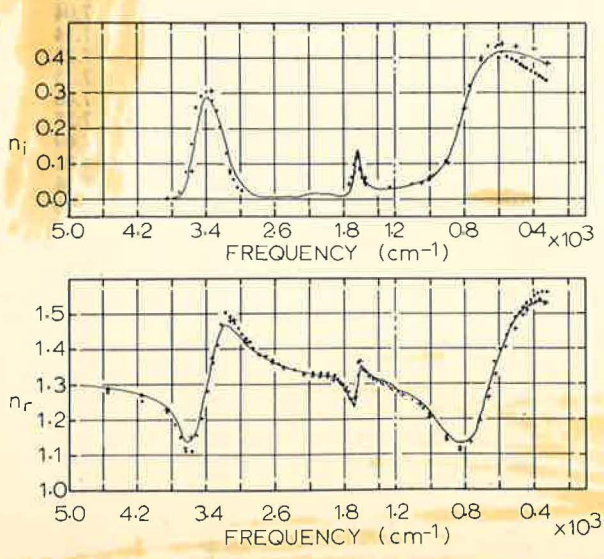

FIG. 13. Comparison of present values of n_r and n_i, given by the solid curves, are compared with the results of Pontier and Dechambenoy given by crosses and with those of Zolatarev *et al.*, given by solid circles.

We note also that our present value of the maximum value of n_i at 3400 cm^{-1} is nearly 70% greater than some of the values cited by Irvine and Pollack on the basis of their survey.[1] Values of n_i in the 1000–300-cm^{-1} region cannot be determined with precision from existing transmittance data.

When the values of the optical constants in Table I were used to calculate values of R_0 and $R_{\theta II}$, the calculated values of these quantities agreed with the measured values well within the limits of experimental error. Agreement between the observed and calculated values serves essentially as a check of the internal consistency of our measurements and computations.

DISCUSSION OF RESULTS

In estimating the uncertainties in the tabulated values of the optical constants, it is necessary to consider not only the scatter of the original reflectance measurements but also possible systematic instrumental errors of various kinds. Detailed analysis of the data leads to the following uncertainties in n_r: $\pm 1\%$ in the 5000–3700-cm^{-1} region, $\pm 2\%$ in the 3700–2900-cm^{-1} region, $\pm 1.5\%$ between 2900 and 900 cm^{-1}, and $\pm 2\%$ in the 900–330-cm^{-1} region. In the case of n_i values based on reflectance data, we estimate an uncertainty of $\pm 7\%$ in the peak value at 3400 cm^{-1}, $\pm 10\%$ in the peak value at 1640 cm^{-1}, and $\pm 5\%$ in the 600-cm^{-1} region. Because the smaller n_i values are based on measurements of published transmittance curves, the tabulated values are accurate to perhaps $\pm 10\%$.

In Fig. 13 we compare the results obtained in other recent studies with the present results, which are given by the solid curves. In the case of n_r, the values obtained by Pontier and Dechambenoy[2] are in excellent agreement with the present results over the entire range between 5000 and 900 cm^{-1}; the maximum deviations, which occur near 3134 and 910 cm^{-1}, fall well within the limits of uncertainty stated in the two investigations. Between 900 and 330 cm^{-1}, the n_r values listed by Pontier and Dechambenoy are consistently lower than the present values but there is some over-

lapping when the estimated uncertainties are considered. The n_r values of Zolatarev *et al.*[4] are consistently lower than the present values between 5000 and 3300 cm^{-1} and consistently higher than the present results between 3300 and 2500 cm^{-1}; there is good agreement between our values and the Zolatarev results between 2500 and 900 cm^{-1}. The Zolatarev values are lower than ours near 800 cm^{-1}, are in excellent agreement with ours between 700 and 450 cm^{-1}, and become progressively greater than ours for frequencies less than 450 cm^{-1}. Zoltatarev *et al.* placed special emphasis on their low extreme of 1.11 for n_r near 3500 cm^{-1} and their high extreme of 1.50 near 3170 cm^{-1}; the present study did not confirm these extreme values.

For n_i, there is good agreement between maximum values for the absorption bands at 3400 and 1640 cm^{-1}. However, there seems to be some disagreement regarding the shape of the 3400-cm^{-1} band; this band, as defined by the four values listed by Pontier and Dechambenoy, appears to be somewhat narrower than the band shown by the solid curve in Fig. 13; this band, as mapped by Zolatarev, has the same width as that noted in the present study but seems to be shifted slightly toward higher frequencies. For the band in the vicinity of 600 cm^{-1} Zolatarev *et al.* report a rather sharp peak at 665 cm^{-1} followed by rapidly decreasing values of n_i at lower frequencies. Pontier and Dechambenoy report the maximum value of n_i at the same frequency as the maximum obtained in our study and obtain a general band shape similar to that we obtained.

At the lowest frequencies, the Pontier values of n_i are in general slightly higher than ours and the Zolatarev values are considerably lower.

Although the recent studies have provided values of optical constants that are sufficiently accurate for use in Mie-theory calculations and for calculations of emissivity, further improvements of accuracy are desirable. Pending the development of improved optical attenuators or amplifier–detector systems of improved linearity, it appears unlikely that $\delta R_0/R_0$ can be made appreciably less than 0.01; however, even with this limitation, the ratio $\delta n_r/n_r$ could be reduced to values smaller than our present value of 0.01 in the high-frequency region, where n_i is less than 0.01. The value of $\delta n_r/n_r$ in other spectral regions is now limited by the value of $\delta n_i/n_i$ obtained in transmittance measurements. Dr. C. Robertson of our laboratory is using an absorption cell of novel design to obtain values of n_i that are more precise than those listed in Table I; his results can, in turn, be used with our present values of R_0 to provide more precise values of n_r.

In view of the necessity for using polarizers and in view of the influence of $\Delta\theta$, for oblique angles of incidence $\delta R_{\theta\Pi}/R_{\theta\Pi}$ is greater than $\delta R_0/R_0$. However, if improved polarizers can be developed, it is possible that more accurate values of the optical constants can be obtained from reflection measurements at some of the special angles suggested by Humphrey-Owens.[5]

We close by noting that several computer techniques have been developed for obtaining n_r and n_i from measurements of R_0 alone. Spitzer *et al.*[9,10] have successfully used the so-called dispersion analysis, which involves the assumption of band models, to obtain the optical constants of quartz. Gottlieb[11] has successfully used Kramers–Kronig relations to obtain the optical constants for LiF from R_0 measurements. Although, in the present study, we have not used these techniques, it is possible to use our R_0 values in such computations and to use our $R_{\theta\Pi}$ values to test the validity of the validity of the computed values of the optical constants.

REFERENCES

* Paper presented at the Annual Meeting of the Optical Society, Hollywood, Florida, October 1970 [J. Opt. Soc. Am. **60**, 1569A (1970)]. Supported in part by the Office of Naval Research through a contract with Kansas State University and by the Missouri Water Resources Research Center (OWRR) through a grant to the University of Missouri, K.C.

[1] W. M. Irvine and J. B. Pollack, Icarus **8**, 324 (1968).
[2] L. Pontier and C. Dechambenoy, Ann. Geophys. **21**, 462 (1965); **22**, 633 (1966).
[3] M. R. Querry, B. Curnutte, and D. Williams, J. Opt. Soc. Am. **59**, 1299 (1969).
[4] V. M. Zolatarev, B. A. Mikhailov, L. I. Aperovich, and S. I. Popov, Opt. Spektrosk. **27**, 790 (1969). [Opt. Spectrosc. **27**, 430 (1969)].
[5] S. P. F. Humphrey-Owens, Proc. Roy. Soc. (London) **77**, 949 (1968).
[6] E. K. Plyler and N. Griff, Appl. Opt. **4**, 1663 (1965).
[7] E. K. Plyler and N. Acquista, J. Opt. Soc. Am. **44**, 505 (1954).
[8] D. A. Draegert, N. W. B. Stone, B. Curnutte, and D. Williams, J. Opt. Soc. Am. **56**, 64 (1966).
[9] W. G. Spitzer, D. A. Kleinman, and D. Walsh, Phys. Rev. **113**, 127 (1959).
[10] W. G. Spitzer, D. A. Kleinman, and C. J. Frosch, Phys. Rev. **113**, 133 (1959).
[11] M. Gottlieb, J. Opt. Soc. Am. **50**, 343 (1960).

PREPRINT:
"Proceedings Seventh International Symposium on the Remote Sensing of Environment"
University of Michigan, Ann Arbor, 17-21 May 1971

SPECULAR REFLECTANCE OF AQUEOUS SOLUTIONS*

M. R. Querry, R. C. Waring, W. E. Holland, and G. R. Mansell

Department of Physics
University of Missouri-Kansas City 64110

ABSTRACT

We have constructed two laboratory instruments for measuring the specular reflectance of aqueous solutions. The instruments are an organic-dye-laser spectrophotometer for the 360-650nm wavelength region and a reflectometer accessory for a Perkin-Elmer E-system spectrophotometer which will operate in the 0.2-20μm wavelength region. We have used the reflectometer accessory to measure the relative, infrared, specular reflectance in limited spectral regions for aqueous solutions of NaCl, K_2SO_4, $ZnSO_4$, $(NH_4)_2SO_4$, and $NH_4H_2PO_4$ with radiant flux incident at about 70° and polarized perpendicular to the plane of incidence. We have used the laser spectrometer to measure the absolute reflectance of aqueous solutions of NaCl in the wavelength region 575-610nm for light incident at angles of about 60°, 65°, and 70° and polarized parallel to the plane of incidence. More extensive use of both instruments to obtain reflectance measurements of aqueous solutions is now under way in our laboratory.

INTRODUCTION

Optical instruments, such as the University of Michigan's multichannel optical-mechanical scanner[1,2] and Long Island University's multispectral color photographic system,[3] to mention only two at random, have been used to collect data for remote sensing applications. Such instruments are mounted in aircraft and typically sense radiant flux as reflected from the substances[4] in an earth surface area that has been apriorily selected for analysis. In the 8-14μm wavelength region of the infrared, only radiant flux naturally emitted by the substance is sensed by the instrument because of the low emissive power of the sun in this wavelength region. The analysis of data from such instruments for purposes of identifying and measuring the quantity of a particular substance must ultimately depend on the characteristic reflectance or emittance of the substance. The characteristic reflectance of different plant leaves therefore has been the subject of several laboratory investigations.[5-12] Though the earth's surface is about 75 per cent covered by aqueous solutions, it is only during the past five years that extensive reflectance measurements have been reported for distilled water,[13-25] and to our knowledge there are no published reports of extensive investigations of the reflectance of aqueous solutions.[26]

With the thoughts listed above as a partial rationale, we have constructed two laboratory instruments for measuring the specular reflectance of aqueous solutions. One instrument is an organic-dye-laser spectrophotometer for the 0.36-0.65μm wavelength region and the other is a reflectometer accessory for a

*Supported in part by the U.S. Geological Survey under Contract 14-08-0001-12636, by the National Aeronautics and Space Administration under Grant NGR 26-001-012, and by the Missouri Water Resources Center under project A-030-MO.

Perkin-Elmer E-system spectrophotometer which will operate in the 0.2-20μm wavelength region. We have used these instruments to measure absolute and relative specular reflectance of selected aqueous solutions in selected spectral regions. Spectral values of the optical constants, i.e. the index of refraction and the extinction coefficient, can be determined from the reflectance measurements[26-28] and we have developed several unique computer codes to make these computations. In this paper, however, we limit the discussion to the instrumentation for measuring reflectance and to the results from the reflectance measurements.

REFLECTOMETER

The new reflectometer for measuring specular reflectance is an improved design of the reflectometer that Querry et al.[23] used in 1968 to measure the specular reflectance of distilled water. The new system was designed for the 0.2-30μm wavelength region, but to date, we have used it only in the 2-20μm region of the infrared. A diagram of the reflectometer-spectrophotometer system is shown in Figure 1. When operating the system in the infrared spectral region, a glower G emits radiant flux which is chopped at C and is then collected and collimated by a Cassegrain unit consisting of spherical mirrors M_1 and M_2. A partially collimated pencil of radiant flux of about 18 mrad divergence passes horizontally to mirror M_3, and then enters a Cassegrain condenser unit consisting of spherical mirrors M_5 and M_6. From the condenser unit a convergent cone of radiant flux, with apex angle of about 75 mrad at the entrance slit of the monochromator, passes through a transmission polarizer consisting of 12 silver chloride plates positioned at the Brewster's angle relative to the system's optical axis. The 12 plate polarizer passes about 0.1 per cent of the undesired polarization component. A thermopile detector having a CsI window provides a measure of the spectral energy. Interference filters at the monochromator's exit slit prevent overlapping diffraction orders and scattered radiant flux from reaching the detector. The monochromator, chopper, detector assembly, amplifier, recorder, and scan control are a Perkin-Elmer E-14 system.

A cathetometer having a protractor ocular is used to determine the angle of incidence Θ to $\pm$ 4 mrad for the central ray of the slightly divergent pencil of radiant flux.

DYE-LASER SPECTROPHOTOMETER

The new laser spectrophotometer, constructed in our laboratory, uses an organic-dye-laser[29] as both the source of radiant flux and the monochromator. A block diagram of the dye-laser spectrophotometer is shown in Figure 2. An AVCO C950 pulsed nitrogen-gas laser, which emits 8 nsec pulses of radiant flux of wavelength 337.1 nm, optically pumps the dye-laser, which is a significantly modified AVCO dye-laser module that emits 5-8 nsec pulses of about 0.25 nm spectral width. A wavelength drive assembly rotates a diffraction grating in a Littrow mount located at one end of the dye-laser cavity and thereby continuously wavelength tunes the dye-laser. The sample area contains a simple arrangement of plane mirrors, similar to M_3 and M_4 of Figure 1, for measuring specular reflectance. A photodiode of 0.35 nsec risetime detects the laser pulses reflected from the sample and a PAR box-car integrator then senses and integrates signals from the photodiode. As an alternate display, a sampling oscilloscope senses many pulses from the photodiode to give a representation of a single pulse. The signal from the integrator is proportional to the energy per laser pulse and is recorded on strip charts. The scan control synchronizes six different recorder chart movements and 36 different rates of rotation of the diffraction grating. A mechanical counter provides a wavelength reference. Synchronous pulses from the nitrogen laser control panel trigger the integrator in such a manner that only the signals representing the dye-laser pulse are integrated.

The dye-laser is continuously wavelength tunable in the region 360-650 nm when the nine different closed dye-cells are used as supplied by AVCO. Temporal decreases as large as 30 per cent in the intensity of the dye-laser pulses were

reduced to less than 2 per cent by continuously circulating the dye solution through the laser cavity. Circulating the dye solution required us to enter a period of testing to determine which dyes and what concentrations are needed for lasing in the 360-650 nm region. Therefore, to date, we have only measured the reflectance of aqueous solutions in the 575-610 nm region of tunability for the dye rhodamine 6G.

The output pulse from the dye-laser is predominately plane polarized with the electric vector being vertical. A polarizer is placed in the laser beam to further reduce the horizontal polarization component. The specular reflectance for aqueous solutions is then measured for the incident laser beam polarized parallel to the plane of incidence.

EXPERIMENTAL TECHNIQUES

Both the reflectometer accessory and the dye-laser system provide measurements of absolute specular reflectance or of specular reflectance relative to a calibrated reflectance standard. To measure absolute reflectance, we remove the sample and then measure the incident radiant flux by keeping the total length of the optical-path unchanged by using a He-Ne laser beam as a reference to carefully reposition two mirrors in the reflectometer accessory; and in the dye-laser system by relocating the detector. These techniques consistently introduce an additional uncertainty of ± 2-3 per cent in the absolute reflectance measurements. To measure relative specular reflectance, we substitute the reflectance standard for the sample and then carefully move the standard reflector to the sample's original position by adjusting a small laboratory jack while viewing the edge of the reflectance surface with a cathetometer. A series of relative reflectance measurements typically have a standard deviation of less than 1.0 per cent. Since the optical constants of distilled water are now known with reasonable certainty[20-25] in the 2-20μm wavelength region of the infrared, we chose distilled water as the reflectance standard and measured the relative reflectance of the aqueous solutions. We are uncertain about the values for the optical constants of water in the visible, especially for short-time, high-power laser pulses, and therefore use the dye-laser system to measure absolute reflectance.

The relative specular reflectances of the aqueous solutions are measured as follows: An aqueous solution is placed at the sample position in the reflectometer. The spectrophotometer's recorder shows a numerical reading N_s which is given by

$$N_s = (mak_pI_p)R_{ps} \quad , \tag{1}$$

where m is a proportionality constant characteristic of the detector-amplifier-recorder system, a is the fraction of the desired component of polarization that passes through the polarizer, k_p is the optical system's efficiency for collecting and transmitting radiant flux of polarization p to the detector, I_p is the luminous intensity of polarization component p at the source, and R_{ps} is the absolute specular reflectance of the aqueous solution for radiant flux of polarization component p. Distilled water is then placed at the sample position in the reflectometer and the recorder shows a numerical reading N_w which is given by

$$N_w = (mak_pI_p)R_{pw} \quad , \tag{2}$$

where R_{pw} is the absolute specular reflectance of distilled water for radiant flux of polarization component p. The instrument settings are held constant for the measurements indicated by both equations (1) and (2). The relative specular reflectance R_p of the aqueous solutions, therefore, is given by

$$R_p = N_s/N_w = R_{ps}/R_{pw} \quad . \tag{3}$$

During a series of infrared reflectance measurements zero references are recorded by scanning the spectrum while the luminous source is several centimeters off the optic-axis of the reflectometer.

We compute the absolute reflectances R_{ps} of the aqueous solutions from the measured values of R_p and with R_{pw} computed from the optical constants of water, the angle of incidence Θ, and the generalized Fresnel equations.30/

The absolute reflectance measurements are obtained with the dye-laser system as follows. An aqueous solution is placed at the sample position in the laser system's reflectometer and the resultant recorder reading is a number N_s given by equation (1). The sample is removed and the detector carefully repositioned to measure the energy per laser pulse of the incident laser beam. The resultant recorder reading is a number N_o given by

$$N_o = mak_p I_p \quad . \tag{4}$$

The product (mak_p) is constant for about three orders of magnitude change in I_p and therefore the absolute reflectance $R_{ps} = N_s/N_o$. Zero and maximum response is carefully noted for each strip chart recording on N_o and N_s.

RESULTS

The relative reflectances of aqueous solutions of NaCl, $ZnSO_4$, $(NH_4)_2SO_4$, and $NH_4H_2PO_4$ as measured relative to distilled water are shown in Figures 3-9 for selected wavelength regions of the infrared. The measurements were made for infrared radiant flux indident at $70.03° \pm 0.23°$ and for plane polarization with the electric field vector perpendicular to the plane of incidence. The absolute reflectance, which also appears in some of the figures, was computed by the techniques outlined in the preceeding section. The relative reflectance values are the mean for three separate measurements. One standard deviation for the three measurements was less than 1 per cent.

The NaCl are in solution as monatomic ions and therefore do not exhibit characteristic infrared reflectance bands. The effect of the NaCl is to broaden and shift the 2.75μm and 6μm vibrational bands and the 16μm association band of the water. The sulfate and phosphate are in solution as XY_4 molecular ions which have strong ν_3-vibration bands in the 8-10μm wavelength region. These vibrational bands produce strong characteristic, spectral signatures in the relative reflectance spectra as shown in Figures 7-9.

The absolute reflectance of distilled water and of an aqueous solution of NaCl as measured in the 575-610 nm wavelength region with the dye-laser spectrophotometer are shown in Figure 10. The measurements were made for radiant flux plane polarized with the electric field vector parallel to the plane of incidence. The straight lines through the data points are to indicate the general trends of the data. The angles of incidence for measurements on the NaCl solution were about 60°, 65°, and 70°. The Brewster angle for distilled water is about 53°. The absolute reflectance values are the mean for three separate measurements and the error bars indicate one standard deviation for the three measurements.

The NaCl was at 1, 3, and 5 molar concentration and the sulfates and phosphate were at 0.5 molar concentration. The temperature of the solutions was about 25°C.

CONCLUSIONS

We have described a new reflectometer-spectrophotometer system and a new organic-dye-laser spectrophotometer for measuring the specular reflectance of aqueous solutions. We have presented interim results from the specular reflectance measurements for aqueous solutions of NaCl, $ZnSO_4$, $(NH_4)_2SO_4$, and $NH_4H_2PO_4$. Characteristic infrared spectral signatures for SO_4^{--} and PO_4^{---} were evident in the relative reflectance spectra. The NaCl broadens and shifts the infrared reflectance bands of the water and in general increases the reflectance.

The aqueous solutions had larger solute content than that ordinarily found in natural waters. The interim results therefore have only specialized applications to remote sensing of water quality, such as in strip mine areas where sulfates and phosphates are abundant by-products of natural chemical reactions. The results from the NaCl solutions should have utility in the reduction of remote sensor data for coastal areas, where target materials are viewed against a background of radiant flux reflected and emitted from sea water.

The reflectance spectra of natural waters will be more complex than that for simple laboratory aqueous solutions with only one solute. Therefore, we are now extending the laboratory measurements of reflectance to the entire 0.2-20μm wavelength region in order to determine the optical constants for several aqueous solutions having different solute content. A knowledge of the optical constants will allow us to construct physical models that represent natural waters; to determine the sensitivity of reflectance techniques for remote monitoring of water quality; and to design remote sensing experiments and techniques for processing data from remote sensors.

SELECTED REFERENCES

1. A. E. Coker, R. Marshall, and N. S. Thomson, Proc. of Sixth Symp. Remote Sensing, p. 65 (Univ. of Michigan 1969).

2. M. C. Kolipinski, A. L. Higer, N. S. Thomson, and F. J. Thomson, Proc. Sixth Symp. Remote Sensing, p. 79, (Univ. of Mich. 1969).

3. E. Yost and S. Wenderoth, Proc. Sixth Symp. Remote Sensing, p. 145, (Univ. of Mich. 1969).

4. F. J. Kriegler, W. A. Malila, R. F. Nalepka, and W. Richardson, Proc. Sixth Symp. Remote Sensing, p. 97 (Univ. of Mich. 1969).

5. H. W. Gausman, W. A. Allen, R. Cardenas, and A. J. Richardson, Proc. Sixth Symp. Remote Sensing, p. 1123 (Univ. of Mich. 1969).

6. W. A. Allen, T. V. Gayle, and A. J. Richardson, J. Opt. Soc. Am. 60, 372 (1970).

7. W. A. Allen and A. J. Richardson, J. Opt. Soc. Am. 58, 1023 (1968).

8. W. A. Allen, H. W. Gausman, A. J. Richardson, and J. R. Thomas, J. Opt. Soc. Am. 59, 1376 (1969).

9. W. A. Allen, H. W. Gausman, A. J. Richardson, J. Opt. Soc. Am. 60, 542 (1970).

10. H. W. Gausman, W. A. Allen, R. Cardenas, and A. J. Richardson, Appl. Opt. 9, 545 (1970).

11. D. L. Spooner, Proc. Sixth Symp. Remote Sensing, p. 1003 (Univ. of Mich.) 1969).

12. J. M. Ward, PROC. Sixth Symp. Remote Sensing, p. 1205 (Univ. of Mich. 1969).

13. W. M. Irvine and J. B. Pollack, Icarus 8, 324 (1968).

14. C. H. Cartwright, Nature 135, 872 (1935).

15. M. Centeno, J. Opt. Soc. Am. 31, 244 (1941).

16. E. N. Dorsey, Properties of Ordinary Water Substance, Reinholt Pub. Co., New York (1948).

17. E. D. McAlister, Appl. Optics 3, 609 (1964).

18. L. D. Kislouskii, Opt. i Spektroskopiya 1, 201 (1959).

19. B. McSwain and J. Berstein, Rept. 539, Naval Ordnance Laboratory Corona, pp. 29-36, 15 Feb. 1961.

20. L. Pontier and C. Dechambenoy, Ann. Geophys. 22, 633 (1966).

21. L. Pontier and C. Dechambenoy, Ann Geophys. 21, 462 (1965).

22. M. R. Querry, Infrared Reflectance of Liquid Water, Ph.D. Dissertation, Kansas State University (1968) (available from Univ. Microfilms, Ann Arbor, Michigan).

23. M. R. Querry, B. Curnutte, D. Williams, J. Opt. Soc. Am. 59, 1299 (1969).

24. V. M. Zolatarev, B. A. Mikhailov, L. I. Aperovich, and S. I. Popov, Opt. Spektrosk. 27, 790 (1969). [Opt. Spectrosc. 27, 430 (1969)].

25. A. Rusk, D. Williams, and M. R. Querry, Optical Constants of Water in the infrared, Accepted for publication in J. Opt. Soc. Am.

26. M. R. Querry, R. C. Waring, W. E. Holland, Second Quarterly Report, U.S. Geological Survey Contract 14-08-0001-12636.

27. M. Gottlieb, J. Opt. Soc. Am. 50, 343 (1960).

28. M. R. Querry, J. Opt. Soc. Am. 59, 876 (1969).

29. J. A. Meyer, C. L. Johnson, E. Kierstead, R. D. Sharma, and I. Itzkan, Dye Laser Stimulation with a Pulsed N_2 Laser Line at 3371 Å, preprint of article for Applied Phys. Letters.

30. J. A. Stratton, "Electromagnetic Theory," McGraw-Hill, New York (1941), pp. 505-506..

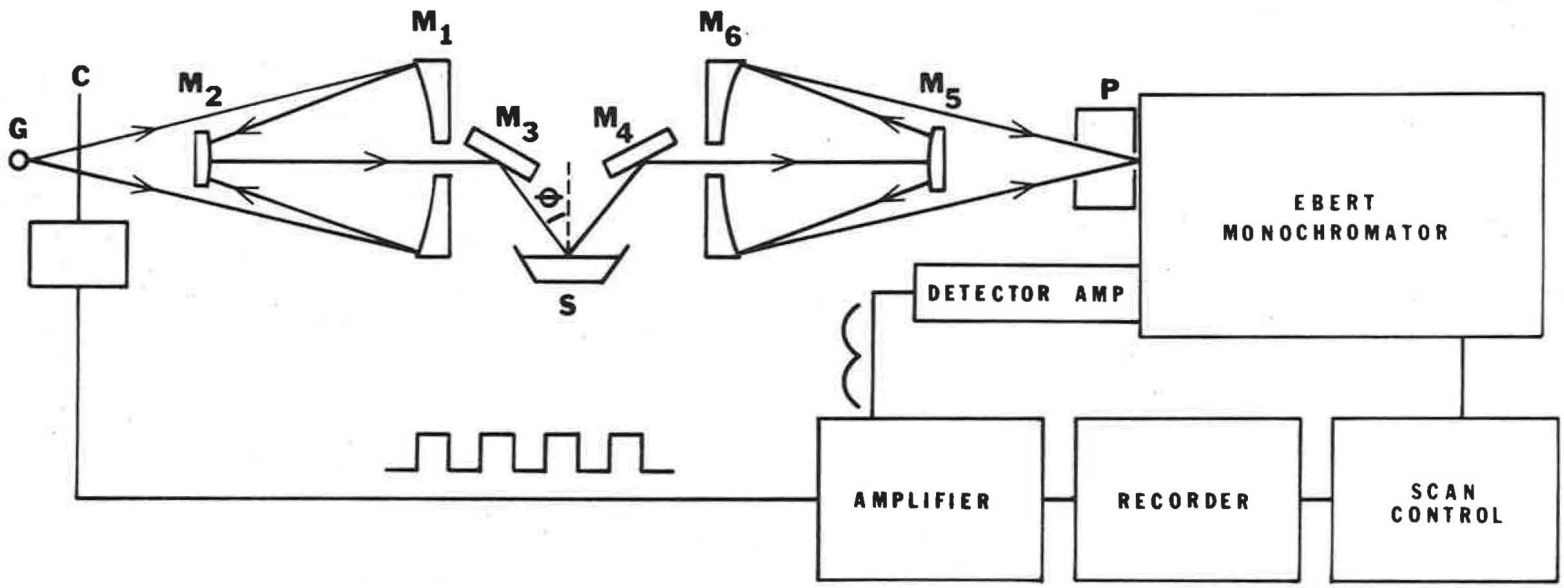

Figure 1. Reflectometer-spectrophotometer system for measuring the specular reflectance of aqueous solutions.

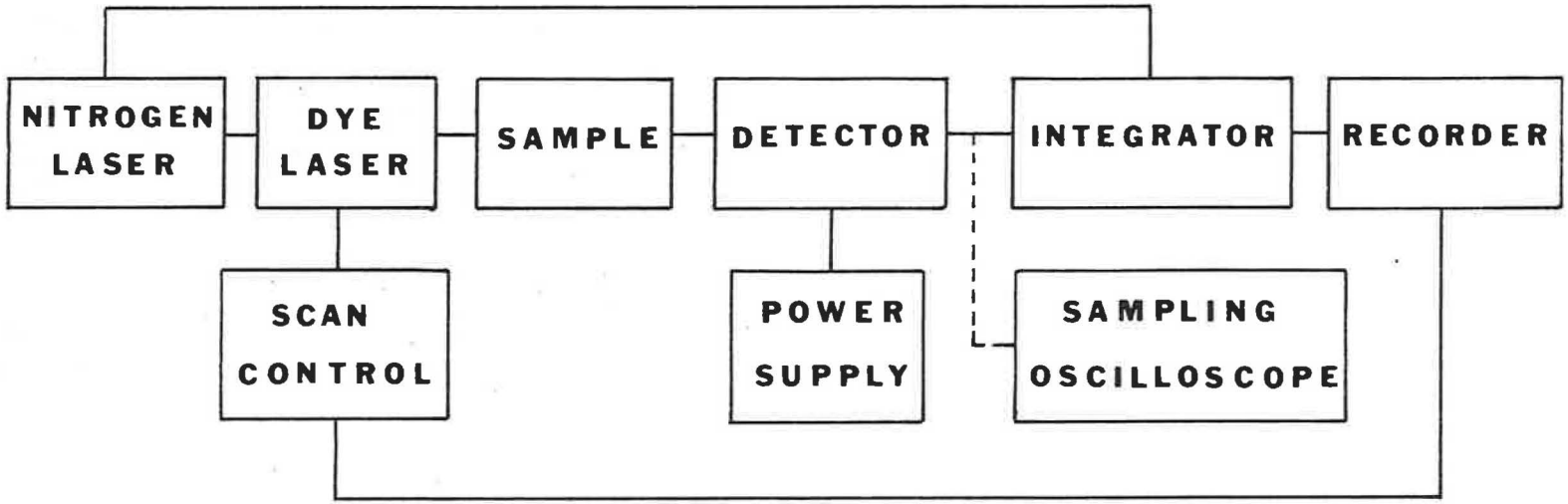

Figure 2. A block diagram of the organic-dye laser spectrophotometer.

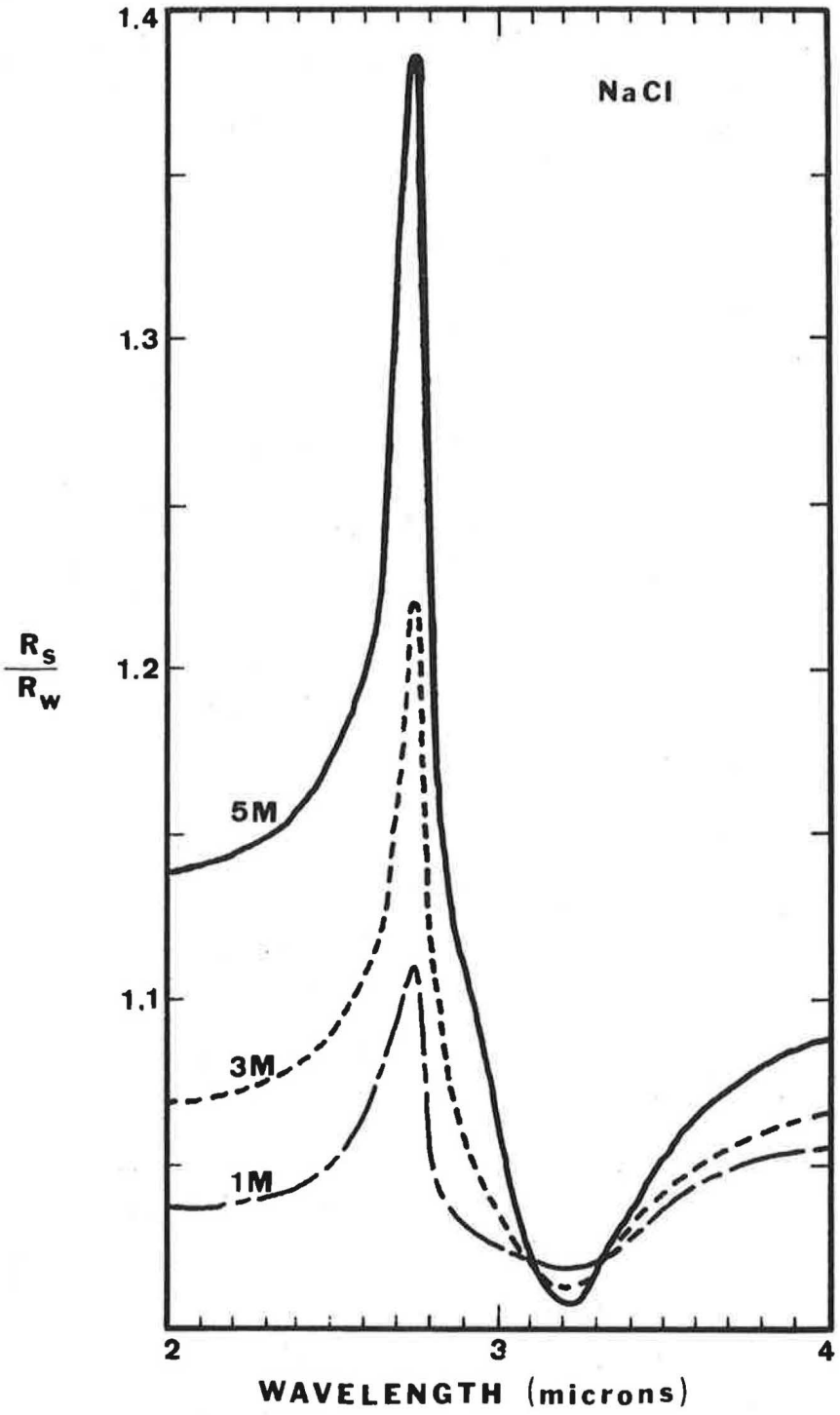

Figure 3. Specular, relative reflectance of 1, 3, and 5 molar aqueous solutions of NaCl in the 2-4μm wavelength region. The angle of incidence was 70.03° ± 0.23°. The radiant flux was plane-polarized with the electric field vector perpendicular to the plane of incidence.

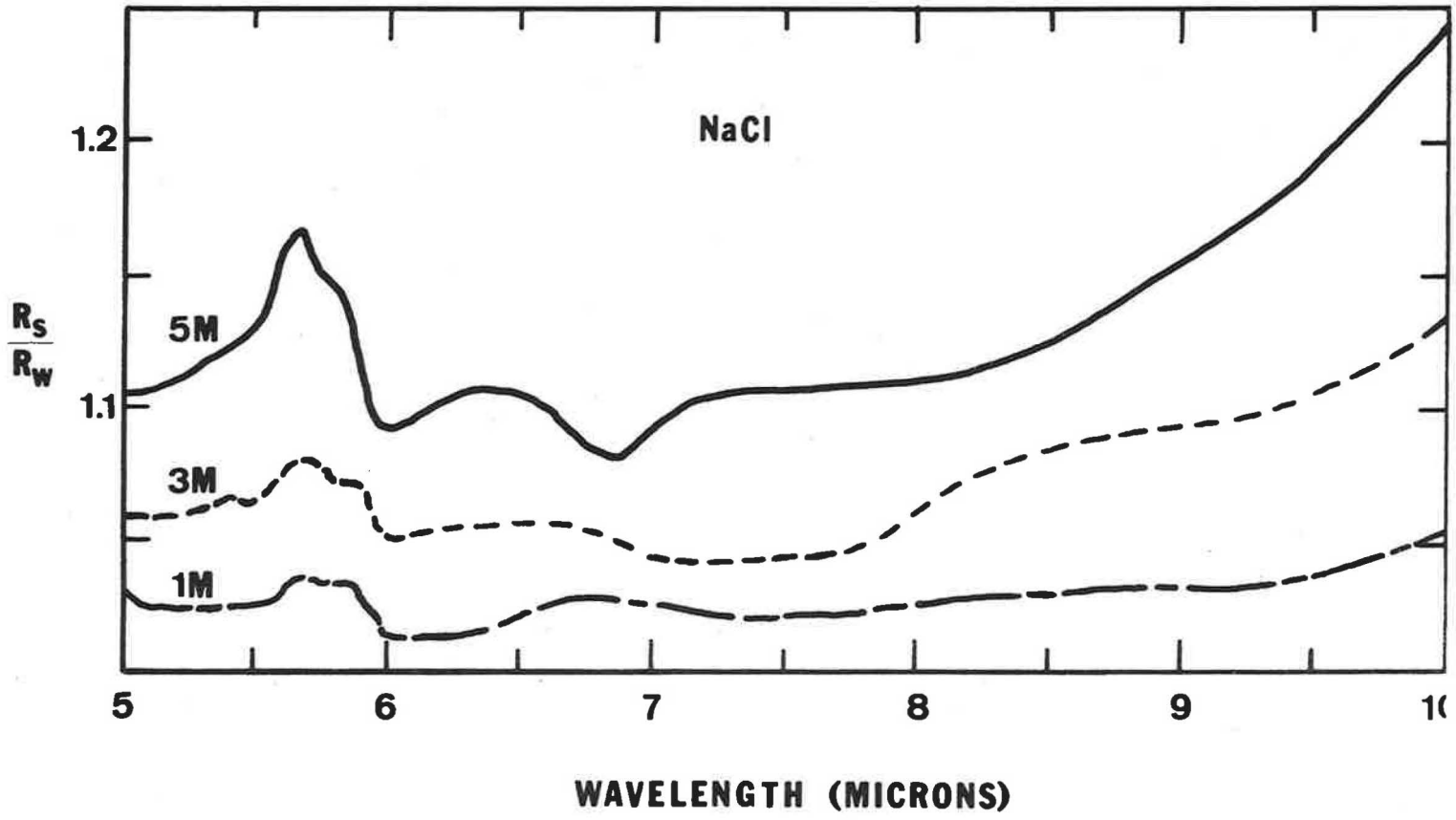

Figure 4. Specular, relative reflectance of 1, 3, and 5 molar solutions of aqueous solutions of NaCl in the 5-10μm wavelength region. The angle of incidence was 70.03°± 0.23°. The incident radiant flux was plane-polarized with the electric field vector perpendicular to the plane of incidence.

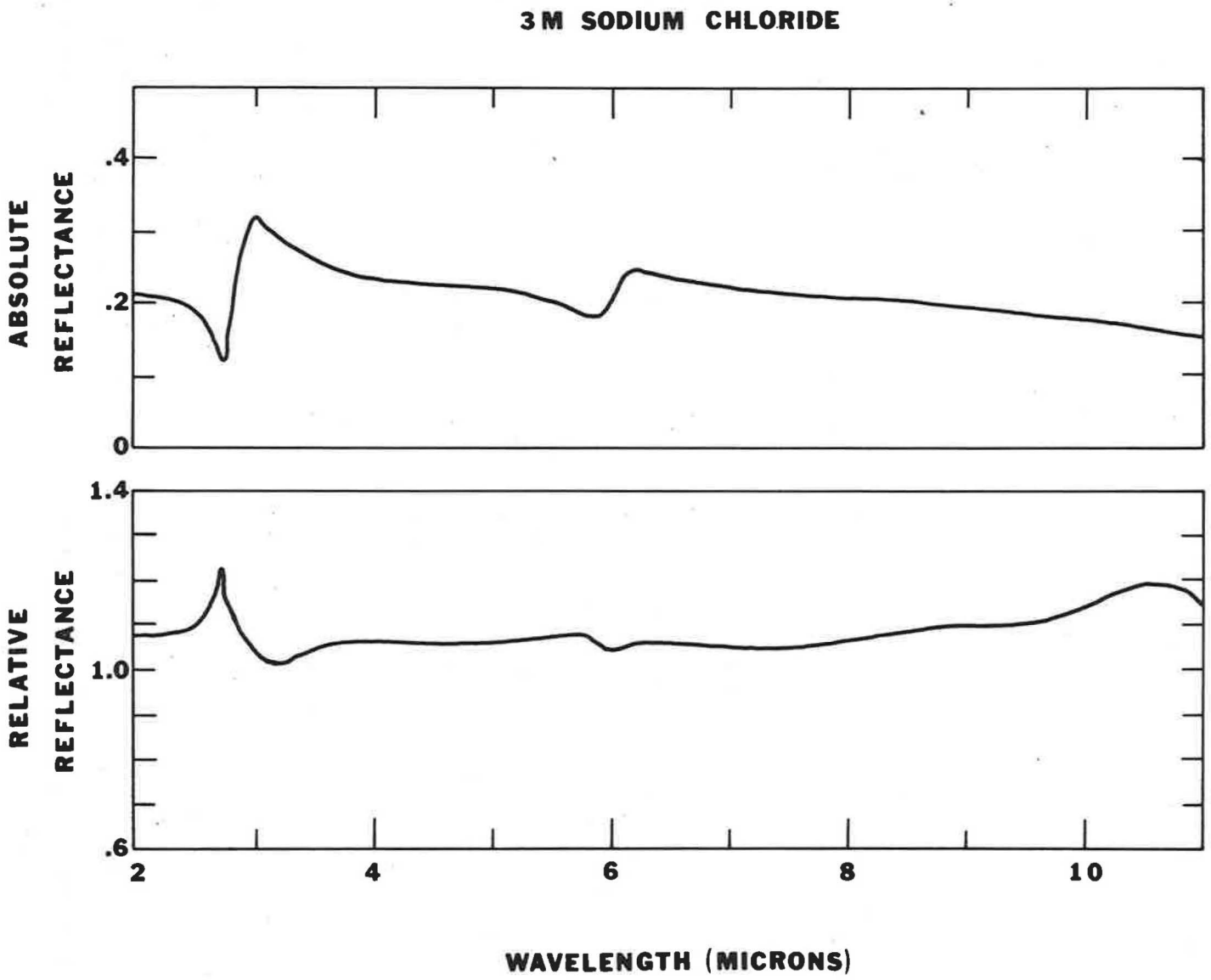

Figure 5. Specular, relative and absolute reflectande of a 3 molar aqueous solution of NaCl in the wavelength region 2-11μm. The angle of incidence was 70.03°± 0.23° for radiant flux plane-polarized with the electric field vector perpendicular to the plane of incidence.

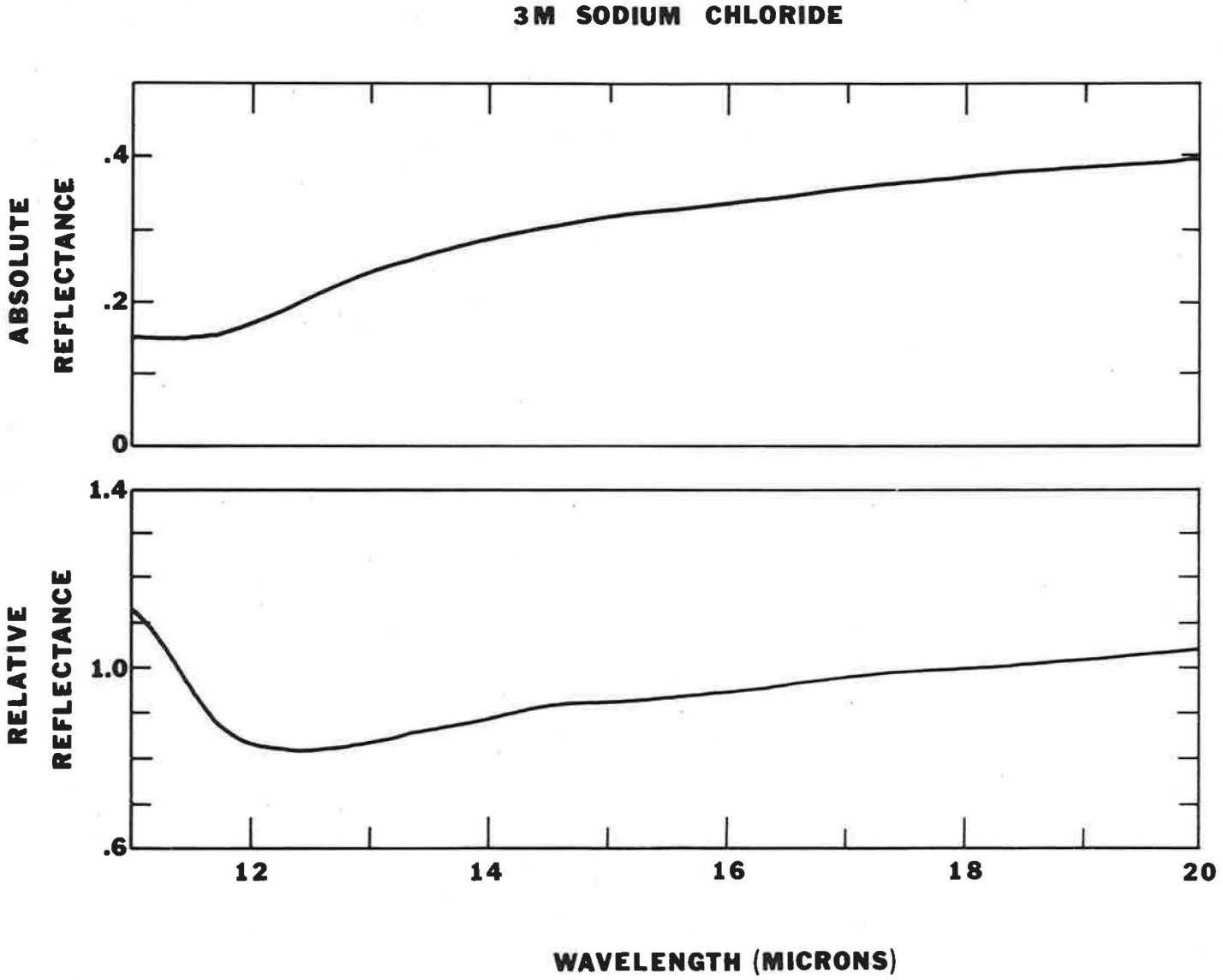

Figure 6. Specular, relative and absolute reflectance of a 3 molar aqueous solution of NaCl in the wavelength region 11-20μn. The angle of incidence was 70.03° ± 0.23° for radiant flux plane-polarized with the electric field vector perpendicular to the plane of incidence.

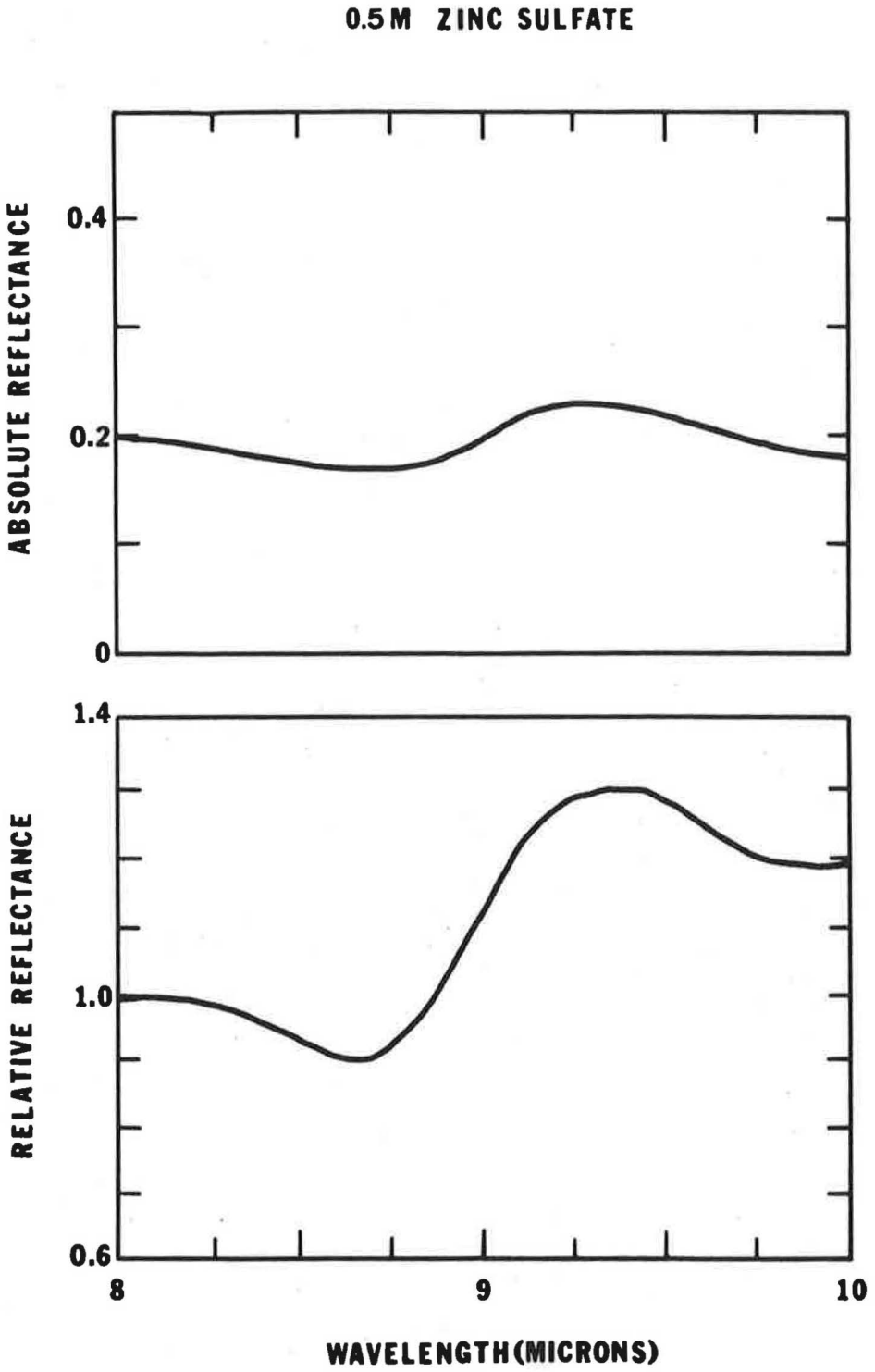

Figure 7. Specular, relative and absolute reflectance of a 0.5 molar aqueous solution of $ZnSO_4$ in the 8-10μm wavelength region. The angle of incidence was 70.03° ± 0.23° for radiant flux plane-polarized with the electric field vector perpendicular to the plane of incidence.

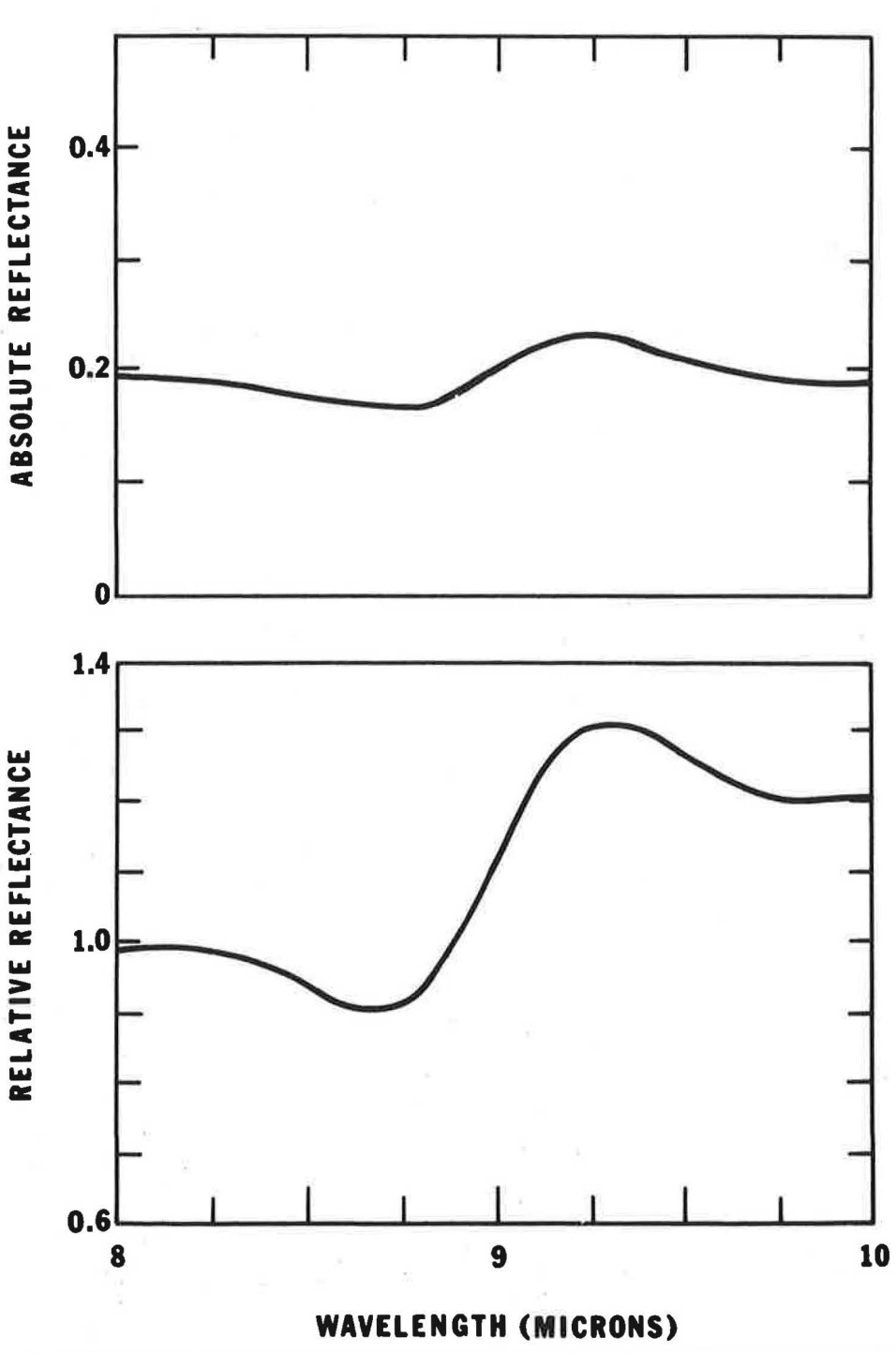

Figure 8. Specular, relative and absolute reflectance of a 0.5 molar aqueous solution of $(NH_4)_2SO_4$ in the 8-10μm wavelength region. The angle of incidence was 70.03° ± 0.23° for radiant flux plane-polarized with the electric field vector perpendicular to the plane of incidence.

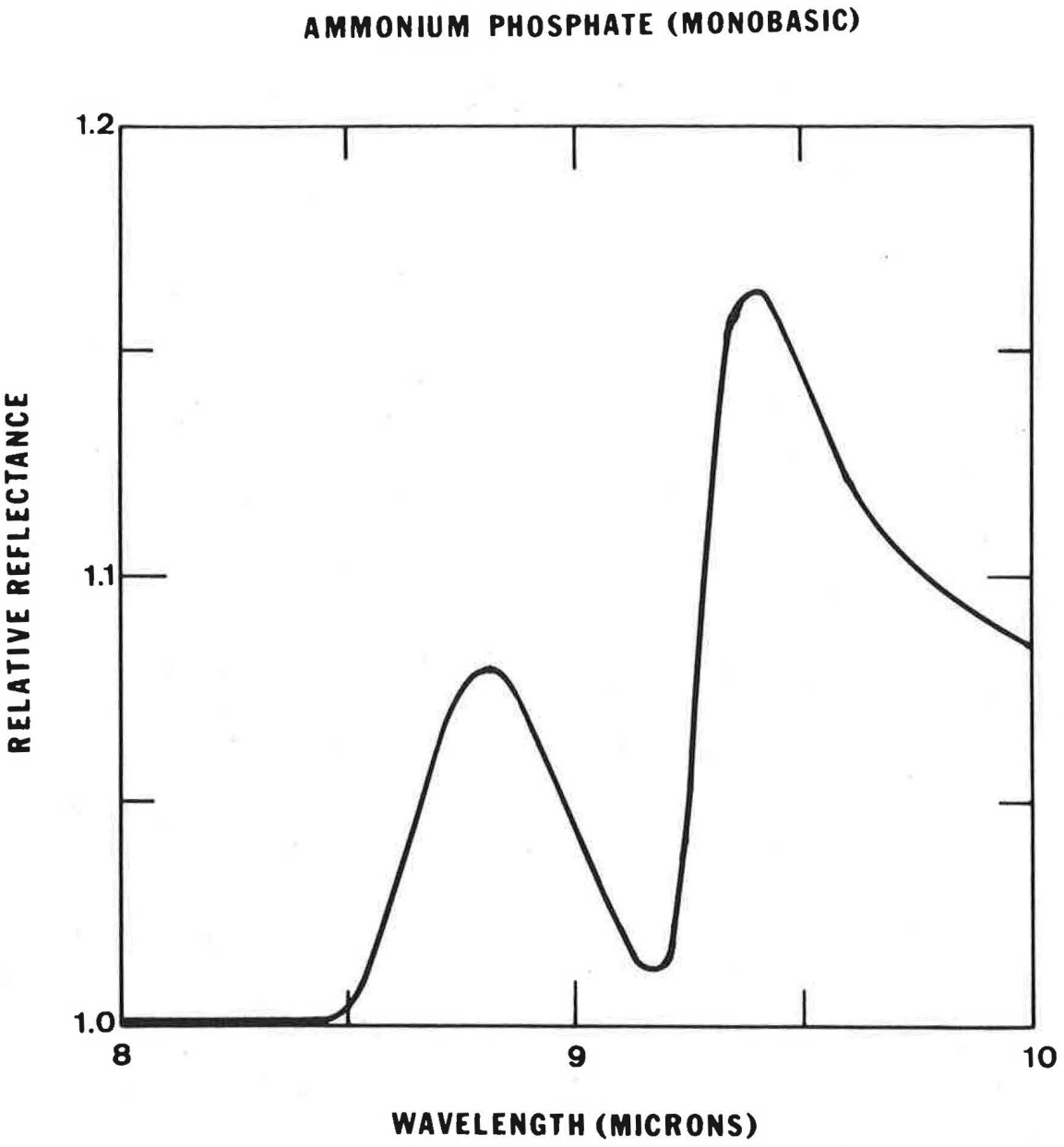

Figure 9. Specular, relative reflectance of a 0.5 molar solution of $NH_4H_2SO_4$ in the 8-10μm wavelength region. The angle of incidence was 70.03 ± 0.23° for radiant flux plane-polarized with the electric field vector perpendicular to the plane of incidence.

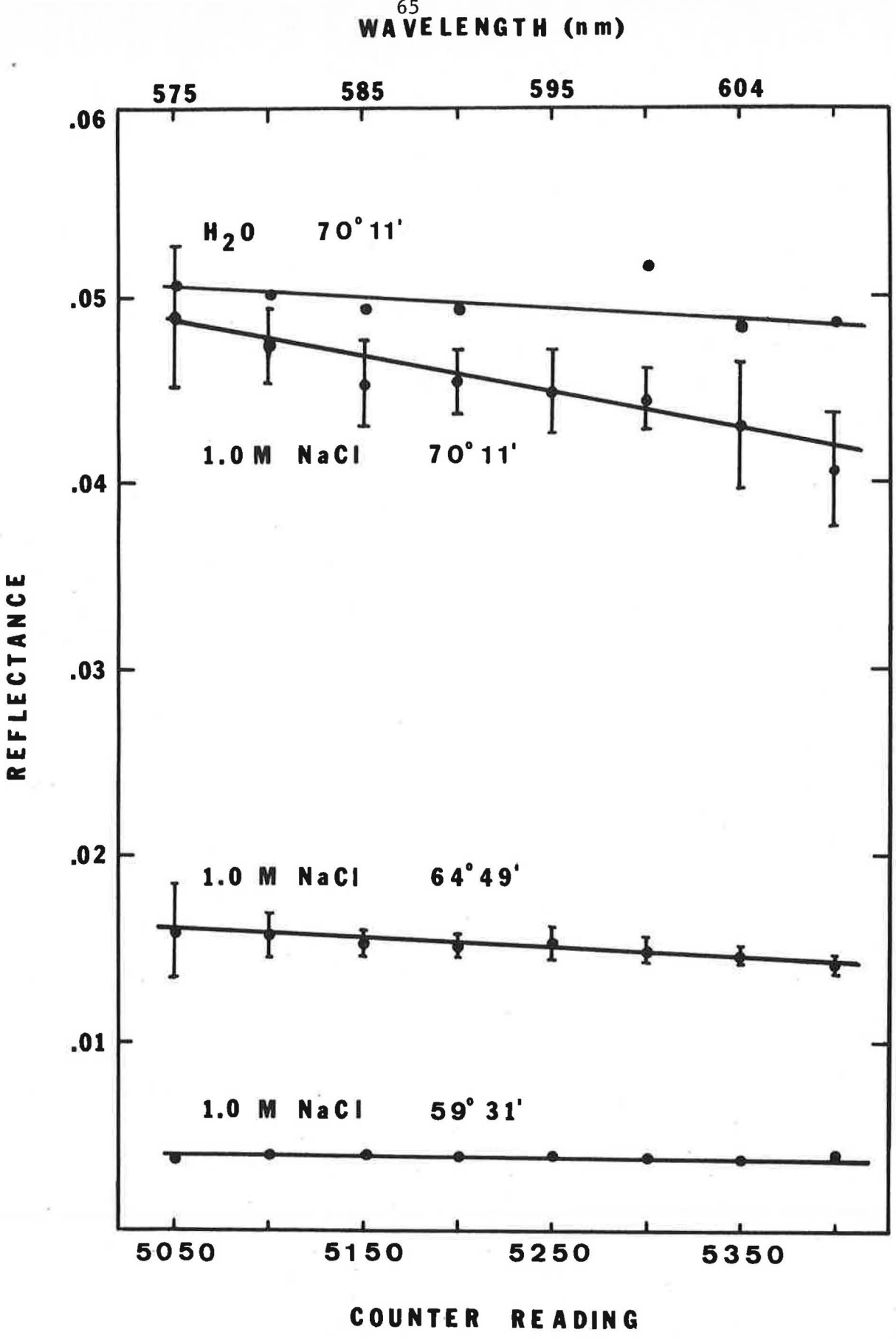

Figure 10. Specular, absolute reflectance of distilled water and a 1 molar aqueous solution of NaCl as measured with the dye-laser spectrophotometer. The angles of incidence are shown in the figure. The incident laser beam was plane-polarized with the electric field vector parallel to the plane of incidence.

APPENDIX II

The following pages are a tablulation of the optical constants of the aqueous solutions of K_2SO_4, $NH_4H_2PO_4$, and $(NH_2)_2CO$ as computed according to the Kramers-Kronig analysis outlined in the text.

WL: Wavelength (Micrometers)

R(REL): Relative Reflectance

R(ABS): Absolute Reflectance

N: Index of refraction

K: Extinction coefficient

Note:

The relative reflectance measurements had three significant digits. The values of N and K therefore have only three significant digits. Some small values of K are shown as negative in the tables. The negative values of K are merely a result of having only three significant digits in the data. For example on page 67 at WL = 2.00 N = 1.302, K = -0.006. Keeping only three significant digits N = 1.30, K = 0.00.

OPTICAL CONSTANTS OF 0.5 M POTASSIUM SULFATE
ANGLE OF INCIDENCE = 1.2223 RADIANS

WL	R(REL)	R(ABS)	N	K
2.00	1.006	0.203	1.302	-0.006
2.05	1.008	0.202	1.301	-0.007
2.10	1.001	0.200	1.297	-0.007
2.15	1.002	0.198	1.294	-0.006
2.20	1.000	0.196	1.290	-0.005
2.25	1.000	0.194	1.287	-0.004
2.30	1.005	0.192	1.284	-0.003
2.35	1.005	0.190	1.280	-0.003
2.40	1.009	0.187	1.275	-0.001
2.45	1.009	0.184	1.270	-0.002
2.50	1.009	0.179	1.262	-0.002
2.55	1.015	0.173	1.252	-0.003
2.60	1.017	0.163	1.237	0.001
2.65	1.031	0.153	1.222	-0.001
2.70	1.044	0.126	1.182	0.015
2.75	1.049	0.103	1.138	0.053
2.80	1.013	0.142	1.141	0.123
2.85	0.990	0.196	1.160	0.192
2.90	0.978	0.250	1.217	0.256
2.95	0.976	0.283	1.295	0.283
3.00	0.984	0.297	1.370	0.264
3.05	0.984	0.302	1.421	0.229
3.10	0.982	0.304	1.460	0.181
3.15	0.983	0.295	1.462	0.130
3.20	0.987	0.287	1.456	0.094
3.25	0.991	0.281	1.448	0.071
3.30	0.993	0.273	1.435	0.049
3.35	0.997	0.266	1.421	0.037
3.40	0.996	0.260	1.409	0.029
3.45	0.997	0.255	1.399	0.025
3.50	0.999	0.251	1.392	0.021
3.55	1.001	0.248	1.386	0.019
3.60	1.002	0.245	1.380	0.015
3.65	0.998	0.240	1.370	0.015
3.70	1.001	0.239	1.368	0.016
3.75	1.000	0.237	1.364	0.015
3.80	0.999	0.234	1.358	0.016
3.85	1.005	0.234	1.358	0.017
3.90	1.003	0.232	1.354	0.017
3.95	1.004	0.230	1.351	0.019
4.00	1.020	0.232	1.354	0.022
4.05	1.020	0.231	1.352	0.020
4.10	1.036	0.234	1.358	0.016
4.15	1.006	0.225	1.341	0.016
4.20	1.045	0.233	1.357	0.015
4.25	1.012	0.225	1.342	0.012

OPTICAL CONSTANTS OF 0.5 M POTASSIUM SULFATE
ANGLE OF INCIDENCE = 1.2223 RADIANS

WL	R(REL)	R(ABS)	N	K
4.30	1.012	0.224	1.340	0.013
4.35	1.012	0.223	1.338	0.017
4.40	1.012	0.221	1.334	0.019
4.45	1.033	0.225	1.341	0.023
4.50	1.030	0.224	1.339	0.018
4.55	1.025	0.222	1.336	0.019
4.60	1.028	0.222	1.336	0.018
4.65	1.028	0.221	1.334	0.021
4.70	1.037	0.223	1.337	0.019
4.75	1.040	0.224	1.340	0.016
4.80	1.016	0.218	1.329	0.011
4.85	1.011	0.217	1.327	0.017
4.90	1.025	0.219	1.330	0.016
4.95	1.030	0.220	1.333	0.009
5.00	0.968	0.206	1.307	0.013
5.05	1.014	0.215	1.322	0.023
5.10	1.019	0.215	1.323	0.020
5.15	1.027	0.215	1.323	0.018
5.20	1.026	0.214	1.321	0.016
5.25	1.028	0.213	1.320	0.013
5.30	1.025	0.210	1.314	0.012
5.35	1.034	0.210	1.314	0.010
5.40	1.026	0.206	1.307	0.007
5.45	1.026	0.202	1.300	0.008
5.50	1.021	0.199	1.295	0.010
5.55	1.039	0.198	1.294	0.009
5.60	1.022	0.190	1.280	0.010
5.65	1.029	0.187	1.275	0.016
5.70	1.036	0.184	1.269	0.020
5.75	1.036	0.180	1.262	0.024
5.80	1.014	0.170	1.245	0.034
5.85	1.039	0.172	1.244	0.049
5.90	1.009	0.168	1.232	0.065
5.95	1.025	0.175	1.231	0.092
6.00	1.038	0.196	1.250	0.124
6.05	1.053	0.219	1.283	0.143
6.10	1.032	0.234	1.315	0.143
6.15	1.035	0.243	1.344	0.128
6.20	1.037	0.245	1.358	0.108
6.25	1.021	0.240	1.356	0.086
6.30	1.026	0.239	1.357	0.076
6.35	1.024	0.235	1.353	0.065
6.40	1.030	0.234	1.353	0.056
6.45	1.004	0.225	1.337	0.050
6.50	1.013	0.225	1.336	0.054
6.55	1.037	0.228	1.343	0.050

OPTICAL CONSTANTS OF 0.5 M POTASSIUM SULFATE
ANGLE OF INCIDENCE = 1.2223 RADIANS

WL	R(REL)	R(ABS)	N	K
6.60	1.025	0.223	1.335	0.042
6.65	1.012	0.219	1.328	0.038
6.70	0.992	0.214	1.318	0.044
6.75	1.021	0.219	1.326	0.046
6.80	1.037	0.221	1.332	0.038
6.85	0.955	0.203	1.299	0.038
6.90	1.042	0.220	1.328	0.047
6.95	0.979	0.206	1.304	0.040
7.00	1.003	0.211	1.312	0.045
7.05	1.002	0.210	1.310	0.048
7.10	1.007	0.210	1.310	0.045
7.15	1.017	0.212	1.314	0.046
7.20	1.001	0.208	1.307	0.040
7.25	1.000	0.207	1.305	0.043
7.30	0.994	0.205	1.302	0.042
7.35	0.995	0.205	1.301	0.045
7.40	0.995	0.205	1.301	0.044
7.45	1.000	0.204	1.300	0.044
7.50	0.986	0.201	1.294	0.045
7.55	1.001	0.204	1.299	0.048
7.60	0.996	0.202	1.296	0.044
7.65	0.988	0.200	1.292	0.046
7.70	0.992	0.200	1.292	0.046
7.75	0.994	0.200	1.292	0.047
7.80	0.989	0.198	1.289	0.046
7.85	0.994	0.199	1.290	0.046
7.90	0.980	0.195	1.284	0.044
7.95	0.977	0.194	1.282	0.047
8.00	0.985	0.195	1.283	0.048
8.05	0.981	0.194	1.282	0.047
8.10	0.979	0.192	1.278	0.046
8.15	0.976	0.191	1.277	0.046
8.20	0.971	0.189	1.273	0.046
8.25	0.965	0.187	1.270	0.046
8.30	0.959	0.185	1.266	0.046
8.35	0.953	0.183	1.263	0.047
8.40	0.944	0.180	1.258	0.046
8.45	0.936	0.177	1.253	0.048
8.50	0.923	0.173	1.246	0.050
8.55	0.910	0.171	1.241	0.054
8.60	0.902	0.168	1.235	0.058
8.65	0.889	0.166	1.229	0.065
8.70	0.886	0.165	1.224	0.072
8.75	0.890	0.165	1.220	0.081
8.80	0.905	0.167	1.218	0.091
8.85	0.939	0.172	1.219	0.104

OPTICAL CONSTANTS OF 0.5 M POTASSIUM SULFATE
ANGLE OF INCIDENCE = 1.2223 RADIANS

WL	R(REL)	R(ABS)	N	K
8.90	0.975	0.178	1.221	0.115
8.95	1.025	0.186	1.226	0.128
9.00	1.096	0.198	1.240	0.141
9.05	1.146	0.206	1.253	0.145
9.10	1.188	0.213	1.267	0.147
9.15	1.227	0.219	1.280	0.146
9.20	1.259	0.223	1.293	0.140
9.25	1.273	0.225	1.303	0.132
9.30	1.278	0.225	1.311	0.120
9.35	1.273	0.222	1.311	0.108
9.40	1.266	0.219	1.310	0.098
9.45	1.255	0.216	1.308	0.090
9.50	1.239	0.212	1.303	0.081
9.55	1.226	0.208	1.298	0.075
9.60	1.214	0.204	1.293	0.070
9.65	1.197	0.199	1.285	0.066
9.70	1.187	0.194	1.277	0.064
9.75	1.180	0.191	1.271	0.064
9.80	1.171	0.187	1.265	0.064
9.85	1.165	0.185	1.260	0.067
9.90	1.163	0.183	1.256	0.068
9.95	1.162	0.181	1.252	0.070
10.00	1.171	0.182	1.253	0.072
10.05	1.169	0.179	1.249	0.070
10.10	1.167	0.177	1.246	0.070
10.15	1.161	0.174	1.240	0.071
10.20	1.158	0.172	1.236	0.072
10.25	1.161	0.171	1.233	0.074
10.30	1.160	0.169	1.230	0.075
10.35	1.164	0.168	1.227	0.077
10.40	1.163	0.166	1.224	0.077
10.45	1.163	0.165	1.221	0.079
10.50	1.159	0.162	1.216	0.079
10.55	1.160	0.161	1.213	0.081
10.60	1.148	0.157	1.206	0.082
10.65	1.149	0.157	1.203	0.087
10.70	1.155	0.157	1.201	0.091
10.75	1.145	0.156	1.197	0.093
10.80	1.142	0.156	1.195	0.096
10.85	1.140	0.155	1.192	0.098
10.90	1.134	0.154	1.189	0.100
10.95	1.127	0.153	1.185	0.103
11.00	1.125	0.153	1.182	0.106
11.05	1.119	0.153	1.179	0.110
11.10	1.103	0.153	1.176	0.113
11.15	1.098	0.154	1.174	0.117

OPTICAL CONSTANTS OF 0.5 M POTASSIUM SULFATE
ANGLE OF INCIDENCE = 1.2223 RADIANS

WL	R(REL)	R(ABS)	N	K
11.20	1.088	0.153	1.170	0.119
11.25	1.074	0.154	1.167	0.123
11.30	1.065	0.155	1.164	0.127
11.35	1.058	0.155	1.160	0.130
11.40	1.049	0.156	1.157	0.134
11.45	1.037	0.158	1.153	0.140
11.50	1.030	0.161	1.151	0.145
11.55	1.019	0.164	1.149	0.151
11.60	1.011	0.167	1.148	0.156
11.65	1.005	0.170	1.146	0.161
11.70	1.006	0.174	1.145	0.167
11.75	1.006	0.178	1.144	0.173
11.80	1.001	0.181	1.144	0.178
11.85	1.001	0.185	1.143	0.183
11.90	0.998	0.189	1.143	0.189
11.95	0.998	0.194	1.145	0.195
12.00	0.971	0.193	1.143	0.194
12.05	0.966	0.196	1.141	0.199
12.10	0.965	0.200	1.139	0.205
12.15	0.970	0.206	1.139	0.212
12.20	0.966	0.209	1.139	0.216
12.25	0.965	0.213	1.139	0.222
12.30	0.961	0.217	1.139	0.227
12.35	0.962	0.220	1.139	0.231
12.40	0.967	0.226	1.140	0.239
12.45	0.962	0.228	1.140	0.242
12.50	0.965	0.233	1.141	0.249
12.55	0.964	0.237	1.141	0.254
12.60	0.964	0.241	1.143	0.259
12.65	0.963	0.245	1.144	0.265
12.70	0.963	0.249	1.146	0.270
12.75	0.965	0.253	1.148	0.276
12.80	0.962	0.256	1.151	0.280
12.85	0.964	0.259	1.153	0.284
12.90	0.966	0.262	1.155	0.288
12.95	0.965	0.264	1.155	0.291
13.00	0.977	0.270	1.158	0.300
13.05	0.978	0.272	1.162	0.303
13.10	0.977	0.275	1.165	0.307
13.15	0.976	0.277	1.168	0.310
13.20	0.977	0.280	1.172	0.314
13.25	0.973	0.280	1.174	0.314
13.30	0.975	0.283	1.176	0.318
13.35	0.972	0.284	1.177	0.320
13.40	0.976	0.287	1.180	0.324
13.45	0.975	0.289	1.182	0.327

OPTICAL CONSTANTS OF 1.0 M UREA
ANGLE OF INCIDENCE = 1.2223 RADIANS

WL	R(REL)	R(ABS)	N	K
2.00	1.029	0.208	1.311	-0.010
2.05	1.022	0.205	1.306	-0.009
2.10	1.024	0.204	1.304	-0.008
2.15	1.025	0.203	1.302	-0.007
2.20	1.024	0.200	1.297	-0.006
2.25	1.030	0.199	1.295	-0.003
2.30	1.037	0.198	1.294	-0.002
2.35	1.041	0.197	1.292	-0.002
2.40	1.038	0.193	1.285	-0.003
2.45	1.041	0.190	1.280	-0.002
2.50	1.044	0.185	1.272	0.0
2.55	1.077	0.184	1.270	-0.002
2.60	1.091	0.174	1.254	-0.007
2.65	1.053	0.157	1.227	-0.007
2.70	1.078	0.130	1.187	0.013
2.75	1.145	0.113	1.152	0.053
2.80	0.983	0.137	1.144	0.113
2.85	0.993	0.197	1.162	0.193
2.90	1.006	0.257	1.219	0.267
2.95	1.001	0.290	1.302	0.294
3.00	1.028	0.311	1.389	0.287
3.05	1.027	0.316	1.452	0.241
3.10	1.027	0.317	1.493	0.185
3.15	1.030	0.309	1.499	0.127
3.20	1.025	0.299	1.487	0.083
3.25	1.026	0.291	1.474	0.055
3.30	1.024	0.281	1.454	0.035
3.35	1.032	0.275	1.442	0.025
3.40	1.034	0.270	1.431	0.016
3.45	1.034	0.264	1.419	0.009
3.50	1.037	0.260	1.411	0.005
3.55	1.036	0.256	1.402	0.002
3.60	1.031	0.252	1.394	-0.0
3.65	1.035	0.249	1.388	-0.001
3.70	1.031	0.246	1.382	-0.001
3.75	1.037	0.245	1.380	-0.001
3.80	1.037	0.243	1.376	-0.003
3.85	1.034	0.240	1.370	-0.004
3.90	1.038	0.240	1.370	-0.005
3.95	1.035	0.237	1.365	-0.008
4.00	1.030	0.235	1.360	-0.013
4.05	0.999	0.226	1.344	-0.010
4.10	0.983	0.222	1.336	0.002
4.15	1.019	0.228	1.347	0.010
4.20	1.032	0.230	1.351	0.006
4.25	1.024	0.227	1.346	0.004

OPTICAL CONSTANTS OF 1.0 M UREA
ANGLE OF INCIDENCE = 1.2223 RADIANS

WL	R(REL)	R(ABS)	N	K
4.30	1.024	0.226	1.344	0.005
4.35	1.024	0.225	1.342	0.006
4.40	1.024	0.224	1.340	0.005
4.45	1.015	0.221	1.334	0.010
4.50	1.021	0.222	1.336	0.016
4.55	1.053	0.229	1.349	0.015
4.60	1.037	0.224	1.340	0.010
4.65	1.062	0.229	1.349	0.003
4.70	1.000	0.215	1.324	0.005
4.75	1.022	0.220	1.332	0.012
4.80	1.030	0.221	1.334	0.016
4.85	1.033	0.221	1.334	0.013
4.90	1.047	0.224	1.340	0.013
4.95	1.019	0.217	1.327	0.012
5.00	1.074	0.228	1.347	0.012
5.05	1.038	0.220	1.333	0.004
5.10	1.061	0.224	1.340	-0.003
5.15	1.016	0.213	1.320	-0.005
5.20	1.010	0.211	1.316	-0.0
5.25	1.023	0.212	1.318	0.002
5.30	1.022	0.210	1.315	-0.001
5.35	1.011	0.206	1.308	-0.001
5.40	1.019	0.205	1.306	-0.001
5.45	1.017	0.200	1.297	-0.001
5.50	1.017	0.198	1.294	-0.001
5.55	1.001	0.191	1.282	0.002
5.60	1.021	0.190	1.280	0.004
5.65	0.996	0.181	1.265	0.006
5.70	0.987	0.175	1.255	0.014
5.75	0.968	0.169	1.245	0.023
5.80	0.977	0.164	1.235	0.035
5.85	0.945	0.157	1.220	0.051
5.90	0.958	0.160	1.214	0.076
5.95	0.954	0.163	1.198	0.109
6.00	1.102	0.208	1.237	0.166
6.05	1.122	0.233	1.275	0.187
6.10	1.108	0.251	1.323	0.185
6.15	1.125	0.264	1.361	0.176
6.20	1.094	0.259	1.373	0.139
6.25	1.116	0.263	1.386	0.131
6.30	1.098	0.256	1.380	0.111
6.35	1.172	0.269	1.409	0.111
6.40	1.141	0.259	1.396	0.084
6.45	1.226	0.275	1.436	0.065
6.50	1.123	0.249	1.387	0.028
6.55	1.121	0.246	1.381	0.021

OPTICAL CONSTANTS OF 1.0 M UREA
ANGLE OF INCIDENCE = 1.2223 RADIANS

WL	R(REL)	R(ABS)	N	K
6.60	1.043	0.227	1.344	0.024
6.65	1.044	0.226	1.341	0.037
6.70	1.059	0.228	1.343	0.048
6.75	1.054	0.226	1.338	0.052
6.80	1.102	0.235	1.354	0.060
6.85	1.116	0.237	1.359	0.052
6.90	1.113	0.235	1.357	0.045
6.95	1.111	0.234	1.355	0.042
7.00	1.107	0.233	1.354	0.039
7.05	1.106	0.232	1.353	0.036
7.10	1.101	0.230	1.349	0.032
7.15	1.091	0.227	1.344	0.032
7.20	1.081	0.225	1.340	0.034
7.25	1.098	0.228	1.345	0.034
7.30	1.084	0.224	1.338	0.031
7.35	1.089	0.224	1.338	0.031
7.40	1.083	0.223	1.336	0.030
7.45	1.085	0.222	1.335	0.028
7.50	1.076	0.219	1.329	0.029
7.55	1.080	0.220	1.331	0.029
7.60	1.077	0.218	1.327	0.028
7.65	1.062	0.215	1.322	0.029
7.70	1.070	0.216	1.323	0.032
7.75	1.071	0.215	1.321	0.032
7.80	1.071	0.215	1.321	0.032
7.85	1.072	0.214	1.320	0.032
7.90	1.071	0.214	1.320	0.031
7.95	1.064	0.211	1.314	0.033
8.00	1.080	0.214	1.319	0.034
8.05	1.079	0.213	1.318	0.032
8.10	1.078	0.212	1.316	0.030
8.15	1.079	0.211	1.314	0.030
8.20	1.076	0.210	1.313	0.028
8.25	1.075	0.208	1.309	0.029
8.30	1.077	0.208	1.309	0.027
8.35	1.073	0.206	1.306	0.025
8.40	1.047	0.199	1.294	0.026
8.45	1.068	0.202	1.298	0.032
8.50	1.060	0.199	1.293	0.032
8.55	1.059	0.198	1.291	0.037
8.60	1.074	0.201	1.295	0.041
8.65	1.077	0.201	1.295	0.040
8.70	1.086	0.202	1.297	0.041
8.75	1.093	0.203	1.299	0.039
8.80	1.095	0.202	1.298	0.035
8.85	1.082	0.198	1.291	0.036

OPTICAL CONSTANTS OF 1.0 M UREA
ANGLE OF INCIDENCE = 1.2223 RADIANS

WL	R(REL)	R(ABS)	N	K
8.90	1.099	0.201	1.296	0.036
8.95	1.099	0.200	1.295	0.032
9.00	1.078	0.195	1.287	0.028
9.05	1.069	0.192	1.281	0.031
9.10	1.073	0.192	1.281	0.033
9.15	1.063	0.190	1.277	0.033
9.20	1.065	0.189	1.276	0.034
9.25	1.065	0.188	1.274	0.037
9.30	1.073	0.189	1.275	0.035
9.35	1.058	0.185	1.269	0.035
9.40	1.064	0.184	1.267	0.037
9.45	1.075	0.185	1.268	0.038
9.50	1.061	0.181	1.262	0.037
9.55	1.078	0.183	1.265	0.038
9.60	1.066	0.179	1.259	0.035
9.65	1.056	0.176	1.254	0.037
9.70	1.070	0.175	1.252	0.038
9.75	1.069	0.173	1.248	0.039
9.80	1.063	0.170	1.243	0.041
9.85	1.079	0.171	1.244	0.043
9.90	1.062	0.167	1.238	0.043
9.95	1.058	0.165	1.234	0.046
10.00	1.064	0.165	1.233	0.049
10.05	1.070	0.164	1.231	0.051
10.10	1.076	0.163	1.229	0.052
10.15	1.075	0.161	1.225	0.053
10.20	1.072	0.159	1.221	0.055
10.25	1.077	0.159	1.220	0.058
10.30	1.077	0.157	1.217	0.059
10.35	1.084	0.156	1.214	0.061
10.40	1.076	0.154	1.211	0.063
10.45	1.078	0.153	1.208	0.065
10.50	1.081	0.151	1.204	0.067
10.55	1.080	0.150	1.201	0.070
10.60	1.080	0.148	1.196	0.073
10.65	1.079	0.148	1.194	0.077
10.70	1.080	0.147	1.191	0.080
10.75	1.077	0.146	1.187	0.083
10.80	1.077	0.147	1.185	0.088
10.85	1.075	0.146	1.182	0.090
10.90	1.068	0.145	1.178	0.094
10.95	1.069	0.145	1.173	0.100
11.00	1.103	0.150	1.175	0.108
11.05	1.100	0.151	1.174	0.111
11.10	1.097	0.152	1.173	0.114
11.15	1.090	0.153	1.171	0.117

OPTICAL CONSTANTS OF 1.0 M UREA
ANGLE OF INCIDENCE = 1.2223 RADIANS

WL	R(REL)	R(ABS)	N	K
11.20	1.085	0.153	1.168	0.120
11.25	1.081	0.155	1.167	0.125
11.30	1.078	0.156	1.165	0.128
11.35	1.069	0.156	1.161	0.131
11.40	1.064	0.158	1.158	0.136
11.45	1.057	0.161	1.156	0.143
11.50	1.052	0.165	1.155	0.149
11.55	1.049	0.169	1.154	0.156
11.60	1.045	0.173	1.155	0.161
11.65	1.040	0.176	1.154	0.166
11.70	1.034	0.179	1.154	0.171
11.75	1.034	0.183	1.153	0.176
11.80	1.027	0.186	1.153	0.181
11.85	1.024	0.190	1.153	0.187
11.90	1.023	0.194	1.153	0.192
11.95	1.021	0.198	1.154	0.198
12.00	1.006	0.200	1.154	0.200
12.05	1.006	0.204	1.153	0.206
12.10	1.003	0.208	1.153	0.212
12.15	1.004	0.213	1.153	0.219
12.20	1.002	0.217	1.155	0.224
12.25	1.000	0.221	1.156	0.229
12.30	0.998	0.225	1.157	0.235
12.35	0.996	0.228	1.157	0.239
12.40	0.998	0.233	1.159	0.246
12.45	0.993	0.236	1.159	0.250
12.50	1.000	0.242	1.161	0.258
12.55	0.999	0.246	1.163	0.264
12.60	1.006	0.251	1.166	0.271
12.65	1.004	0.255	1.169	0.276
12.70	1.003	0.259	1.173	0.282
12.75	1.001	0.262	1.176	0.286
12.80	1.006	0.268	1.182	0.294
12.85	1.001	0.269	1.186	0.295
12.90	1.000	0.271	1.190	0.298
12.95	1.000	0.274	1.193	0.302
13.00	0.991	0.274	1.196	0.301
13.05	1.000	0.279	1.198	0.309
13.10	1.001	0.282	1.204	0.313
13.15	0.999	0.283	1.207	0.314
13.20	1.003	0.287	1.213	0.320
13.25	0.994	0.286	1.217	0.317
13.30	0.990	0.287	1.220	0.318
13.35	0.984	0.287	1.219	0.319
13.40	0.990	0.292	1.223	0.326
13.45	0.989	0.293	1.226	0.327

OPTICAL CONSTANTS OF 1.0 M UREA
ANGLE OF INCIDENCE = 1.2223 RADIANS

WL	R(REL)	R(ABS)	N	K
13.50	0.983	0.293	1.229	0.327
13.55	0.987	0.296	1.231	0.332
13.60	0.986	0.297	1.235	0.332
13.65	0.987	0.300	1.239	0.337
13.70	0.975	0.297	1.239	0.331
13.75	0.979	0.300	1.238	0.337
13.80	0.989	0.305	1.242	0.345
13.85	0.984	0.305	1.245	0.345
13.90	0.994	0.310	1.251	0.353
13.95	0.991	0.310	1.255	0.352
14.00	0.991	0.311	1.260	0.352
14.05	0.988	0.311	1.260	0.352
14.10	0.990	0.313	1.265	0.355
14.15	0.985	0.313	1.265	0.355
14.20	0.991	0.316	1.270	0.359
14.25	0.984	0.315	1.270	0.357
14.30	0.984	0.316	1.272	0.359
14.35	0.988	0.319	1.273	0.364
14.40	0.992	0.321	1.277	0.367
14.45	0.996	0.324	1.281	0.372
14.50	0.995	0.325	1.288	0.372
14.55	0.989	0.324	1.289	0.370
14.60	0.986	0.324	1.290	0.370
14.65	0.989	0.326	1.289	0.374
14.70	0.997	0.331	1.296	0.382
14.75	0.995	0.331	1.299	0.381
14.80	0.993	0.331	1.303	0.380
14.85	0.998	0.333	1.303	0.384
14.90	1.000	0.335	1.306	0.388
14.95	1.017	0.342	1.315	0.400
15.00	1.015	0.342	1.328	0.396
15.05	0.993	0.335	1.324	0.382
15.10	0.995	0.337	1.322	0.387
15.15	1.011	0.344	1.327	0.401
15.20	1.013	0.345	1.336	0.400
15.25	1.017	0.347	1.343	0.402
15.30	1.017	0.348	1.354	0.400
15.35	0.999	0.343	1.352	0.389
15.40	0.997	0.343	1.353	0.389
15.45	1.005	0.346	1.354	0.395
15.50	1.004	0.347	1.362	0.394
15.55	1.001	0.347	1.364	0.394
15.60	0.990	0.344	1.362	0.387
15.65	1.014	0.352	1.369	0.403
15.70	1.017	0.353	1.382	0.400
15.75	1.008	0.350	1.385	0.391

OPTICAL CONSTANTS OF 1.0 M UREA
ANGLE OF INCIDENCE = 1.2223 RADIANS

WL	R(REL)	R(ABS)	N	K
15.80	1.004	0.349	1.390	0.387
15.85	0.998	0.347	1.387	0.383
15.90	1.001	0.348	1.392	0.383
15.95	1.008	0.350	1.401	0.384
16.00	0.974	0.338	1.388	0.359
16.05	0.980	0.341	1.382	0.370
16.10	0.995	0.346	1.388	0.380
16.15	0.981	0.341	1.379	0.372
16.20	0.997	0.348	1.384	0.387
16.25	1.023	0.357	1.401	0.402
16.30	1.001	0.350	1.406	0.381
16.35	0.997	0.349	1.405	0.379
16.40	0.991	0.347	1.402	0.375
16.45	0.993	0.349	1.402	0.380
16.50	1.000	0.352	1.410	0.384
16.55	0.991	0.349	1.406	0.378
16.60	0.990	0.350	1.406	0.381
16.65	1.009	0.357	1.414	0.395
16.70	1.013	0.359	1.430	0.392
16.75	1.000	0.355	1.429	0.381
16.80	0.994	0.353	1.429	0.376
16.85	1.012	0.360	1.439	0.389
16.90	1.002	0.357	1.448	0.375
16.95	1.006	0.360	1.464	0.373
17.00	0.953	0.341	1.438	0.335
17.05	0.961	0.345	1.435	0.349
17.10	0.958	0.344	1.430	0.349
17.15	0.955	0.344	1.429	0.350
17.20	0.959	0.346	1.431	0.355
17.25	0.954	0.345	1.430	0.352
17.30	0.952	0.345	1.430	0.353
17.35	0.954	0.346	1.430	0.355
17.40	0.950	0.345	1.429	0.353
17.45	0.953	0.347	1.432	0.357
17.50	0.951	0.346	1.433	0.353
17.55	0.939	0.343	1.426	0.349
17.60	0.946	0.346	1.428	0.357
17.65	0.956	0.350	1.435	0.364
17.70	0.945	0.346	1.432	0.354
17.75	0.950	0.349	1.437	0.359
17.80	0.935	0.344	1.429	0.350
17.85	0.941	0.346	1.426	0.358
17.90	0.952	0.351	1.432	0.368
17.95	0.955	0.353	1.441	0.368
18.00	0.949	0.351	1.442	0.362
18.05	0.941	0.348	1.436	0.357

OPTICAL CONSTANTS OF 1.0 M UREA
ANGLE OF INCIDENCE = 1.2223 RADIANS

WL	R(REL)	R(ABS)	N	K
18.10	0.947	0.351	1.438	0.364
18.15	0.947	0.351	1.439	0.364
18.20	0.947	0.351	1.439	0.363
18.25	0.943	0.350	1.433	0.364
18.30	0.961	0.357	1.444	0.377
18.35	0.958	0.356	1.446	0.374
18.40	0.957	0.356	1.449	0.372
18.45	0.962	0.358	1.451	0.376
18.50	0.964	0.359	1.458	0.374
18.55	0.959	0.358	1.458	0.372
18.60	0.953	0.355	1.453	0.366
18.65	0.964	0.360	1.459	0.377
18.70	0.958	0.358	1.459	0.371
18.75	0.963	0.360	1.463	0.374
18.80	0.961	0.359	1.463	0.371
18.85	0.950	0.355	1.452	0.367
18.90	0.969	0.363	1.461	0.384
18.95	0.969	0.363	1.461	0.385
19.00	0.983	0.368	1.473	0.392
19.05	0.988	0.370	1.480	0.393
19.10	0.983	0.368	1.485	0.383
19.15	0.982	0.368	1.483	0.385
19.20	0.992	0.372	1.495	0.389
19.25	0.993	0.372	1.500	0.385
19.30	0.975	0.366	1.492	0.372
19.35	1.005	0.377	1.513	0.392
19.40	0.988	0.370	1.512	0.369
19.45	0.974	0.365	1.502	0.361
19.50	0.981	0.368	1.503	0.370
19.55	0.985	0.370	1.507	0.373
19.60	0.990	0.372	1.516	0.373
19.65	0.987	0.371	1.516	0.369
19.70	0.998	0.375	1.531	0.371
19.75	0.991	0.372	1.534	0.358
19.80	0.972	0.365	1.524	0.341
19.85	0.963	0.362	1.508	0.345
19.90	0.997	0.374	1.534	0.365
19.95	0.998	0.375	1.551	0.353
20.00	0.956	0.359	1.527	0.316

OPTICAL CONSTANTS OF 0.5 M AMMONIUM PHOSPHATE (MONOBASIC)
ANGLE OF INCIDENCE = 1.2223 RADIANS

WL	R(REL)	R(ABS)	N	K
2.00	1.038	0.209	1.312	-0.014
2.05	1.029	0.206	1.307	-0.014
2.10	1.030	0.205	1.306	-0.012
2.15	1.030	0.203	1.302	-0.011
2.20	1.035	0.203	1.302	-0.011
2.25	1.039	0.201	1.299	-0.012
2.30	1.038	0.198	1.293	-0.012
2.35	1.036	0.196	1.290	-0.012
2.40	1.039	0.193	1.285	-0.012
2.45	1.036	0.189	1.278	-0.013
2.50	1.035	0.184	1.270	-0.014
2.55	1.042	0.178	1.260	-0.017
2.60	1.019	0.163	1.236	-0.014
2.65	1.027	0.153	1.221	-0.013
2.70	1.011	0.122	1.177	0.005
2.75	1.006	0.099	1.135	0.047
2.80	0.956	0.134	1.135	0.115
2.85	0.972	0.193	1.154	0.191
2.90	0.982	0.251	1.210	0.260
2.95	0.985	0.286	1.293	0.289
3.00	0.993	0.300	1.371	0.272
3.05	0.996	0.306	1.426	0.237
3.10	0.998	0.309	1.468	0.190
3.15	1.001	0.301	1.475	0.137
3.20	1.010	0.294	1.471	0.099
3.25	1.011	0.287	1.462	0.072
3.30	1.023	0.281	1.452	0.049
3.35	1.022	0.273	1.437	0.032
3.40	1.020	0.266	1.423	0.022
3.45	1.015	0.259	1.408	0.019
3.50	1.021	0.256	1.402	0.018
3.55	1.032	0.255	1.400	0.015
3.60	1.031	0.252	1.394	0.009
3.65	1.026	0.247	1.384	0.007
3.70	1.025	0.245	1.380	0.007
3.75	1.029	0.243	1.376	0.006
3.80	1.022	0.240	1.370	0.007
3.85	1.035	0.241	1.372	0.005
3.90	1.025	0.237	1.365	0.003
3.95	1.021	0.234	1.359	0.005
4.00	1.047	0.238	1.367	0.002
4.05	1.008	0.228	1.348	0.002
4.10	1.026	0.232	1.355	0.005
4.15	1.020	0.229	1.349	0.004
4.20	1.014	0.226	1.344	0.005
4.25	1.022	0.227	1.345	0.009

OPTICAL CONSTANTS OF 0.5 M AMMONIUM PHOSPHATE (MONOBASIC)
ANGLE OF INCIDENCE = 1.2223 RADIANS

WL	R(REL)	R(ABS)	N	K
4.30	1.022	0.226	1.344	0.008
4.35	1.022	0.225	1.342	0.009
4.40	1.022	0.223	1.338	0.010
4.45	1.031	0.225	1.342	0.012
4.50	1.028	0.224	1.340	0.007
4.55	1.013	0.220	1.333	0.007
4.60	0.996	0.215	1.323	0.016
4.65	1.034	0.223	1.337	0.021
4.70	1.031	0.222	1.336	0.018
4.75	1.039	0.223	1.338	0.015
4.80	1.031	0.222	1.336	0.014
4.85	1.023	0.219	1.330	0.013
4.90	1.040	0.222	1.336	0.014
4.95	1.011	0.216	1.325	0.014
5.00	1.042	0.222	1.336	0.017
5.05	1.043	0.221	1.334	0.012
5.10	1.052	0.222	1.336	0.005
5.15	1.023	0.215	1.324	0.002
5.20	1.023	0.213	1.320	0.003
5.25	1.021	0.211	1.316	0.005
5.30	1.025	0.210	1.315	0.004
5.35	1.020	0.207	1.309	0.004
5.40	1.023	0.206	1.308	0.004
5.45	1.025	0.202	1.301	0.004
5.50	1.032	0.201	1.299	0.003
5.55	1.018	0.194	1.287	0.005
5.60	1.034	0.192	1.283	0.008
5.65	1.024	0.186	1.273	0.012
5.70	1.025	0.182	1.266	0.018
5.75	1.028	0.179	1.260	0.026
5.80	1.049	0.176	1.254	0.034
5.85	1.029	0.171	1.243	0.047
5.90	1.047	0.174	1.242	0.065
5.95	1.037	0.178	1.239	0.087
6.00	1.040	0.197	1.259	0.113
6.05	1.027	0.214	1.283	0.129
6.10	1.011	0.229	1.313	0.130
6.15	1.013	0.238	1.337	0.121
6.20	1.012	0.239	1.348	0.102
6.25	1.009	0.238	1.351	0.089
6.30	1.012	0.236	1.351	0.078
6.35	1.040	0.239	1.359	0.069
6.40	1.025	0.232	1.349	0.054
6.45	1.016	0.228	1.342	0.050
6.50	1.016	0.226	1.339	0.047
6.55	1.016	0.223	1.334	0.044

OPTICAL CONSTANTS OF 0.5 M AMMONIUM PHOSPHATE (MONOBASIC)
ANGLE OF INCIDENCE = 1.2223 RADIANS

WL	R(REL)	R(ABS)	N	K
6.60	1.016	0.221	1.331	0.041
6.65	0.984	0.213	1.316	0.044
6.70	1.008	0.217	1.322	0.049
6.75	1.010	0.217	1.322	0.049
6.80	0.999	0.213	1.315	0.048
6.85	1.019	0.216	1.319	0.054
6.90	1.021	0.216	1.319	0.053
6.95	1.039	0.219	1.325	0.053
7.00	1.032	0.217	1.322	0.049
7.05	1.035	0.217	1.322	0.047
7.10	1.029	0.215	1.319	0.045
7.15	1.027	0.214	1.317	0.045
7.20	1.028	0.214	1.318	0.044
7.25	1.027	0.213	1.316	0.043
7.30	1.018	0.210	1.311	0.042
7.35	1.019	0.210	1.310	0.044
7.40	1.020	0.210	1.311	0.042
7.45	1.016	0.208	1.307	0.041
7.50	1.013	0.206	1.304	0.041
7.55	1.007	0.205	1.302	0.042
7.60	1.007	0.204	1.300	0.043
7.65	1.006	0.203	1.298	0.044
7.70	1.001	0.202	1.296	0.045
7.75	1.003	0.202	1.296	0.046
7.80	1.002	0.201	1.294	0.045
7.85	0.995	0.199	1.291	0.045
7.90	0.995	0.198	1.289	0.047
7.95	0.992	0.197	1.286	0.049
8.00	0.998	0.197	1.286	0.051
8.05	1.002	0.197	1.286	0.052
8.10	1.002	0.197	1.286	0.051
8.15	1.000	0.195	1.282	0.051
8.20	0.995	0.194	1.280	0.052
8.25	0.999	0.193	1.278	0.055
8.30	1.001	0.193	1.278	0.055
8.35	0.998	0.192	1.276	0.056
8.40	0.996	0.189	1.270	0.057
8.45	0.999	0.189	1.269	0.061
8.50	1.003	0.188	1.266	0.065
8.55	1.015	0.190	1.267	0.071
8.60	1.031	0.193	1.271	0.075
8.65	1.045	0.195	1.274	0.077
8.70	1.066	0.198	1.279	0.077
8.75	1.075	0.199	1.282	0.075
8.80	1.077	0.199	1.283	0.071
8.85	1.079	0.198	1.283	0.067

OPTICAL CONSTANTS OF 0.5 M AMMONIUM PHOSPHATE (MONOBASIC)
ANGLE OF INCIDENCE = 1.2223 RADIANS

WL	R(REL)	R(ABS)	N	K
8.90	1.064	0.195	1.279	0.062
8.95	1.055	0.192	1.274	0.060
9.00	1.040	0.188	1.268	0.060
9.05	1.038	0.186	1.264	0.062
9.10	1.022	0.183	1.258	0.064
9.15	1.012	0.180	1.251	0.068
9.20	1.013	0.180	1.247	0.078
9.25	1.043	0.184	1.249	0.090
9.30	1.112	0.195	1.263	0.099
9.35	1.157	0.202	1.278	0.096
9.40	1.164	0.201	1.282	0.085
9.45	1.157	0.199	1.281	0.076
9.50	1.146	0.196	1.279	0.069
9.55	1.123	0.190	1.269	0.065
9.60	1.132	0.190	1.270	0.064
9.65	1.113	0.185	1.262	0.061
9.70	1.110	0.182	1.258	0.060
9.75	1.105	0.179	1.252	0.060
9.80	1.097	0.176	1.247	0.060
9.85	1.092	0.173	1.241	0.063
9.90	1.094	0.173	1.241	0.064
9.95	1.089	0.170	1.236	0.065
10.00	1.085	0.169	1.234	0.065
10.05	1.079	0.166	1.229	0.066
10.10	1.072	0.163	1.224	0.066
10.15	1.073	0.161	1.219	0.069
10.20	1.065	0.158	1.213	0.071
10.25	1.065	0.157	1.210	0.075
10.30	1.060	0.154	1.204	0.077
10.35	1.059	0.153	1.200	0.081
10.40	1.059	0.151	1.194	0.086
10.45	1.076	0.152	1.190	0.093
10.50	1.096	0.154	1.189	0.100
10.55	1.127	0.156	1.188	0.106
10.60	1.163	0.159	1.188	0.112
10.65	1.197	0.164	1.191	0.119
10.70	1.225	0.167	1.194	0.122
10.75	1.241	0.169	1.197	0.123
10.80	1.246	0.170	1.199	0.123
10.85	1.239	0.169	1.199	0.121
10.90	1.228	0.167	1.197	0.119
10.95	1.216	0.165	1.193	0.119
11.00	1.184	0.162	1.188	0.118
11.05	1.178	0.161	1.183	0.121
11.10	1.162	0.161	1.180	0.124
11.15	1.149	0.161	1.176	0.127

OPTICAL CONSTANTS OF 0.5 M AMMONIUM PHOSPHATE (MONOBASIC)
ANGLE OF INCIDENCE = 1.2223 RADIANS

WL	R(REL)	R(ABS)	N	K
11.20	1.137	0.160	1.171	0.130
11.25	1.125	0.161	1.167	0.135
11.30	1.126	0.163	1.165	0.140
11.35	1.122	0.164	1.161	0.144
11.40	1.123	0.167	1.158	0.150
11.45	1.125	0.171	1.157	0.157
11.50	1.122	0.176	1.158	0.164
11.55	1.109	0.178	1.158	0.167
11.60	1.093	0.181	1.158	0.172
11.65	1.079	0.182	1.156	0.174
11.70	1.073	0.186	1.156	0.180
11.75	1.058	0.187	1.154	0.182
11.80	1.049	0.190	1.153	0.187
11.85	1.041	0.193	1.151	0.192
11.90	1.037	0.197	1.151	0.197
11.95	1.033	0.201	1.151	0.203
12.00	1.020	0.203	1.151	0.205
12.05	1.010	0.205	1.148	0.209
12.10	1.009	0.209	1.147	0.215
12.15	1.012	0.215	1.147	0.223
12.20	1.004	0.218	1.149	0.227
12.25	1.000	0.221	1.148	0.231
12.30	1.000	0.225	1.148	0.237
12.35	1.000	0.229	1.148	0.242
12.40	0.997	0.233	1.149	0.247
12.45	0.999	0.237	1.149	0.253
12.50	0.994	0.241	1.151	0.258
12.55	0.997	0.245	1.152	0.264
12.60	0.991	0.248	1.154	0.268
12.65	0.991	0.252	1.154	0.274
12.70	0.992	0.256	1.156	0.279
12.75	0.996	0.261	1.159	0.286
12.80	0.991	0.264	1.163	0.290
12.85	0.991	0.267	1.166	0.295
12.90	0.987	0.268	1.169	0.296
12.95	0.983	0.269	1.168	0.297
13.00	0.997	0.275	1.171	0.306
13.05	0.996	0.278	1.174	0.311
13.10	0.998	0.281	1.179	0.315
13.15	0.992	0.281	1.180	0.315
13.20	0.995	0.285	1.185	0.321
13.25	1.001	0.288	1.189	0.325
13.30	0.981	0.285	1.192	0.320
13.35	0.985	0.288	1.191	0.325
13.40	0.982	0.289	1.193	0.326
13.45	0.984	0.292	1.194	0.331